

# SECOND MEXICAN WORKSHOP ON NANOSTRUCTURED MATERIALS

May 15–18, 2007

Instituto de Física, Benemérita Universidad Autónoma de Puebla  
Puebla, Mexico

## Book of abstracts



Instituto de Física Luis Rivera  
Terrazas  
Edificios 14A-B. C.U.  
Av. San Claudio y 18 Sur  
Puebla, Pue.  
Tel: (222) 229 55 00, ext. 5610  
<http://www.ifuap.buap.mx/index.htm>



Universidad Popular  
Autónoma del Estado de  
Puebla  
21 Sur 1103, Col. Santiago  
Puebla, Pue.  
Tel: (222) 229 94 00  
<http://web.unaep.mx>



aspelab de México  
S.A. de C.V.  
Victor Hugo 48 Desp. 302  
Col. Anzures, Mexico, D.F.  
Tel: (55) 5255-5900  
<http://www.aspelab.com.mx>



Sociedad Mexicana de  
Nanociencias  
y Nanotecnología, A.C.  
<http://www.somenano.org.mx>



Tecnología y Equipamiento  
S.A. de C.V.  
Durango No. 69, Col. Roma  
Mexico, D.F.  
Tel: (55) 5208 1165  
<http://www.tveq.com>



Facultad de Ciencias de la Electrónica  
Edificio 129. C.U.  
Av. San Claudio y 18 Sur  
Puebla, Pue.  
Tel: (222) 229 55 00, ext. 7401  
<http://www.ece.buap.mx>

## FOREWORDS

Like its first edition, the Second Mexican Workshop on Nanostructured Materials (SMWNM) is aimed to provide a common forum for the scientists, technologists, and students involve in the design, fabrication/synthesis, and application of nanomaterials in Mexico and in the world, to present their recent results, difficulties and exchange informations.

The Workshop is focused on all aspects of nanomaterials; from controlled synthesis, understanding the physics and chemistry of nanomaterials to their applications. Therefore, this is a common area of interest for the physicists, chemists, materials scientists and technologists.

The organizers tried to gather eminent personalities from Mexico and other countries, experts in several areas of nanomaterials and nanotechnologies as invited speakers, to provide best opportunity for the young researchers to update their knowledge on the recent progress in this highly emerging research filed. This is a small event with relatively small budget. We tried to keep the event free of registration fee, so that all the interested students can attend. On the other hand, the organizers arranged two courses on the microscopic characterization and analysis of nanomaterials, imparted by specialists in these fields considering their usefulness and demand among the young researchers.

The workshop covered two courses, 8 invited talks, 29 oral presentations and 78 poster presentations. Apart from that, there was one lecture from Tecnologia y Equipamiento on the application of field emission microscope and ultra high resolution FIB for the inspection of nanomaterials, and one special meeting on the Normalization of Nanotechnology in Mexico. The proceedings of the workshop containing full length papers or extended abstracts of all 8 invited lectures and contributed papers will be published in a special issue of the Journal of Nanoscience and Nanotechnology, after reviewing. Therefore, the participants are advised to prepare their full length articles according to the guidelines of the journal and submit before 30<sup>th</sup> June, 2007.

We wish to express our thanks to the sponsors of the workshop for their courageous support. I would like to thank the invited speakers and the members of the organizing committee and support staff for their contribution to make the event successful.

Puebla, May 15, 2007.



**Dr. Umapada Pal**

Chairman of the SMWNM

## **ORGANIZING COMMITTEE**

Dr. Umapada Pal (Chairman), IFUAP

Dr. Gregorio Hernández Cocolletzi, IFUAP

Dra. Patricia Santiago Jacinto, IFUNAM

Dr. Marcelino Barboza Flores, UNISON

M.C. Jaime Cid, FCE, BUAP

M.C. Fidel Pacheco, UPAEP

## **SPONSORS**

Instituto de Física “Luis Rivera Terrazas”, BUAP

Universidad Popular Autónoma del Estado de Puebla

Sociedad Mexicana de Nanociencia y Nanotecnología, A.C.

Asesoría y Proveedora de Equipos para Laboratorio S.A. de C.V.

Facultad de Ciencias de la Electrónica, BUAP

Tecnología y Equipamiento, S.A. de C.V.

Instituto Mexicano de Normalización y Certificación, A.C.

# SHORT COURSES



## **Z-Contrast Electron Microscopy for Evaluation of Inhomogeneous Nanostructured Materials**

Luis Rendón

*Laboratorio Central de Microscopia (LCM), Instituto de Física, Universidad Nacional Autónoma de Mexico, Mexico D.F, 01000 Mexico.*

Atomic number contrast (Z-contrast) imaging using a High angle annular dark field (HAADF) detector is used to study nanostructured materials such as nanostructured metals, semiconductors, mixed oxides and even soft matter composites of inhomogeneous nature. By HAADF-STEM imaging technique, it is possible to determinate the crystalline properties of the nanostructured materials even at atomic level with a spatial resolution of 0.2 nm. Even more, by a simple intensity contrast analysis, the High resolution-HAADF images give us the position of atomic inhomogeneities produces by non-uniformity intercalation of atoms in specific compounds. HAADF technique is superior to HRTEM in determining surface inhomogeneities and defects in the stoichiometric composition even at atomic resolution because it is possible to determine the chemical specie of the atoms involved by Z-contrast imaging process. The main aim of the present course is to give an introduction of HAADF-HR technique in order to apply this knowledge in the characterization of nanostructured system including biological and soft matter issues.

## **Application of EELS in Nanostructured Materials**

**Dr. Miguel Avalos Borja**

*Centro de Ciencias de la Materia Condensada, Universidad Nacional Autónoma de México,  
Apdo. Postal 2681, Ensenada, BC, México.*

This short course will cover the fundamentals of electron energy loss spectroscopy (EELS) both, from the fundamental point of view, and from the instrumentation requirements as implemented on a transmission electron microscope. It will cover in some detail the following topics, including applications for each of them: zero loss peak, plasmons, chemical identification, chemical quantification, chemical maps, fine effects, and radial distribution functions.

# INVITED TALKS



## Cathodoluminescence of Semiconductor Nanowires

J. Piqueras

*Departamento de Física de Materiales, Facultad de Ciencias Físicas*

*Universidad Complutense de Madrid, 28040 Madrid, Spain.*

The characterization of elongated semiconductor nano- and microstructures, with shapes of wires, belts, needles or tubes is a subject of increasing interest due to the potential use of such structures in future nanoelectronic systems, optical nanodevices or other applications as gas-sensing or in transparent electrodes. The one-dimensional semiconductor structures have often different electronic behavior than the bulk material, due to different factors, as the influence of surface states, defect structure or size effects. In this work, cathodoluminescence (CL) in SEM has been applied to the characterization of elongated nano- and microstructures of ZnO, Ga<sub>2</sub>O<sub>3</sub>, In<sub>2</sub>O<sub>3</sub>, SnO<sub>2</sub>, TiO<sub>2</sub>, GeO<sub>2</sub>, CdSe and other compounds.

The samples were prepared by compacting high purity powder to form disks of about 7 mm diameter, and then annealing under argon flow. This method leads to the growth of the structures directly on the sample surface, which acts as the source as well as the substrate.<sup>1,2,3</sup> The growth mechanism is a vapour-solid process which does not involve a foreign substrate or a catalyst. The morphology and luminescence of the obtained nano- and microstructures were investigated by SE imaging and CL in SEM.

The formation of the elongated structures induces, in all the investigated cases, marked changes in the CL intensity and spectra. Some examples of specific spectral features have been found in ZnO, where nanoneedles present an intense band corresponding to deep level state not observed in bulk material or in SnO<sub>2</sub> tubes whose inner wall does not show the 1.9 eV emission characteristic of oxygen vacancies, present in bulk samples. CL images reveal in different elongated structures an inhomogeneous distribution of defects.

The application of CL to the characterization of the above mentioned elongated structures will be discussed.

*This work was supported by MEC (Project MAT2006-01259)*

---

<sup>1</sup> A.Urbieto, P.Fernández and J.Piqueras, Appl.Phys. Lett. **85** (2004) 596

<sup>2</sup> A.Urbieto, P.Fernández and J.Piqueras, Appl.Phys. Lett. **85** (2004) 596

<sup>3</sup> D.A.Magdas, A.Cremades and J.Piqueras, Appl. Phys. Lett. **88**, (2006) 113107



## **Novel Optical and Dynamic Properties and Emerging Applications of Nanomaterials**

Jin Z. Zhang

*Department of Chemistry and Biochemistry, University of California Santa Cruz,  
Santa Cruz, CA 95064 USA.*

*[http://chemistry.ucsc.edu/zhang\\_j.html](http://chemistry.ucsc.edu/zhang_j.html)*

Nanomaterials are of strong interest for both fundamental and technological reasons. At the fundamental level, nanomaterials possess novel physical and chemical properties that differ from those of isolated atoms or molecules and bulk matter due to quantum confinement effects and exceedingly larger surface area relative to volume. These novel properties are highly promising for applications in emerging technologies such as nanoelectronics, nanophotonics, non-linear optics, miniaturized sensors and imaging devices, solar cells, and detectors.

Semiconductor nanoparticles have been studied extensively because of their potential application in electronic devices and the opportunity they offer to study the effects of quantum confinement. A unique subset of semiconductor nanoparticles is doped semiconductor nanoparticles. We have recently studied several doped semiconductor nanoparticle systems with the goal to understand the relation between their optical properties and the structure of the host nanoparticles as well as that of the dopant. In the case of  $\text{Mn}^{2+}$ -doped ZnSe nanoparticles, we have found that the location of the  $\text{Mn}^{2+}$  significantly influences its optical emission properties. This understanding is important for designing new nanophotonics materials. We have also investigated the bioconjugation of silica-coated CdSe quantum dots to IgG proteins for potential applications in cancer biomarker detection and have found that the silica coating significantly enhance the stability of the CdSe quantum dots in buffer solutions based on photoluminescence properties.

Metal nanoparticles have also attracted considerable attention due to their interesting properties and potential applications. We have studied the optical and structural properties of different metal nanostructures including aggregates, nanorods, and nanoshells with the goal to optimize their SERS (surface-enhanced Raman scattering) activities. For example, we have very

recently demonstrated SERS from single, hollow gold nanostructures. Exceptional sample homogeneity leads to a nearly tenfold increase in signal consistency over standard silver substrates. We have also discovered that it is possible to make long gold nanotubes using magnetic nanoparticles as templates. Unique hollow Au-Ag double nanoshell structures have been designed and successfully synthesized in our lab that show enhanced SERS activities over hollow gold nanoshells. SERS offers a unique combination of molecular specificity and extremely high sensitivity that few other analytical techniques can offer. SERS based on metal nanoparticles, in conjunction with photoluminescence from semiconductor quantum dots, have been exploited for detection of cancer biomarkers.

In addition, my lab has been engaged in the study of metal oxide nanostructures for solar energy applications based on photovoltaics, photocatalysis, or photoelectrochemistry. One example is hydrogen generation from photoelectrochemical splitting of water based on  $\text{WO}_3$  and  $\text{TiO}_2$  nanostructures doped with nitrogen or sensitized with quantum dots.

## **Nanostructured Semiconductor Materials and their Applications for Renewable Energies**

Gerardo Contreras Puente

*Escuela Superior de Física y Matemáticas-IPN, Edificio -9, UPALM, Mexico D.F., Mexico.*

The possibility of making the characterization, control and manipulation of condensed matter in the submicrometric dimensions, and even below, allows the design and processing of novel structures with defined purposes. We present in this talk the results obtained in nanostructured semiconductors of silicon, silicon dioxide, and of the binary compounds of the II–VI groups, as processed by several cheap chemical and physical techniques of easy and rapid implementation. Our main interest in these basic and applied studies lies in the uses of these nanostructured materials in photovoltaics and photoelectrolyzers, with the aim of increasing the efficiency of such devices.

## **In Situ High Temperature Electron Irradiation Effects in Carbon Nanostructures**

Humberto Terrones<sup>1</sup>, Julio A. Rodríguez Manzo<sup>1</sup>, Litao Sun<sup>2</sup>, Florian Banhart<sup>2</sup>,  
Mauricio Terrones<sup>1</sup>, and Harold W. Kroto<sup>3</sup>

<sup>1</sup> *Advanced Materials Department, IPICyT, Camino a la Presa San José 2055, Col. Lomas 4a. sección, 78216 San Luis Potosí, Mexico.*

<sup>2</sup> *Institut für Physikalische Chemie, Universität Mainz, 55099 Mainz, Germany.*

<sup>3</sup> *Department of Chemistry and Biochemistry, Florida State University, Tallahassee, Florida 32306-4390, USA.*

Using a high resolution transmission electron microscope, equipped with a heating stage, we have been able to produce important changes in carbon nanostructures and shed some light in the processes involved during the growth of carbon nanotubes. In addition, the role of pressure inside carbon nanotubes is studied; it is found that metal nanowires inside multiwalled carbon nanotubes are extruded due to high pressures. Finally, it is shown that carbon atoms diffuse through transition metals to catalyze the growing of single walled carbon nanotubes. The importance of electron irradiation to study nanomaterials is discussed.

## Dynamic Behavior of $\text{WO}_x/\text{ZrO}_2$ Nanostructures and Catalytic Efficiency for Oxidative Desulfurization

J. A. Ascencio, E. Torres-Garcia, and A. Medina

*Instituto Mexicano del Petroleo, Lazaro Cardenas 152, Col San Bartolo Atepehuacan Mexico,  
Distrito Federal 07730 Mexico.*

*Universidad Michoacana de San Nicolas de Hidalgo. Edificio U, C. U., Morelia, Michoacán,  
58000 Mexico.*

The use of catalyst based on the presence of a thin layer of  $\text{WO}_x$  over  $\text{ZrO}_2$  supports has been well sustained for oxidative desulfurization phenomena. In this way, the capability to deposit controlled size  $\text{WO}_x$  films over  $\text{ZrO}_2$  nanostructures has been determined as the most important parameter to increase the efficiency of the material. In previous reports we have determined the influence of the  $\text{WO}_x$  surface density in the sulfur removal,<sup>1</sup> but also on the content in the production of different configurations of  $\text{WO}_x/\text{ZrO}_2$  materials, with the corresponding effects to the physicochemical properties.<sup>2</sup> The use of transmission electron microscopy techniques, including high resolution images, allows a chemical composition and structural evaluation of the materials deriving into the understanding of several important parameters.

In this case, we are focused to determine the possible effects of electron irradiation on the induction of dynamic phenomena, which must affect the catalytic properties of the materials. Consequently a review about the physicochemical parameters that are involved in the catalytic efficiency of this material is evaluated, and following the formation of clusters of  $\text{WO}_x$  over the  $\text{ZrO}_2$ . As part of this clusters formation, we report an observed effect of structural transition, which is associated to a kind of quasi-melting behavior.

This effect has been reported for metal nanoparticles, which has been even associated to coalescence and the production of bigger structures. However, in case of a metal oxide the possible reduction phenomenon imply chemical repercussions on the characteristics of the material. Based on the structural and physicochemical characterization, here is discussed the main parameters to have the optimum catalysts for sulfur removal with this kind of materials

---

<sup>1</sup> E. Torres-García, G. Canizal, L.F. Ramírez-Verduzco, F. Murrieta-Guevara, and J. A. Ascencio. *Influence of surface phenomena in oxidative desulfurization with  $\text{WO}_x/\text{ZrO}_2$  catalysts*. **Applied Physics A**. 79, 2037-2040 (2004).

<sup>2</sup> Iribarren, A., Rodriguez-Gattorno, G., Ascencio, J. A., Medina, A., Torres-Garcia E. *Tailoring chemical hardness in  $\text{WO}_x\text{-ZrO}_2$  system*. **Chemistry of Materials**. 18 (23): 5446-5452 (2006).

## Interactions of Cu<sub>2</sub>O, SnO<sub>2</sub>, ZnO Nanoparticles with Different Molecular Species

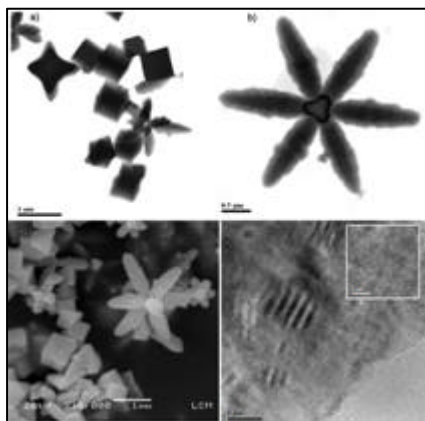
David Díaz\*, Guadalupe Osorio-Monreal, Donaji Velasco-Arias,

Víctor-Fabián Ruiz-Ruiz, Héctor García –Ortega, Rita Patakfalvi, and Luis Ortiz-Frade

Facultad de Química, Universidad Nacional Autónoma de México, Coyoacán, 04510 México D.F., México.

\*e-mail: david@servidor.unam.mx

A variety of fundamental studies have been carried out related to photoinduced energy and electron transfer in non-covalently bonded donor–acceptor (D–A) systems. For example, metal oxide nanoparticles with attached photosensitizers such as porphyrins are used as an *in vivo* agent for photodynamic therapy (PDT)<sup>1</sup>. Here we present the direct interaction of metal oxide well characterized nanoparticles (NPs) and two different kind of organic molecules, cholic acid (CA) and *meso*-tetraphenylporphyrin (TPP). These interaction reactions take place under mild reaction conditions in polar organic solvents, such as DMSO and DMF, where ZnO, SnO<sub>2</sub> and Cu<sub>2</sub>O NPs are dispersed. UV-visible electronic absorption and emission spectroscopies are used to follow those reactions.



TPP was prepared by a previously published method<sup>2</sup>. The synthesis and characterization of ZnO and SnO<sub>2</sub> is reported elsewhere<sup>3</sup>. Cuprous oxide nanoparticles were obtained by three different methods, in colloid dispersions.

Figure 1. (a), (b) TEM images of Cu<sub>2</sub>O particles; (c) SEM image of these particles; and, (d) HR-TEM image of selected particles prepared by Benedict's reaction (the insert shows an amplified area of same image).

<sup>1</sup> H. Gu, K Xu., Z. Yang, C. K. Chang, and B Xu., *Synthesis and cellular uptake of porphyrin decorated iron oxide nanoparticles -a potential candidate for bimodal anticancer therapy*. Chem. Comm. 34, (2005), 4270.

<sup>2</sup> J. S. Lindsey, I. C. Schreiman, H. C. Hsu, P. C. Kearney, and A. M. Marguerettaz. *Rothenmund and Adler-Longo reactions revisited: synthesis of tetraphenylporphyrins under equilibrium conditions*. J. Org. Chem. 52, (1987), 827.

<sup>3</sup> (a) G. Rodríguez-Gattorno, P. Santiago-Jacinto, L. Rendon-Vázquez, J. Németh, I. Dékány, and D. Díaz\*. [Novel Synthesis Pathway of ZnO Nanoparticles from the Spontaneous Hydrolysis of Zinc Carboxylate Salts](#). J. Phys. Chem. B. 107, (2003), 12597. (b) D. Velasco-Arias, D. Díaz, P. Santiago-Jacinto, G. Rodríguez-Gattorno, A. Vázquez-Olmos and S. E. Castillo -Blum. Direct Interaction of Colloidal Nanostructured ZnO and SnO<sub>2</sub> with NO and SO<sub>2</sub>. Submitted to JNN

The first method is a modification, in a DMSO-H<sub>2</sub>O mixture, of the well known Benedict's reaction and involves the use of a reducing agent; large particles are obtained (70–100 nm). The second method is a basic hydrolysis of CuCl salt in DMSO, which gives smaller nanoparticles (2.1–2.4 nm). Stable and small Cu<sub>2</sub>O nanoparticles (2.2 nm) are prepared by the spontaneous hydrolysis of CuCl in DMSO-H<sub>2</sub>O mixtures. The cuprous oxide NP characterization techniques include UV-visible absorption and emission spectra, HR-TEM, and Xray powder diffraction. Cyclic voltammetry and potentiometric measurements were performed to demonstrate the presence of Cu(I) ions in solution, and then, to explain the formation of Cu<sub>2</sub>O NPs.

## Third-order optical nonlinearities of metal and semiconductor nanostructures

A. I. Ryasnyanskiy

*Institut des Nano-Sciences de Paris, CNRS – Université Pierre et Marie Curie, Case 80,  
140 rue de Lourmel, F75015 Paris, France.*

*Samarkand State University, 703004 Samarkand, Uzbekistan.*

e-mail: ryaasn2000@yahoo.com

The nonlinear optical parameters such as nonlinear refractive index, nonlinear absorption coefficient, real and imaginary parts of the third-order nonlinear susceptibility are very important for many practical applications. Moreover, the sign of these parameters determines the area of applicability. For example negative nonlinear refraction and positive nonlinear absorption can be efficiently used for optical limiting<sup>1</sup>, reduction of intensity fluctuations<sup>1</sup>, stabilization and compression of picosecond pulses in the passive negative feedback schemes.<sup>2</sup> On the other hand material with positive sign of nonlinear refraction can be used for soliton formation in optical waveguides and the negative absorption is used for mode-locking. All these show the importance of determination both the values and the signs of nonlinear optical parameters.

In this paper the results of investigation of nonlinear-optical parameters of metal and semiconductor nanoparticle systems are presented in the field of both picosecond and nanosecond pulsed of Nd:YAG laser radiation using Z-scan technique and its modifications like Reflective Z-scan and Off-axis Z-scan. The dependence of the sign and the value of these parameters on the laser radiation intensity, wavelength and pulse duration are shown. The mechanisms of nonlinear refraction (thermal effect, electronic Kerr effect) and absorption are considered.

The possible areas of application are considered both theoretically and experimentally.

---

<sup>1</sup> Ryasnyanskiy A. I., Palpant B., Debrus S., Ganeev R. A., Stepanov A., Can N., Buchal Ch., Uysal S. "Nonlinear optical absorption of ZnO doped with copper nanoparticles in the pico- and nanosecond pulse laser field" *Applied Optics* **44** (2005) 2839.

<sup>2</sup> Ganeev R. A., Usmanov T. "Investigation of negative feedback regimes for generation of compressed pulses" *Jpn. J. Appl. Phys.* **39** (2000) 5111.



**Nano-structured ZnO thin films for field-emission and spintornic application**

Dr. Pijush Bhattacharya

*FISK University, 17<sup>th</sup> Ave. North, Nashville TN 37209.*

Zinc oxide (ZnO) is a unique material that exhibits both semiconducting and piezoelectric properties. It has asymmetric growth property, grown preferential along c-axis that makes ZnO as an attractive candidate for fabrication of different kind of nano-structured thin films. These nanostructures could have many novel applications in optoelectronics, sensors, transducers and biomedical sciences. Several growth techniques are reported for synthesis of ZnO nano-structures such as, vapor-liquid-solid (VLS), hydrothermal, closed space pulsed laser deposition (PLD) etc. In this work, detail fabrication technique of VLS growth of ZnO structure on patterned Si substrates using self assembled polystyrene sphere and their different characterizations will be discussed. Fabrication of ZnO nano-rod by close-spaced PLD technique and doping with 3d transition metal impurities will be presented.

# TALKS



## **Efecto de la Implantación de Iones de Al en las Propiedades Ópticas de $\alpha$ -Al<sub>2</sub>O<sub>3</sub>**

**L. Herrera-Colín<sup>1\*</sup> and A. García-Bórquez<sup>1</sup>**

<sup>1</sup> *Departamento de Ciencia de Materiales, ESFM – IPN Edif. 9 UPALM, 07738 Mexico D.F.,  
Mexico.*

\*e-mail: lizherr@hotmail.com

La búsqueda continua de materiales avanzados para aplicaciones específicas se extiende cada vez más hacia los cerámicos, los cuales son de particular interés pues presentan muy buena resistencia al desgaste, a la corrosión, a la temperatura, al paso de la electricidad, etc., además son ligeros y de costo accesible. Sin embargo, bajo la irradiación de un haz de partículas, la superficie de los cerámicos es muy sensible y aparecen en ella manchas pardas visibles debidas probablemente a desplazamientos atómicos en el material.<sup>1</sup>

El estudio de los defectos superficiales y su relación con los cambios estructurales puede ser de considerable interés práctico para predecir el comportamiento y la estabilidad de los materiales sometidos a ambientes de irradiación constante. Algunos estudios han mostrado que durante la irradiación, los iones pesados depositan su energía en las capas superficiales del material, lo cual conlleva a la producción de una alta densidad de defectos que afectan propiedades ópticas como la transmitancia y la reflectancia.<sup>2</sup>

En este trabajo, se irradiaron muestras de  $\alpha$ -Al<sub>2</sub>O<sub>3</sub> con dosis altas de iones de Al de 3.66 MeV a 1000 °C, usando un acelerador tipo Tandetron GIC. La muestra control y las muestras irradiadas fueron analizadas empleando microscopía electrónica de barrido (MEB) y espectroscopia de UV-VIS (UV-VIS) para caracterizar los cambios en la morfología y en la respuesta óptica, respectivamente.

Por MEB, se observa la presencia de nanorugosidad con formaciones piramidales en la superficie de las muestras irradiadas. UV-VIS revela la disminución en transmitancia y reflectancia con respecto a la muestra no irradiada.

---

<sup>1</sup> Chiari M., Migliori A., Mandó P. A., Nuclear Instruments and Methods in Physics Research B 188 (2002) 151-155.

<sup>2</sup> T. Aruga, Y. Katano, T. Ohmichi, S. Jitsukawa, Surface and Coatings Technology 158/159 (2002) 444-448.

## **Study of Defects in ZnO:Yb by Cathodoluminescence and Tunneling Microscopy**

A. Susarrey<sup>1</sup>, M. Herrera<sup>1\*</sup>, J. Valenzuela<sup>1</sup>, and U. Pal<sup>2</sup>.

<sup>1</sup> *Centro de Ciencias de la Materia Condensada, Universidad Nacional Autónoma de México,  
Apdo. Postal 2681, Ensenada, B.C. 22800, México.*

<sup>2</sup> *Instituto de Física, B. Universidad Autónoma de Puebla, Apdo. Postal J-48, Puebla, Puebla  
72570, México.*

\*e-mail: zaldivar@ccmc.unam.mx

The morphology and optical characteristics of ZnO nanoparticles doped with Yb were studied by cathodoluminescence (CL) and scanning tunneling microscopy (STM) techniques. Hydrothermal and thermal diffusion methods were used to prepare ZnO nanoparticles doped with < at 1% Yb and > at 1% Yb respectively. Agglomeration of nanoparticles was observed in the samples with higher Yb content. Relatively higher CL emissions related to point defects in ZnO were observed for the samples doped by thermal diffusion method. STM images of weakly doped samples show monocrystalline surface characteristics.

*We acknowledge to V. García and A. Pérez by their technical support. This work was partially supported by CONACyT, Mexico through projects No. 47505 and 46269.*

## **Directing the Spectroscopic States of CdS Nanoparticles by Chemical Surface Modification**

M. Quintana<sup>1\*</sup>, F. Mendez<sup>2</sup>, and E. Pérez<sup>1</sup>

<sup>1</sup>*IF- Universidad Autónoma de San Luis Potosí, Manuel Nava 6, Zona Universitaria, 78290 San Luis Potosí, SLP, Mexico.*

<sup>2</sup>*Universidad Autónoma Metropolitana-Iztapalapa, Mexico DF, Mexico.*

\*e-mail: mildred@ifisica.uaslp.mx

Size-tunable optical properties in nanoscales derive primarily from the physical size and shape of the materials. In II-VI semiconductor nanoparticles the size-tuning is attributed to the confinement of the exciton in a nanocrystal significantly smaller than the bulk exciton. The excitons can be engineered in a material according to structure. Interesting spectroscopic properties are governing by the size, including the band gap and the exciton binding energy, which are often minuscule in bulk materials, and are greatly accentuated in nanometer sized materials. In this work we presented a surface chemical modification of CdS nanoparticles by different Lewis bases. The spectroscopy studies reveals details of the collective excited states that capture and redistributed the excitation causing a blue shift and fluorescence enhancement depending on the adsorbed molecules. The experimental results are explained by theoretical DFT calculations.

***Acknowledgements.** This work was partially supported by SEP-2004-C01-45951 Conacyt and UNAM-UASLP 2006 projects. Mildred Quintana is a CONACYT postdoc fellow.*

## One-dimension Core-Shell Zn/ZnO Structures Synthesized by Solvothermal Approach

M. Trejo<sup>1</sup>, P. Santiago<sup>1,\*</sup>, L. Rendón<sup>1</sup>, M. Villagran-Muñoz<sup>2</sup>,  
M. Sobral<sup>2</sup>, and J.M. Hernández<sup>3</sup>

<sup>1</sup>*Departamento de Materia Condensada, Instituto de Física, Universidad Nacional Autónoma de México, Coyoacan, 04510, A.P. 20-364, C.P. 01000, Mexico City.*

<sup>2</sup>*Laboratorio de Fotofísica (CCADET) Circuito Exterior s/n A.P. 70-186 Ciudad Universitaria, 04510 Mexico D.F., Mexico.*

<sup>3</sup>*Departamento de Estado Sólido, Instituto de Física, Universidad Nacional Autónoma de México, Coyoacan, 04510, A.P. 20-364, 01000, Mexico City, Mexico.*

\*e-mail: paty@fisica.unam.mx

Binary metal-semiconductor Zn/ZnO core-shell nanorods have been synthesized by a solvothermal technique. The core is form by metallic single crystal Zn nanorods growing in the [0002] direction, while the shell corresponds to ZnO growing epitaxially in the [0002] of the hexagonal Wurtzite phase; this direction is perpendicular to the [0002] of Zn. The ZnO layer is about 5 nm in thickness. The structural properties of the binary one dimension structures were studied by HRTEM and EDS. Photoluminescence (PL) measurements were performed at room temperature using a pulsed laser line at 248 nm as excitation source.

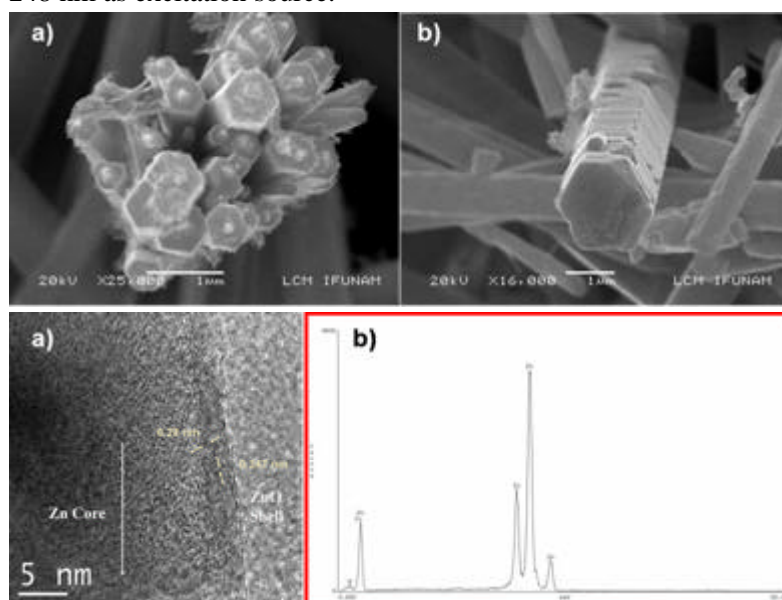


Figure1.a) SEM micrograph of Zn/ZnO metal-semiconductor core-shell nanorods. The micrograph shows the hexagonal habit. b) Single crystal Zn nanorod.

Figure2. a) HRTEM micrograph of Zn/ZnO core-shell nanorod. b) EDS obtained from the core zone were the absence of O is evident

We kindly acknowledge to Instituto de Física at UNAM for allowing the use of their microscopy facilities and CUDI project for financial support.

## Solvent-free Obtaining of $\text{Co}_3\text{O}_4$ and $\text{CuO}$ Nanoparticles

A. Vázquez-Olmos<sup>\*a</sup>, A. L. Fernández-Osorio<sup>b</sup>,

R. Sato-Berrú<sup>a</sup>, and A. L. Ramos Bautista<sup>a</sup>

<sup>a</sup>*Centro de Ciencias Aplicadas y Desarrollo Tecnológico, <sup>b</sup>Facultad de Estudios Superiores, Cuautitlán-I, Universidad Nacional Autónoma de México, Coyoacán, México D. F., 04510, México.*

\*e-mail: america.vazquez@aleph.cinstrum.unam.mx

Transition metal oxide nanoparticles are an important kind of materials due to their optical, magnetic and electronic properties. In particular, cobalt oxide  $\text{Co}_3\text{O}_4$ , a mixed valence compound  $[\text{Co(II)Co(III)}_2\text{O}_4]$  with a normal spinel structure, has a wide range of industry applications including anode materials for rechargeable Li-ion battery, catalyst, pigments, gas sensors, magnetic materials and as intercalation compounds for energy storage. These applications are highly related to the particle size and surface effects.

On the other hand, copper oxide  $\text{CuO}$ , is a covalent semiconductor with a band gap between 1.21 and 1.5 eV.  $\text{CuO}$  has a large, but almost constant, paramagnetic susceptibility at low temperatures. The effect of the electronic configuration of  $\text{Cu(II)}$  on electronic and phononic characteristics of mixed oxides, has made  $\text{CuO}$  a fundamental compound of several high- $T_c$  superconductors.

In this work, we present the obtaining of  $\text{Co}_3\text{O}_4$  and  $\text{CuO}$  nanoparticles with average diameters of 8 nm, by a solvent-free solid-solid synthesis method from  $\text{Cu(II)}$  or  $\text{Co(II)}$  salts (chloride or acetate) with sodium hydroxide ( $\text{NaOH}$ ) in 1:2 stoichiometric ratio.

The nanostructures were studied by UV-visible electronic absorption, electronic paramagnetic resonance (EPR) and Raman spectroscopy,<sup>1</sup> and their crystal structures, as well as their average diameter, were determined from XRD patterns and by HR-TEM images.

**Acknowledgments.** The support of PAPIIT project IN109205

---

<sup>1</sup> R. Y. Sato-Berru, A. Vazquez-Olmos, A. L. Fernandez-Osorio, S. Sotres-Martinez, "Micro-Raman investigation of transition-metal doped  $\text{ZnO}$  nanoparticles", *J. Raman Spectrosc.* In press

## TL and OSL Properties of $\text{TiO}_2\text{:Yb}$ Nanophosphors

Mou Pal<sup>1</sup>, U. Pal<sup>2</sup>, V. Chernov<sup>3</sup>, R. Meléndrez<sup>3</sup>, and M. Barboza-Flores<sup>3\*</sup>

<sup>1</sup>*Posgrado en Ingeniería y Ciencias Aplicadas, UAEM-CIICAP, Cuernavaca, Morelos, Mexico.*

<sup>2</sup>*Instituto de Física, Benemérita Universidad Autónoma de Puebla, Apartado Postal J-48, Puebla, Puebla, 72570 Mexico.*

<sup>3</sup>*Centro de Investigación en Física, Universidad de Sonora, Apartado Postal 5-088, Hermosillo, 83190 Mexico.*

\*e-mail: mbarboza@cajeme.cifus.uson.mx

The development of nanostructured material capable of assessing ionizing radiation doses, by thermoluminescence (TL), has been recently demonstrated.<sup>1</sup> In the present work, we report on the TL and optically stimulated luminescence (OSL) properties of nanostructured 28-40 nm grain size  $\text{TiO}_2\text{:Yb}$  prepared by controlled hydrolysis of glycolated precursors. It exhibited a characteristic TL glow curve after irradiation with beta rays. The TL glow curve shape of non-irradiated samples displayed some distinctive TL peaks around 100-125 and 200-300 °C which may associated to the transition of amorphous  $\text{TiO}_2$  to its rutile phases structures. Several TL glow peaks were found in  $\text{TiO}_2\text{:Yb}$  and the maximum temperature and intensity of each peak was strongly dependent on Yb doping concentration. The  $\text{TiO}_2\text{:Yb}$  nanophosphor showed an IR optically stimulated luminescence (IROS) signal that increased as the dose increased in the range of 10-300 Gy. It was determined that the OSL signal involves mainly the detrapping of charge carriers at trapping levels around 65-75 °C. The TL and OSL properties exhibited by  $\text{TiO}_2\text{:Yb}$  nanophosphor indicates that it worth to perform further investigation on this material in order to improve its qualities as ionizing radiation dosimeter.

*The work was partially supported by UC-MEXUS and CONACyT (Grant # CN-05-215, # 46269), Mexico.*

---

<sup>1</sup> U. Pal, R. Meléndrez, V. chernov, M. Barboza-Flores. Appl. Phys. Lett. 89(18), 183118 (2006).



## Effect of UV Light on the Isoelectric Point of Nanosized TiO<sub>2</sub> (Anatase) Sol-Gel Prepared at Different Water/Alkoxide Molar Ratios

J. A. Pedraza-Avella<sup>1</sup>, P. Acevedo-Peña<sup>2</sup>, R. Gómez<sup>3</sup>, and J. E. Pedraza-Rosas<sup>2,\*</sup>

<sup>1</sup> Centro de Investigaciones en Catálisis - CICAT, Universidad Industrial de Santander, Sede Guatiguará, Km. 2 vía El Refugio, Piedecuesta, Santander, Colombia.

<sup>2</sup> Grupo de Investigaciones en Minerales, Biohidrometalurgia y Ambiente - GIMBA, Universidad Industrial de Santander, Sede Guatiguará, Km. 2 vía El Refugio, Piedecuesta, Santander, Colombia.

<sup>3</sup> Grupo ECOCATAL, Área de Catálisis, Departamento de Química, Universidad Autónoma Metropolitana-Iztapalapa, Av. San Rafael Atlixco 186, 09340 Mexico D.F., Mexico.

\*e-mail: apedraza@uis.edu.co, jpedraza@uis.edu.co

It is well known that the isoelectric point (IEP) of a catalyst plays an important role in heterogeneous catalysis. It is related to the strength of the electrostatic interaction between the solid surface and the substrate. In heterogeneous photocatalysis, it is also important to keep in mind that additional charges are generated when a semiconductor photocatalysts is illuminated (electron-hole pairs)<sup>1,2</sup>. In this work, different samples of TiO<sub>2</sub> sol-gel were prepared by gelling

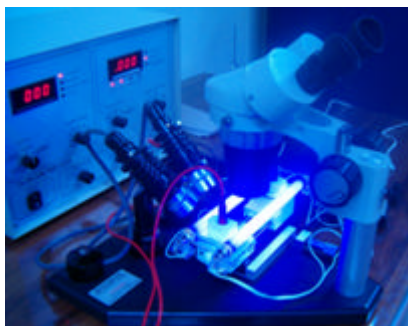


Fig. 1. Equipment used for electrophoretic measurements in the presence of UV-light.

titanium *n*-butoxide in aqueous acid media (pH=3, HNO<sub>3</sub>) using *n*-butanol as solvent. Molar ratio water/alkoxide was varied from 4 to 16. XRD patterns showed only nanocrystalline anatase phase in all samples. The IEP of materials was measured in the absence and presence of UV-light (see Fig. 1). In the absence of UV-light, IEP depends on the molar ratio water/alkoxide. However, in the presence of UV-light, IEP was the same for all materials. This result proves that TiO<sub>2</sub> surface speciation is strongly affected by the generation of electron-hole pairs.

We acknowledge the partial financial supports of UIS (DIEF Ciencias, Project 5125), COLCIENCIAS, UAM-I and CONACYT, as well as the doctoral scholarship given by COLCIENCIAS to J.A. Pedraza-Avella in 2003.

<sup>1</sup> W.W. Dunn, Y. Aikawa and A.J. Bard, "Characterization of Particulate Titanium Dioxide Photocatalysts by Photoelectrophoretic and Electrochemical Measurements", J. Am. Chem. Soc. **103** (1981) 3456.

<sup>2</sup> C. Boxall, "The Electrophoresis of Semiconductor Particles", Chem. Soc. Rev. **23** (1994) 137.

## The Hydriding Behavior of Nanostructured Mg-Based Alloy Powders

A. F. Palacios-Lazcano, J. L. Luna-Sánchez, L. F. Dámaso-Custodio, F. Cruz -  
Gandarilla, and J. G. Cabañas-Moreno\*

*Instituto Politécnico Nacional, ESFM, Depto. de Ciencia de Materiales, UPALM,  
Col. Lindavista, Apdo. Postal 75-373, Mexico D.F., 07300. Mexico.*

\*e-mail: gcabanas@esfm.ipn.mx

Hydrogen storage in the form of metal hydrides is of importance for the realization of the so-called “Hydrogen Economy”. Mg and Mg-based alloys are promising candidate materials for hydrogen storage due to their low density and high storage capacity (~7.6 wt. %). The kinetics of hydrogen storage and release are improved in nanostructured Mg alloys. In the present work, we report the preparation by mechanical alloying of nanocrystalline, solid solution Mg-M alloys (M = Zn, Al, Ag), and their hydriding behavior at different temperatures and hydrogen pressures.

The powder alloys were produced by ball milling under argon atmosphere. The as-milled powders were hydrided at 200 and 300 C under 0.5 and 3 MPa  $P_{H_2}$ . The  $MgH_2$  phase was already present after hydriding under relatively mild conditions (200 C and 0.5 MPa  $P_{H_2}$ ) in the amount of 4 to 23 vol. %, depending on the alloy composition, as determined by Rietveld analysis of XRD data. The  $MgH_2$  content in samples hydrided under more severe conditions (300 C and 3 MPa  $P_{H_2}$ ) ranged from 3 to 76 vol. %. In contrast, the  $MgH_2$  phase was not found in commercial polycrystalline Mg powders after hydriding under the same conditions.

The advantages provided by the nanocrystalline structure on the hydriding behavior of the Mg alloys will be highlighted, as well as the effects observed from the alloying additions.

*Financial support from PIFI-IPN, SPI-IPN and CONACyT is gratefully acknowledged. JGCM is a recipient of a COFAA-IPN fellowship.*

## Computational Study of Organometallic Structures for Hydrogen Storage

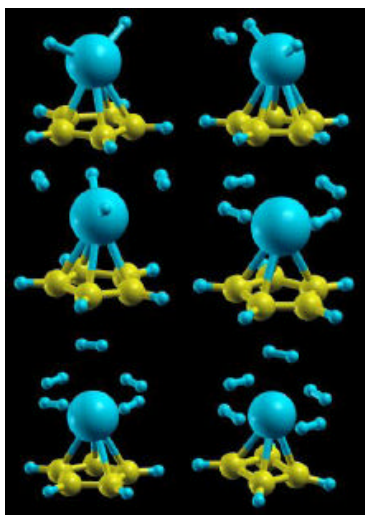
A.I. Martinez\* and M.E. Sanchez

*Center for Research and Advanced Studies of the National Polytechnic Institute (CINVESTAV-IPN) Saltillo, Carr. Saltillo-Mty. Km 13, 5900 Ramos Arizpe Coahuila, Mexico.*

\*e-mail: mtz.art@gmail.com

Currently, hydrogen is compressed at pressures of around 700 bar in tanks of demonstration automobiles; this storage way waste up to 30% of the total energy used for transportation. Study of materials for hydrogen storage with high gravimetric/volumetric densities and adsorption/desorption reversibility at near room-temperature, represents a critical challenge for applications in hydrogen powered vehicles. If weak-interactions between  $H_2$ /adsorbent are present, desorption occurs at very low temperatures, while higher binding energies require very high temperatures; then, the ideal form of binding in  $H_2$  storage is in between physisorption and chemisorption. By density functional theory (DFT) calculations, it has been reported that transition metal (TM) atoms bound to fullerenes or carbon nanotubes are ideal adsorbents for high density, room temperature and ambient pressure hydrogen storage.<sup>1</sup> A theoretical  $H_2$  storage density of ~9 wt % has been predicted, which meets the U.S. Department of Energy target for the year 2015 -6.0 wt % of hydrogen in gravimetric capacity-.

In order to characterize the  $H_2$ -metal interaction, 3d TM (Sc, Ti, V) bounded to  $C_xH_x$  ( $x = 4, 5$ ) molecules and lithium atoms interacting with  $C_5H_5$ ,  $C_5F_5$  and  $B_3N_3H_6$  are studied in this work. DFT



calculations suggest that Li binds weakly to  $C_5H_5$  and  $B_3N_3H_6$ , but strongly to  $C_5F_5$  (3.03 eV), this is comparable to the binding energy of Li to boron-carbon nanotubes (~ 2.7 eV). While for Sc, Ti and V the first  $H_2$  molecule dissociates to form hydride bonds, Li- $C_5F_5$  adsorbs  $H_2$  molecularly. The adsorption energy of  $H_2$  on the studied structures is in the range of 0.10-0.6 eV, which would be suitable for reversible  $H_2$  adsorption/desorption at near ambient conditions.

*Figure 1. Optimized geometries of Sc-C5H5-(H2)<sub>n</sub> (n=1-5) and Ti-C4H4-(H2)<sub>5</sub>.*

<sup>1</sup> Y. Zhao, Y.H. Kim, A.C. Dillon, M.J. Heben, S.B. Zhang, "Hydrogen storage in novel organometallic buckyballs", Phys. Rev. Lett. 94 (2005) 155504.

## Photoluminescence from Si Nanocrystals in a SiO<sub>2</sub> Matrix Deposited by Reactive Sputtering

J. Carrillo López<sup>1\*</sup>, G. García Salgado<sup>1</sup>, and M. Meléndez Lira<sup>2</sup>

<sup>1</sup>*Centro de Investigación en Dispositivos Semiconductores-ICUAP, BUAP.*

*Av. San Claudio y 14 Sur Colonia San Manuel, C.P. 72570, Puebla, Mexico.*

<sup>2</sup>*Departamento de Física-CINVESTAV. Av. IPN 2508, San Pedro Zacatenco, 07360 Mexico D.F., Mexico.*

\*e-mail: jecarril@siu.buap.mx

The optical properties of Si nanocrystals in SiO<sub>2</sub> have been studied extensively since visible room temperature photoluminescence (PL) was first observed in such systems<sup>1</sup>. However, despite intense study, the physical origins of the PL remain unclear. For example, some researchers explain their results using a three-dimension quantum confinement model<sup>2</sup>, while others believe that interface defects and defect centres outside the nanocrystal are responsible for PL emission<sup>3</sup>. In this paper, the dependence of the PL from Si nanocrystals embedded in a SiO<sub>2</sub> matrix deposited by reactive sputtering and after annealing is presented. Red PL has been observed at room temperature from deposited films, before and after annealing. The intensity of the A band shows dependence on the temperature and time of annealing. Fourier transform infrared (FTIR) spectra are used to discuss the emission mechanisms.

*We acknowledge the partial financial support of VIEP-BUAP through the project 06/EXC/06-G.*

---

<sup>1</sup> L.T Cahnam, Appl. Phys. Lett. 57 (1990) 1046.

<sup>2</sup> Y. Maeda, Phys. Rev. B 51 (1995) 1658.

<sup>3</sup> F. Flores, M. Aceves, J. Carrillo, C. Domínguez, C. Falcony, Superficies y Vacío 18(2) (2005) 7.

## Nanoparticles of Rhodium for Catalytic Wet Air Oxidation of Gasoline Additives

I. Cuauhtémoc<sup>1</sup>, G. Del Angel<sup>1\*</sup>, G. Torres<sup>2</sup>, and V. Bertin<sup>1</sup>

(1) *Universidad Autónoma Metropolitana-Iztapalapa, Laboratorio de Catálisis, Departamento de Química, DCBI, Av. San Rafael Atlixco No. 186, CP 09340, Mexico DF, Mexico.*

(2) *Universidad Juárez Autónoma de Tabasco, Laboratorio de catálisis heterogénea, Área de Química, DACB, Km.-1 carretera Cunduacán-Jalpa de Méndez AP. 24, C.P. 86690, Cunduacán Tabasco, Mexico.*

\*e-mail: gdam@xanum.uam.mx

Nanoparticles of Rhodium were deposited on  $\gamma\text{-Al}_2\text{O}_3$  and  $\gamma\text{-Al}_2\text{O}_3\text{-CeO}_2$  supports. These materials were characterized with techniques of BET areas, TPR, TPD and XPS. The results showed low superficial areas as a function of the Ce load. The particle sizes were distributed in the range of 1 to 3 nm in diameter. The XPS spectroscopy characterization showed the presence of  $\text{Rh}^{\delta+}$  and  $\text{Ce}^{4+}$ , this last specie increase with the increase of Ce loading. The Rh nanoparticles supported on  $\gamma\text{-Al}_2\text{O}_3\text{-CeO}_2$  were tested for the catalytic wet air oxidation of gasoline additives as ETBE and TAME. Catalytic Wet Air Oxidation of gasoline ETBE and TAME were carried out in a Parr reactor at 100°C, 120°C and 150°C using oxygen as oxidant source at 10 bar of pressure. Cerium emphasizes the oxidative capacity of the Rhodium nanoparticles<sup>1</sup> at 100°C in both reactions. In these reactions, the addition of Cerium to  $\text{Rh}/\gamma\text{-Al}_2\text{O}_3$  improved the selectivity to  $\text{CO}_2$ , due to support-metal interaction,  $\text{Ce}^{4+}\text{-O}^{2-}\text{-M}^{+2}$ .

*We thank for to the National Council of Science and Technology of Mexico CONACYT for the financing of project No. 46689 for the accomplishment of this work and the scholarship for the Mr. Ignacio Cuauhtémoc Lopez.*

---

<sup>1</sup> Z. L. Zhang, V. A. Tsipouriari, A. M. Efstathiou, *J Catal*, 158 (1996) 51.

<sup>2</sup> S. Hosokawa, H. Kanai, K. Utani, Y. I. Taniguchi, Y. Saito, S. Imamura, *Appl. Catal. B: Environmental*, 43 (2003) 181.

## **Molecular Hydrogen Adsorption upon the Fullerene Hemisphere for the (5,5) Carbon Nanotube**

J. S. Arellano

*Area de Física Atómica Molecular Aplicada, División de Ciencias Básicas e Ingeniería, UAM-Azcapotzalco. Av. San Pablo No. 180. Mexico 02200, D.F. Mexico.*

e-mail: jsap@correo.azc.uam.mx

It is studied the adsorption of metallic hydrogen along the axis of the (5,5) carbon nanotube when each extreme of the nanotube is joined with a fullerene hemisphere. It has been considered a total of 140 carbon atoms for the system, besides the hydrogen molecule. The basis of the study is Density Functional Theory, as implemented in fhi98md code. This code has been used to obtain the total energy of the system, as a function of the relative distance between the hydrogen molecule and the nearest carbon of the fullerene hemisphere. Previously we have studied the atomic and molecular hydrogen adsorption on a graphene layer and outside and inside the (5,5) and (6,6) carbon nanotubes. In view of those results, and because the diameter of the (5,5) carbon nanotube is less than for (6,6) carbon nanotube, it was expected a barrier energy for the hydrogen adsorption along the axis of the nanotube. This has been confirmed with the calculations and it is made a comparison between the barrier energy found for the lateral insertion, through an hexagonal cavity of the nanotube wall and for the insertion through the pentagonal cavity of the fullerene hemisphere. To explain the barrier energy for the hydrogen adsorption in the later case, there has been obtained the total energy curves when it is considered only 1, 2 or 3 carbon rings of the fullerene hemisphere. These rings are formed respectively by 5, 5 and 10 carbon atoms. The obtained barrier energy is around 2.25 a.u.

## **Photocatalytic Activity under VIS-Irradiation of Nanoparticles of $\text{Bi}_2\text{Mo}_3\text{O}_{12}$ Prepared by an Amorphous Complex Precursor**

A. Martínez-de la Cruz<sup>1\*</sup>, S. Marcos Villarreal<sup>1</sup>, E. López Cuéllar<sup>1</sup>,  
U. Oriz Méndez<sup>1</sup>, and Leticia M. Torres-Martínez<sup>2</sup>

<sup>1</sup>*Facultad de Ingeniería Mecánica y Eléctrica, Universidad Autónoma de Nuevo León,  
Ciudad Universitaria, C.P. 66451, San Nicolás de los Garza, N.L., Mexico.*

<sup>2</sup>*Departamento de Ecomateriales y Energía, Universidad Autónoma de Nuevo León,  
Ciudad Universitaria, C.P. 66451, San Nicolás de los Garza, N.L., Mexico.*

\*e-mail: azmartin@gama.fime.uanl.mx

In the last decades, heterogeneous photocatalysis has been positioned as a promissory efficient technology to resolve problems associated with environmental and energy. The so-called soft chemistry methods have shown to be efficient to prepare better photocatalysts than those synthesized by classical methods.

In this work, we have synthesised nanoparticles of  $\text{Bi}_2\text{Mo}_3\text{O}_{12}$  prepared by using the respective salts solutions of the ions involved and diethylenetriaminepentaacetic acid ( $\text{H}_5\text{TDPA}$ ) as chelating agent. Thermal treatments at 350, 400, 450, 500, 600 and 700 °C were employed in order to check the formation of  $\text{Bi}_2\text{Mo}_3\text{O}_{12}$  from low temperatures. The effects of calcination temperature on the morphology, surface area and properties of  $\text{Bi}_2\text{Mo}_3\text{O}_{12}$  nanoparticles have been investigated in detail. The photocatalytic activity of  $\text{Bi}_2\text{Mo}_3\text{O}_{12}$  nanoparticles was evaluated by degradation of rhodamine B molecules in water under visible light irradiation. The kinetic degradation of rhodamine B followed a first order reaction with  $k = 1.36 \times 10^{-2} \text{ min}^{-1}$  and  $t_{1/2} = 51.1 \text{ min}$  for the best material obtained.

*We wish to thank to CONACYT for supporting the project 43800 and the UANL for its support through the project PAICYT-2006.*

**Assembly of Bromobenzethiol Functionalized Gold Nanoparticles with the  
Fluorescent Poly(Phenyleneethynylene) pPET3OC12-sqS for the Detection  
and Attack to the Fungus *Paecilomyces Variotii***

J. C. Ramos<sup>1,2\*</sup>, E. Vázquez<sup>1</sup>, A. Ledezma<sup>1</sup>, D. I. Medellín, I. Moggio<sup>1</sup>, E. Arias<sup>1</sup>,  
C. Martínez<sup>2</sup>, J. Romero<sup>1</sup>, and P. García<sup>2</sup>

<sup>1</sup>CIQA, Boulevard Enrique Reyna 140, 25253 Saltillo, Mexico.

<sup>2</sup>Universidad Autónoma de Ciudad Juárez, Henry Dunant 4016, C.P. 32310, Ciudad Juárez,  
Mexico.

\*e-mail: juankarlosramos@hotmail.com Tel. 0052 656 688 48 00 Ext. 4571.

Bromobenzethiol functionalized gold nanoparticles have been synthesized by the phase transfer method and mixed in solution with the fluorescent poly(phenyleneethynylene) pPET3OC12-sqS. Thin films have been prepared by self assembly on quartz and glass slides in order to develop a biosensor, which could not only detect the fungus *P. variotii* by the emission of the polymer but also attack it by profiting the fungicidal effect of the gold nanoparticles. The spectroscopic characterization of the films by UV-Vis and fluorescence spectroscopy before and after its immersion in the *P. variotii* culture reveals a net decrease of the emission that can be related to the detection of the fungus. The microscopic characterization by optical and laser confocal microscopy of the samples after the microbiological tests indicates a lyses with formation of pores and total collapses on the fungical mycelium according to our hypothesis that gold nanoparticles could attack the fungus cells.

**Keywords:** poly(phenyleneethynylene), gold nanoparticles, thin films, *P. variotii*.

*We acknowledge financial support by SEP-CONACyT (43166-R project).*



## Energy Transfer Driven Visible Upconversion in $\text{Y}_2\text{O}_3:\text{Yb}^{3+},\text{Er}^{3+}$ Nanorods

O. Meza,<sup>1</sup> LA Diaz-Torres,<sup>1,\*</sup> P Salas,<sup>2</sup> C. Angeles-Chavez,<sup>2</sup>

A. Martinez,<sup>3</sup> E. de la Rosa,<sup>1</sup> and J. Morales<sup>3</sup>

<sup>1</sup> Centro de Investigaciones en Optica A.C. Departamento de Fotonica, C.P. 37150 Leon, Gto., Mexico.

<sup>2</sup> Instituto Mexicano del Petroleo, Programa de Simulación Molecular, C.P. 07730, Mexico, D.F.

<sup>3</sup> Universidad Autonoma Metropolitana-Azcapotzalco, DCBI-Ciencias básicas, c.p. 02200 Mexico D.F.

\*e-mail: ditlacio@cio.mx

Codoped Yb-Er nanophosphors have a broad range of potential applications from Displays to High Power lasers. The main characteristic of this codoped nanophosphors is the possibility of generate visible Green, red, and even blue upconversion emission besides the usual 1.03 and 1.5  $\mu\text{m}$  NIR emissions from Yb and Er, respectively. In recent years many nanocrystalline materials

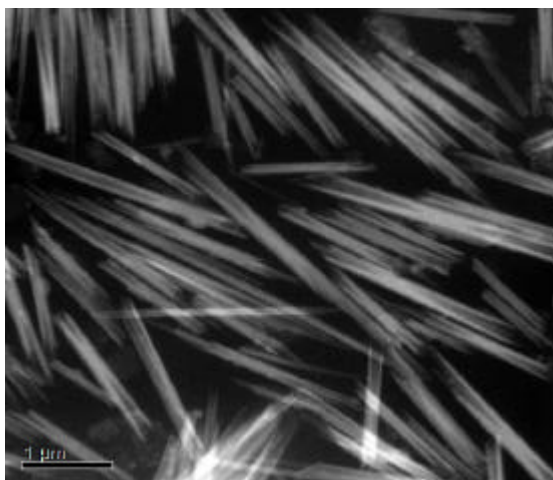


Figure 1. TEM image of  $\text{Y}_2\text{O}_3:\text{Yb}(2\%),\text{Er}(1\%)$  nanorods

have been proposed has efficient upconverters, among these, the nanosized cubic sesquioxide  $\text{Y}_2\text{O}_3$  has proved to be one of the best candidates for High Power laser generation. The performance of sinterized ceramic of such nanosized phosphors depends both on the morphology of the nanoparticles and on the energy transfer processes that lead to the upconverted emission under NIR excitation. In this work we present the fluorescence characterization of nanocrystalline codoped  $\text{Y}_2\text{O}_3:\text{Yb}^{3+},\text{Er}^{3+}$  with to different morphologies: arbitrary shape and Rods. An estimation of the upconversion parameters for both morphologies and their corresponding efficiencies are compared and discussed.

This work was partly supported by CONACYT trough grants 46971-F and 43168-F. O. Meza. Perez acknowledges CONACYT by a PhD scholarship at Centro de Investigaciones en Optica A.C.

## Preparation and Study of Magnetic – Optically Transparent Nanocomposites

M. Garza<sup>1\*</sup>, M. Hinojosa<sup>1</sup>, and V. González<sup>1</sup>

<sup>1</sup> *Facultad de Ingeniería Mecánica y Eléctrica, Universidad Autónoma de Nuevo León,  
C. P. 66451, San Nicolás de los Garza, Nuevo León, Mexico.*

\*e-mail: ingmarcogarza@gmail.com

The preparation of optically transparent magnetic chitosan/magnetite nanocomposite films is reported. Nanocomposite films were prepared by *in-situ* co-precipitation process of ferrous chloride ( $\text{FeCl}_2$ ) and ferric chloride ( $\text{FeCl}_3$ ) into a low molecular weight chitosan matrix, in the necessary proportion to obtain, under NaOH addition, chitosan/magnetite nanocomposites at weight ratios of 25/75, 50/50 and 75/25. After solvent evaporation at room temperature, 6 cm diameter circular films were obtained. To these films were added concentrate sodium hydroxide aqueous dissolutions to obtain 0.1 gr of each nanocomposite. The resultant darkish nanocomposite films were dissolved in formic acid to obtain dissolutions, which were putted into a Petri dish in order to evaporate the dissolved at room conditions, obtaining 6 cm diameter reddish – transparent films. The studies performed to the crystalline structure of the dispersed phase using transmission electron microscopy (TEM) micrographs and selected area electron diffraction (SAED) suggest, that even after dissolved nanocomposite samples, the magnetite phase remains stabilized by the chitosan matrix, resulting onion-like arrangements of the polymer chains surrounding magnetite nanoparticles. Magnetization – temperature dependent (M-T) measurements at zero field cooling (ZFC) and field cooling (FC), as well as magnetization – applied field (M-H) hysteresis loops depicts that the magnetic character of nanocomposite materials can be well describe as paramagnetic with partial antiferromagnetic coupling.

*We acknowledge the partial financial support of CONACYT and PAICYT, Mexico, as well as the assistance from R. Escudero and M. Yacamán.*

## The Monitoring of Process of Laser Irradiation of Si-Al<sub>2</sub>O<sub>3</sub> Sandwich Target

M. Vlasova<sup>1</sup>, P. A. Márquez Aguilar<sup>1\*</sup>, M. C. Reséndiz-González<sup>1</sup>, I. González Morales<sup>1</sup>, M. Kakazey<sup>1</sup>, V. Stetsenko<sup>2</sup>, T. Tomila<sup>2</sup>, and A. Ragulua<sup>2</sup>

<sup>1</sup>*The Autonomous University of the State of Morelos, Av. Universidad, 1001, Cuernavaca, Mexico.*

<sup>2</sup>*The Institute for Problems of Materials Science, National Academy of Sciences of Ukraine, Str. Krzhizhanovskogo 3, Kiev, 252680, Ukraine.*

\*e-mail: pmarquez@uaem.mx

The purpose of this work is a study of the special features of shaping of nano-films and their morphology, formed by the products of the ablation of silicon and oxide of aluminum during the intensive and continuous laser irradiation in the nitrogen atmosphere. Data of study can be useful for creating the films with the specific electrophysical and optical properties.

By methods of electron microscopy, atomic force microscopy, X-ray microanalysis, IR-spectroscopy the influence of continuous IR laser irradiation ( $\lambda = 1064$  nm,  $P = 210$  W) on Si-Al<sub>2</sub>O<sub>3</sub> target is investigated.

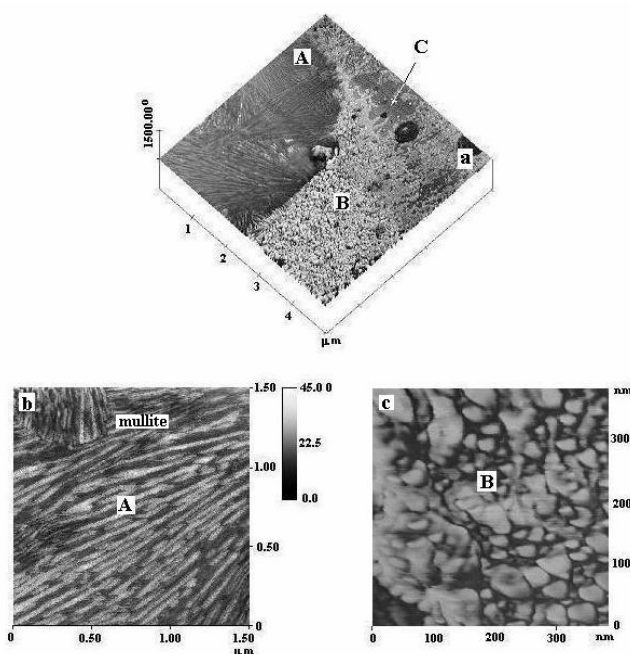


**Fig. 1.** AFM images in regime of phase the surface of precipitated film (a). (b) image in region A; (c) image in region (B).

We acknowledge the partial financial supports of CONACyT through the grant #48361.

The irradiation was in O<sub>2</sub> + N<sub>2</sub> medium. It is established that on the surface of target at first the process of the melting, evaporation and oxidation of Si take place. Then the interaction of Al<sub>2</sub>O<sub>3</sub> with SiO<sub>2</sub> is realized. On a surface of collection plate a nano-film is formed. Its composition and morphology reflects stages of a heating, melting, and evaporation both a separate layers of a target, and products of their interaction. Besides SiO<sub>2</sub>, in a film the mullite is present.

## **Study of the Mobility of DR1 Molecules Embedded in Amorphous and Nanostructured PMMA Films**

**J. García-Macedo<sup>1\*</sup>, A. Franco<sup>1</sup>, and C. Aguilar-Gutiérrez<sup>1</sup>.**

*1. Departamento de Estado Sólido, Instituto de Física, Universidad Nacional Autónoma de Mexico, Mexico, D.F. C.P. 04510.*

\*e-mail: gamaj@fisica.unam.mx

Kinetics of the orientation of Disperse Red 1 (DR1) molecules embedded in amorphous and nanostructured Polymethylmetacrylate (PMMA) films under the effect of a strong constant electric poling field was studied. The changes in the orientation distribution of the DR1 molecules were followed by Second Harmonic Generation (SHG) measurements. The SHG signal was recorded as function of time at three different temperatures. We considered two cases: the signal increment under the presence of the poling field and the signal decay without the poling field. The nanostructured PMMA films were templated by the incorporation of the two different ionic surfactants, Sodium Dodecyl Sulfate (SDS) and Cetyltrimethyl Ammonium Bromide (CTAB). The structure of the films was determined by means of Xray diffraction (XRD) measurements. Substantial differences in the intensity of the signal and in growth and decay rates were detected between amorphous and nanostructured films. Some comparisons are presented with results from SiO<sub>2</sub>:DR1 films.

*We acknowledge the financial support of CONACyT 43226-F, NSF-CONACyT, PUNTA, PAPIIT 116506-3. The authors are thankful to M. Sc. Manuel Aguilar-Franco (XRD) for technical assistance.*

## Optical Macroscopic Birefringence in Anisotropic Silver Nanoparticles

J. A. Reyes-Esqueda<sup>1\*</sup>, C. Torres-Torres<sup>1</sup>, J. C. Cheang-Wong<sup>1</sup>, A. Crespo<sup>1</sup>, L. Rodríguez-Fernández<sup>1</sup>, C. Noguez<sup>1</sup>, and A. Oliver<sup>1</sup>

<sup>1</sup> *Instituto de Física, Universidad Nacional Autónoma de México, México, D. F. 04510.*

\*e-mail: reyes@fisica.unam.mx

MeV silver ions have been implanted in silica plates, leading to the formation of silver nanoparticles embedded in silica. To a first approximation, the shape of these particles can be considered essentially spherical, giving an isotropic nanocomposite. By means of a subsequent Si ion irradiation, these Ag nanoparticles have been deformed into anisotropic particles. As a result of the Si irradiation, we succeeded in obtaining an anisotropic system composed of oriented Ag nanoellipsoids<sup>1</sup>. The major axis of these ellipsoids are oriented along the ion beam direction, and in consequence their optical response exhibits two optical surface plasmon resonances, each one associated with the two main axes of the ellipsoid. This splitting of the surface plasmon resonance into two contributions depends on the fluence of the ion irradiation.

Therefore, in this work, we have measured the optical birefringence of these nanocomposites with an ellipsometric technique using wavelengths close to both resonances, allowing us to quantify the light transmission through our samples when placed and rotated between crossed polarizers. This birefringence can be physically associated with the selective optical absorption of one component of the linear polarization of the incident light with respect to the anisotropic axis of the sample, depending on the wavelength used to perform the measurement.

*We acknowledge the partial financial supports from DGAPA-UNAM, through grants No. IN108807-3, No. IN101605, No. IN119706-3 and No. IN108407; and CONACyT-Mexico, through grants No. 42823-F, No. 44306-F, No. 42626-F and No. 50504.*

---

<sup>1</sup> A. Oliver et al, "Controlled anisotropic deformation of Ag nanoparticles by Si ion irradiation". PRB **74** (2006) 245425.

## Green Synthesis of Au and Ag Nanoparticles

J. García-Serrano<sup>1\*</sup>, A. M. Herrera<sup>1</sup>, P. Salas<sup>2</sup>, C. Ángeles-Chávez<sup>2</sup>, and U. Pal<sup>3</sup>

<sup>1</sup> *Centro de Investigaciones en Materiales y Metalurgia, Universidad Autónoma del Estado de Hidalgo, Carretera Pachuca Tulancingo Km 4.5, Pachuca, Hidalgo, Mexico.*

<sup>2</sup> *Instituto Mexicano del Petróleo, Eje Central Lázaro Cárdenas 152, C.P. 07730, Mexico.*

<sup>3</sup> *Instituto de Física, Universidad Autónoma de Puebla, Apdo. Postal J-48, Puebla, Pue. 72570, Mexico.*

\*e-mail: jserrano@uaeh.reduaeh.mx

In the last few decades, much effort has been devoted to the studies of metal nanoparticles, due to their unique properties and potential applications in nanotechnology.<sup>1</sup> We report on the use of aqueous solutions of ionic polymers containing arsonic acid groups for the green synthesis of Au and Ag nanoparticles at ambient temperature without using additional reducing reagent. The results indicate that these ionic polymers not only are capable of reducing metal ions, but also can protect the nanoparticles in the colloidal solutions. In general, the process of metal ions reduction using these ionic polymers is very slow, but the ability of the polymers to protect the Au and Ag nanoparticles permits to obtain colloidal solutions which are stable for several months. This method would be very much helpful for the preparation of other metal nanoparticles.

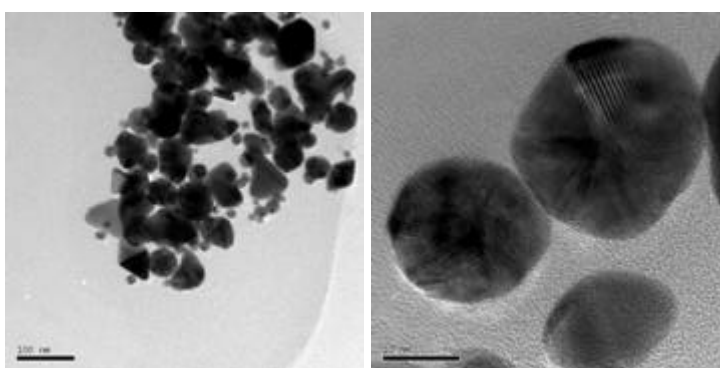


*Figure 1. Typical TEM micrographs of Au nanoparticles prepared in H<sub>2</sub>O at room temperature.*

---

<sup>1</sup> V.M. Rotello, *Nanoparticles: Building Blocks for Nanotechnology*; Kluwer Academic Publishers, New York, 2004.

## On the Homogenization of 1D Phononic Crystals

J. Flores-Méndez and F. Pérez-Rodríguez\*

*Instituto de Física, Universidad Autónoma de Puebla,  
Apdo. Post. J-48, Puebla, Pue. 72570, Mexico.*

\*e-mail: fperez@sirio.ifuap.buap.mx

We have developed a new method for calculating the effective sound velocities in a 1D phononic crystal when the lattice constant is much smaller than the acoustic wave length and, therefore, the periodic medium can be regarded as a homogeneous one. The method is based on the expansion of the displacements field into Bloch waves. The expansion allows us to obtain a wave equation for the amplitude of the macroscopic displacements field. From the form of this equation we identify the effective parameters, namely the effective sound velocities for the transverse and longitudinal macroscopic displacements in the homogenized 1D phononic crystal. We have obtained explicit expressions for the effective sound velocities in terms of the parameters of the inclusions in the unit cell: mass density, transverse and longitudinal elastic moduli. We have used these expressions for studying the dependence of the effective, transverse and longitudinal, sound velocities upon the filling fraction for a binary 1D phononic crystal. In particular, we will present results for 1D phononic crystals composed of Al/W and Si/Polyethylene.

*We acknowledge the partial support from CONACYT, Mexico, through the grant SEP-2004-C01-46425.*

## Optical Properties of Disordered Multilayer: A comparison of Periodic, Quasi-periodic and Random Multilayer Heterostructures

B. Alvarado Tenorio and V. Agarwal\*

Centro de Investigación en Ingeniería y Ciencias Aplicadas (CIICAp)-Universidad Autónoma del Estado de Morelos, Av. Universidad 1001, col. Chamilpa, CP 62209, Cuernavaca Morelos, Mexico.

\*e-mail Corresponding author : vagarwal@uaem.mx

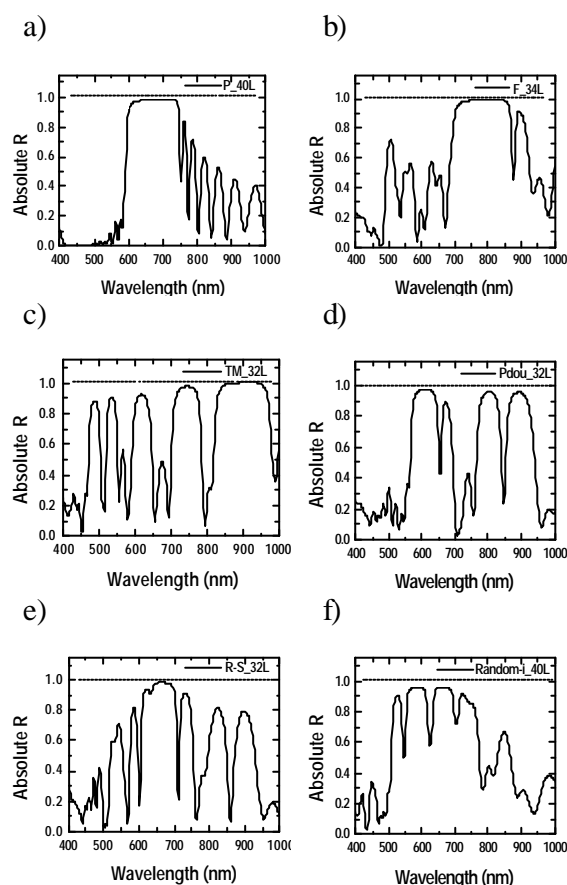


Figure 1. Reflectance spectrum of (a) Periodic, (b) Fibonacci, (c) Thue-Morse, (d) Period doubling, (e) Rudin Shapiro and (f) Random photonic bandgap structures with  $nd=1/4$ , for 650 nm of wavelength.

In recent years, there has been much interest in the photonic applications of porous silicon<sup>1</sup> (PS). The high optical sensitivity of PS due to its large surface area has attracted the attention as a promising material for photonic devices like Bragg filters and optical microcavities.<sup>2</sup> We report the fabrication and analysis of the optical properties of one dimensional Quasi-periodic (Fibonacci, Thue–Morse, Period doubling and Rudin Shapiro) and Random PS-based heterostructures. The comparison with the periodic structures is also done. All multilayered heterostructures were fabricated by the porous silicon layers (A and B) having the refractive indices of  $n_a=1.2$  and  $n_b=2$ , except for the Rudin Shapiro heterostructure where four different refractive indices were required (A, B, C and D layers) with  $n_a=2$ ,  $n_b=1.7$ ,  $n_c=1.1$  and  $n_d=1.5$  respectively. In Figure 1, the reflectance spectrum of the Quasi-periodic and Random photonic band gap structures with  $nd=\lambda/4$  for 650 nm shows many narrow resonances, which can localize the light very effectively. The high quality optical responses are relevant for its application in optical interferometric biosensors.

<sup>1</sup> Mulloni.; Pavesi, L., "Porous Silicon as Optical Chemical sensors". Appl.Phys. Lett. **76** (2000) 2523

<sup>2</sup> L. Pancheri, C.J. Oton, Z. Gaburro, G. Soncini, and L. Pavesi "Very Sensitive Porous Silicon NO<sub>2</sub> Sensor ". Sens. Actuators B **89** (2003) 237.



## Ab-Initio Calculations in Small Gadolinium Systems

J.F. Rivas-Silva<sup>1</sup>, T. Delgado-Vitols<sup>2</sup>, and M. Berrondo<sup>3</sup>.

<sup>1</sup> *Instituto de Física de la BUAP, Apdo. Postal J-48, Puebla, Pue. 72570 Mexico.*

<sup>2</sup> *Departamento de Computación, Electrónica, Física e Innovación, UDLA, Santa Catarina  
Mártir s/n, Cholula, Puebla, Mexico.*

<sup>3</sup> *Dept. of Physics and Astronomy, Brigham Young University, Utah, USA.*

\*e-mail: [rivas@sirio.ifuap.buap.mx](mailto:rivas@sirio.ifuap.buap.mx)

The study of nanoparticles made with rare-earth elements is important in some applications that take advantage of their magnetic properties. Since a theoretical point of view, working with those elements confronts special challenges due to the high correlated electronic f levels. In this work we show that the *ab initio* standard DFT (density functional theory) approach to calculate the electronic structure of systems will contain a systematic error in handling clusters of Gd atoms, by its lack to take into account correctly the high correlations effects of those levels. This error can be traced since the smallest clusters: Gd, Gd<sub>2</sub>, Gd<sub>3</sub>, etc. We used for this purpose the Gaussian, ADF, and LMTO+U codes.

*We acknowledge to VIEP-BUAP for the financial support.*

## Nanoparticles from a Cu-Zn-Al Shape Memory Alloy, Physically Synthesized

L. López Pavon<sup>1</sup>, E. López Cuéllar<sup>1\*</sup>, A. Torres Castro<sup>1</sup>, A.M. Condó<sup>2</sup>,  
U. Ortiz Mendez<sup>1</sup>, and M. José-Yacamán<sup>3</sup>

<sup>1</sup> FIME, Universidad Autónoma de Nuevo León, A.P. 076 Suc. "F", Cd. Universitaria C.P. 66450, San Nicolás de los Garza, N.L., Mexico.

<sup>2</sup> Centro Atómico Bariloche, CONICET, 8400 San Carlos Bariloche, Argentina.

<sup>3</sup> Department of Chemical Engineering, The University of Texas at Austin, 1 University Station C0400, Austin, TX 78712-1062, USA.

\*e-mail: lopezcuellar@gama.fime.uanl.mx

Recent works of nanoparticle synthesis from a TiNi shape memory alloy by physical etching have been done. These results have shown that this method of synthesis produce nanoparticles with a homogenous particle size distribution between 2-3 nm of diameter. Moreover the obtained nanoparticles seem to keep their crystal structure suffering a small decrease in the lattice parameter and possibly a composition variation. In this work, the results of the synthesis of CuZnAl nanoparticles by Ar<sup>+</sup> beam etching following the same procedure reported in previous works are presented. Nanoparticles were obtained from targets of CuZnAl originally presenting the shape memory effect. Two different compositions were used, sample A of 75.22Cu 17.12Zn 7.66Al at% with an Ms of ~10°C and sample B of 76.18Cu 15.84Zn 7.98Al at% with an Ms of ~20 °C. Nanoparticles were characterized by Scanning Transmission Electron Microscopy (STEM), High Resolution Transmission Electron Microscopy (HRTEM), High Angle Annular Dark Field (HAADF), Electron Diffraction (ED), Energy Dispersive X-ray Spectroscopy (EDXS) and images simulation. Results of morphology, composition and crystal structure are discussed, and are in agreement with results reported before for the TiNi alloy.

*We acknowledge the partial financial supports of CONACyT through the grants for PhD #55899, of UANL for the grant Paycit CA1269-06, and the UT of Texas for their technical support.*

## **Estudio del Auto-ensamble de Cúmulos de Oro por Coalescencia: Interacción e Impactos**

**J. Antúñez García<sup>1\*</sup>, S. Mejía Rosales<sup>1</sup>, E. Pérez Tijerina<sup>1</sup>, and M. José Yacamán<sup>2</sup>**

<sup>1</sup>*Postgrado en Ingeniería Física Industrial, FCFM, UANL, San Nicolás de los Garza,  
N. L. 66450 Mexico.*

<sup>2</sup>*Department of Chemical Engineering, The University of Texas at Austin, Austin, TX 78712 USA.*

\*e-mail: jantunez@fcfm.uanl.mx

Hoy en día se conoce que átomos de algún elemento o aleación dispuestos en estructuras de tamaño nanométrico, presentan propiedades distintas a las observadas en bulto. Por otro lado, estas propiedades pueden ser sintonizadas si el tamaño o la geometría de tales estructuras son modificadas. En la actualidad, se ha logrado por diferentes métodos tanto físicos como químicos, disponer de manera ordenada nanopartículas de tamaño y forma similar. Sin embargo, tales tamaños son relativamente grandes ( $>100$  nm), y sólo hasta el momento, para ciertos elementos (*i.e.* Si, Au, etc). De manera más general, diferentes métodos experimentales arrojan partículas de tamaño nanométrico con diferentes dispersiones en tamaños y geometrías. A pesar de ello aparecen ciertas estructuras que se distinguen muy por encima de las demás, dentro de ellas la icosaedra. Es claro entonces, que existen ciertos parámetros que no dependen de las particularidades experimentales bajo las cuales estas estructuras aparecen. El estudio del auto-ensamble de pequeños cúmulos atómicos, puede ayudar a comprender la fenomenología involucrada en la formación de una estructura y las condiciones propicias para su aparición. Con tal finalidad, en el actual trabajo se discuten los resultados de simulaciones de dinámica molecular obtenidos considerando dos casos: a) coalescencia por interacción de dos cúmulos cercanos y b) por impacto. Para ello, cada sistema fue sujeto a una variedad de condiciones iniciales tales como orientación relativa entre partículas, temperatura de termalización y velocidad relativa de impacto. Las geometrías elegidas en el estudio fueron dos: una partícula icosaedra con 147 átomos (ó de tercer orden) y una partícula esférica obtenida de una red fcc de 142 átomos. Bajo las condiciones consideradas, nuestros resultados muestran en la mayoría de los casos la aparición de una nueva partícula con una clara tendencia a un icosaedro de cuarto orden. Adicionalmente encontramos de manera singular, un nanorod coaxial quiral con número de átomos por capa 18-12-6-1 equivalente a uno de los obtenidos por optimización en términos de algoritmos genéticos<sup>1</sup> y similar a los observados experimentalmente para Oro<sup>2</sup>.

*Agradecemos al CONACYT el apoyo financiero otorgado para el proyecto NL-2004-C05-60 y a The University of Texas at Austin por el tiempo de computo otorgado.*

<sup>1</sup> B. Wang, S. Yin, G. Wuang, A. Buldum, and J. Zhao, PRL **86**, 2046 (2001).

<sup>2</sup> Y. Kondo and K. Takayanagi, Science **289**, 606 (2000).

## DFT Study of $\text{Au}_N$ Icosahedral Cage-like Clusters

José Luis Rodríguez-López

*División de Materiales Avanzados, IPICYT, Camino Presa Sn. José 2055, Lomas 4a Secc.*

*78216, San Luis Potosí, SLP, Mexico.*

e-mail: jlrdez@ipicyt.edu.mx

Cagelike clusters with icosahedra ( $I_h$ ) symmetry are studied in the framework of Density Functional Theory (DFT) and pseudopotentials scheme. Full relaxed geometries, stability and electronic structure for neutral, anionic and cationic clusters are discussed in the intermediate size range of  $\text{Au}_N$  clusters ( $N = 32, 42, 72, 92, \& 162$  atoms). We have found that energy stability decreases as the cluster size increases, but with the inclusion of  $\text{Au}_{72}$  atoms cluster we extend the candidates list for possible stable cagelike clusters previously reported. Also, excellent agreement with these previous DFT studies applied to  $\text{Au}_{32}$  and  $\text{Au}_{42}$  clusters is found.

Although still there is not any experimental report of these structures, the present study is included in the new trend of fullerene-like, non-carbon results previously reported for B, Al & Au systems. Discussion on the stability and experimental searches of these systems are addressed.

## Silver Core-Silver Oxide Shell Nanoparticles Embedded in Mesostructured Silica Films

G. Valverde-Aguilar<sup>1</sup>, J. A. García-Macedo<sup>1\*</sup>, and V. Rentería<sup>1</sup>

<sup>1</sup>*Departamento de Estado Sólido. Instituto de Física, Universidad Nacional Autónoma de México. 04510 Mexico D.F., Mexico.*

\*e-mail: gamaj@fisica.unam.mx

Silver nanoparticles were obtained by spontaneous reduction process of  $\text{Ag}^+$  ions to metallic silver nanoparticles ( $\text{Ag}^0$ ). A hexagonal mesostructured sol-gel films were prepared by dip-coating method by using the non-ionic diblock copolymer (Brij58) to produced channels into the film, which house the silver nanoparticles. The optical properties of the metallic nanoparticles were studied by UV-vis spectroscopy and HRTEM images. The experimental absorption spectrum of silver metallic nanoparticles exhibits an absorption band located at 438 nm and a shoulder at longer wavelength. The HRTEM images show silver nanoparticles randomly distributed (Type I) and silver nanoparticles oriented as long line (Type II), both distributions possess a silver oxide shell around of them. The optical absorption spectrum was modeled using the Gans theory. It shows two main contributions related to metallic silver nanoparticles with different axial ratio surrounding of a dielectric medium with high refractive index. This index is justified due to the presence of the silver oxide shell. This study shows that the metallic surface of the nanoparticles, play an important role on the optical properties of the mesostructured sol-gel silica films.

*We acknowledge the financial supports of CONACYT 43226-F, NSF-CONACYT, PUNTA and PAPIIT 116506-3. GVA and VRT are grateful for CONACYT postdoctoral fellowships. The authors are thankful to M. in Sci. Manuel Aguilar-Franco (XRD) for technical assistance.*

## Gold Nanoparticles on Titania Mixed Oxides: Influence of the Support on the Gold Growth

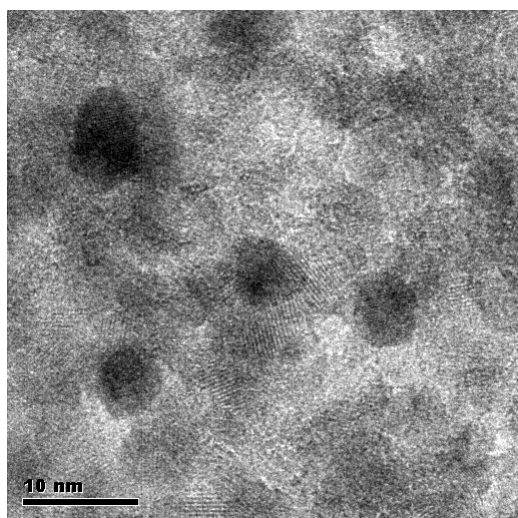
V. Rodríguez-González<sup>1</sup>, J. Navarrete<sup>1</sup>, F. M. Morán-Pineda<sup>1</sup>,  
B. Cerón<sup>1</sup>, and R. Gómez<sup>2\*</sup>

<sup>1</sup>*Instituto Mexicano del Petróleo, Dirección de Investigación y Postgrado / Eje Central 152,  
07730 Mexico D. F., Mexico.*

<sup>2</sup>*Universidad Autónoma Metropolitana-I, Depto. de Química/Av. San Rafael Atlixco No 186,  
09340 Mexico D.F., México.*

\*e-mail: vrgonzal@imp.mx

The present paper reports findings in the preparation and characterization of Au nanoparticles deposited over supported over TiO<sub>2</sub>, TiO<sub>2</sub>-Al<sub>2</sub>O<sub>3</sub> and TiO<sub>2</sub>-In<sub>2</sub>O<sub>3</sub>. The gold nanoparticles were prepared by the deposition-precipitation method with urea<sup>1</sup> and the supports by controlled sol-gel method.<sup>2</sup> Gold nanoparticles were obtained and characterized by X-ray diffraction, Nitrogen adsorption, UV-Vis, STEM and by the FTIR-CO adsorption. The spectroscopic characteristics of CO adsorption at 90 K on these catalysts showed that the IR-CO stretching bands appear at different wavelength upon the support TiO<sub>2</sub>, TiO<sub>2</sub>-Al<sub>2</sub>O<sub>3</sub> and TiO<sub>2</sub>-In<sub>2</sub>O<sub>3</sub>. The findings are



significant because important insights will be gained into the gold binding properties. Our study demonstrated that gold deposition on TiO<sub>2</sub>-doped nanostructure gives rise to highly uniform gold nanoparticles in the 4-15 nm size range and provides new path to generate supported gold catalysts with controlled catalytic properties.

*Fig. 1. STEM image of Au1%/TiO<sub>2</sub>-Al<sub>2</sub>O<sub>3</sub> sol-gel photocatalyst.*

We would like to acknowledge the technical support of C. Castillo

<sup>1</sup> R. Zanella, S. Giorgio, C.R. Henry, C. Louis, J. Phys. Chem. B, 106(2002)7634

<sup>2</sup> V. Rodríguez-González, R. Gómez, M. Moscosa-Santillan, J. Amouroux, React. Kinet. Catal. Lett., 90(2007)331

## Photophysical Properties of Nano-sized $\text{TiO}_2\text{-M}$ ( $\text{M} = \text{Cu}, \text{Mo}$ ) Sol-Gel: on the Reductive Character of the Thermal Dehydroxylation Process

J. A. Pedraza-Avella<sup>1</sup>, F. Martínez-Ortega<sup>1</sup>, E. A. Páez-Mozo<sup>1</sup>, and R. Gómez<sup>2,\*</sup>

<sup>1</sup> Centro de Investigaciones en Catálisis - CICAT, Universidad Industrial de Santander, Sede Guatiguará, Km. 2 vía El Refugio, Piedecuesta, Santander, Colombia.

<sup>2</sup> Grupo ECOCATAL, Área de Catálisis, Departamento de Química, Universidad Autónoma Metropolitana-Iztapalapa, Av. San Rafael Atlixco 186, 09340 Mexico D.F., Mexico.

\*e-mail: gomr@xanum.uam.mx, apedraza@uis.edu.co

Heterogeneous photocatalysis has been intensely investigated in recent years from both fundamental and practical perspectives. Doping constitutes a useful approach to enhance the poor visible-light photoresponse of  $\text{TiO}_2$ . Although, titania has been already doped by various transition metal ions the reported results have been conflicting. In this work, titania doped with copper and molybdenum were prepared through a sol-gel method by using  $\text{Cu}(\text{NO}_3)_2 \cdot 2.5\text{H}_2\text{O}$  and  $(\text{NH}_4)_6\text{Mo}_7\text{O}_{24} \cdot 4\text{H}_2\text{O}$  as precursors (0.1, 0.5, 1.0 and 5.0% wt.), followed by a thermal treatment at  $500^\circ\text{C}$  in air. XRD patterns showed only the anatase phase for all doped samples. The particle size obtained by DLS was at the nanometer scale. The band gap energy ( $E_g$ ) estimated by UV-VIS DRS was 2.22 eV (558 nm) for  $\text{TiO}_2\text{-Cu}$  and 3.01 eV (412 nm) for  $\text{TiO}_2\text{-Mo}$ , both at 1.0 wt. %. XPS studies reveal the presence of  $\text{Cu}^{+1}$  in  $\text{TiO}_2\text{-Cu}$  and a mixture of  $\text{Mo}^{+6}$  and  $\text{Mo}^{+4}$  in  $\text{TiO}_2\text{-Mo}$ , which evidence the strong reductive character of dehydroxylation during the annealing. These observations can explain the photophysical behavior of the resulting materials in agreement with the solid-state physics.

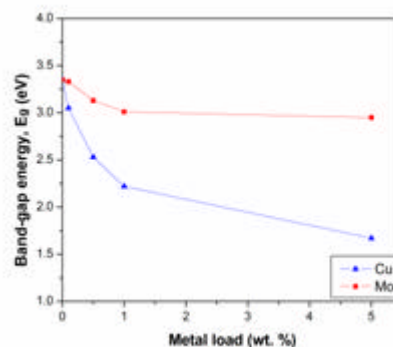


Figure 1. Band-gap energy vs. metal load for  $\text{TiO}_2\text{-Cu}$  and  $\text{TiO}_2\text{-Mo}$  materials.

We acknowledge the partial financial supports of UIS (DIEF Ciencias, Project 5125), COLCIENCIAS, UAM-I and CONACYT, as well as the doctoral scholarship given by COLCIENCIAS to J.A. Pedraza-Avella in 2003.

## **Una Nueva Herramienta de Inspección, el CrossBeam® combinando un SEM de Emisión de Campo de Ultra Alta Resolución y un FIB de Alta Resolución**

Harumi Kimura

*Tecnología y Equipamiento, S.A. DE C.V., Durango No. 69 Col. Roma Norte, C.P. 06700,  
Mexico, D.F., Mexico.*

Tel: 55 5208 1165, Fax: 55 5207 2590

\*e-mail: kimura@tyeq.com, Web site: www.tyeq.com

La combinación de la Microscopía Electrónica de Barrido con Emisión de Campo (FESEM) y el Haz de Iones Enfocado (FIB) es una tecnología clave en el futuro para aplicaciones relacionadas con Semiconductores, Ciencia de Materiales y todos aquellos aspectos relacionados con las nanotecnologías. Una nueva herramienta se analiza en esta presentación.

Mediante la combinación del SEM de Emisión de Campo de Ultra Alta Resolución con su columna de tecnología de punta Gemini y el Cañón de Galio de alto desempeño con la columna FIB, un gran campo de aplicaciones puede ser ahora alcanzado. Esto incluye cortes transversales estructurales para aplicaciones en SEM y TEM, modificación de dispositivos, análisis de fallas, medición de subcapas y evaluación, así como técnicas analíticas relacionadas al SEM y FIB tales como Espectroscopía de Energía Dispersiva de Rayos X (EDS), Espectroscopía de longitud de onda dispersiva de Rayos X (WDS), Espectrometría de Masas de Iones Secundarios (SIMS), etc.

La obtención de micrografías de Alta Resolución en SEM durante el proceso de corte y deposición permite al investigador desarrollar análisis tridimensionales estructurales muy precisos y modificaciones de dispositivos.



# POSTERS



## Characterization of Photoluminescent Photonic Devices Fabricated Using Electrochemical Etching of Low Doped Silicon Wafer

O. Sarracino Martínez<sup>1</sup>, J. M. Gracia-Jiménez<sup>2</sup>, and V. Agarwal<sup>1\*</sup>

<sup>1</sup>CIICAP- Universidad Autónoma del Estado de Morelos, Av. Universidad 1001, Col Chamilpa, CP 62210, Cuernavaca, Morelos, Mexico.

<sup>2</sup>Instituto de Física, BUAP, Apdo. Postal J-48, San Manuel, 72570 Puebla, Pue., Mexico.

\*e-mail: vagarwal@uaem.mx

In this work, we report the fabrication of porous silicon multilayers using p<sup>-</sup> type silicon wafers of high resistivity (14-22 ohm-cm) by pulsed anodic etching. The optical properties have been found to strongly depend on the duty cycle and frequency. The duty cycle of less than 50 %, at low frequencies, is found to show a very rough interface (porous silicon – crystalline silicon). Apart from 50 % of duty cycle the interface is found to be smooth. Hence the optical properties of the samples were investigated for 50 % and 75 % of duty-cycle, for different frequencies in the range of 0-1000 Hz, for 10, 90 and 150 mA/cm<sup>2</sup> of current density.

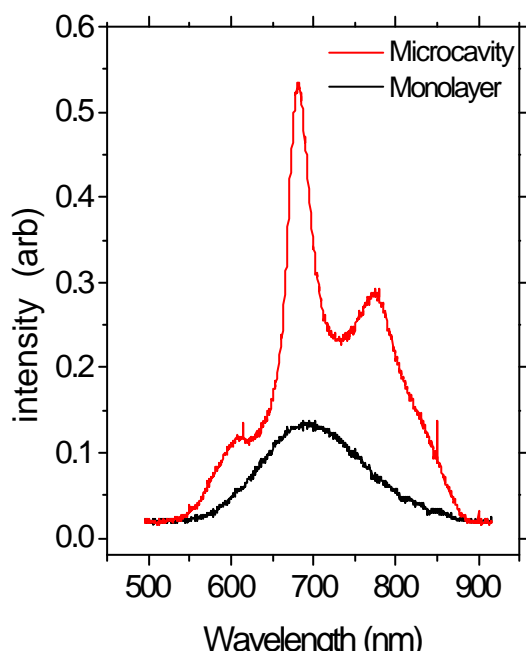


Figure 1 shows a comparison between the monolayer and multilayer microcavity.

The structural analysis was done by HRSEM and optical properties were studied with the help of UV-vis-NIR spectrophotometer. Photoluminescence measurements were carried out by 488nm line of Ar ion laser. The samples fabricated under the above mentioned conditions were found to show an increase in the PL intensity and decrease in the interface roughness. The microcavity is found to show much higher intensity and a decrease in linewidth of the photoluminescence as compared with the monolayer.

## Biocompatibility of $\text{ZnAl}_2\text{O}_4$ Nanostructured Material

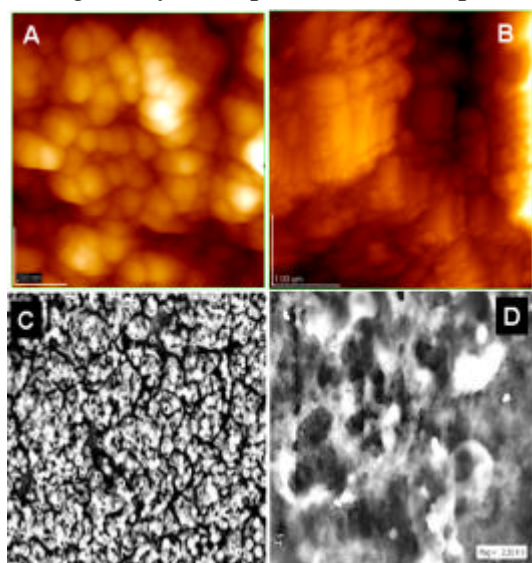
M.A. Alvarez-Pérez<sup>1</sup>, M. García-Hipolito<sup>2</sup>, H. Arzate<sup>1</sup>, B. Carmona-Rodriguez<sup>1</sup>,  
L.A. Ximenez-Fyvie<sup>1</sup>, and O. Alvarez-Fragoso<sup>2</sup>

<sup>1</sup>*Laboratorio de Biología Celular y Molecular, Facultad de Odontología, Universidad Nacional Autónoma de México, Coyoacán 04510, México, D.F.*

<sup>2</sup>*Instituto de Investigación en Materiales, Universidad Nacional Autónoma de México, Coyoacán, 04510 México D.F., México.*

e-mail: transduct6@yahoo.com

Recent progress in the synthesis, characterization and biological compatibility of nanostructured materials for biomedical implants has been proposed. Here we have used  $\text{ZnAl}_2\text{O}_4$  nanostructured materials deposited onto corning glass 7059 by spray pyrolysis to determine its biocompatibility assessed by cells attachment and cell differentiation by testing its potential in promoting mineralization and gene expression associated to mineralized tissues. Cell attachment of HGF-CEMP1 showed an increase of 53, 81 and 86% at 3, 5 and 7 hrs ( $p < 0.05$ ) when compared to controls. Mineralization was evaluated by Alizarin red S staining of the mineral-like tissue deposited onto  $\text{ZnAl}_2\text{O}_4$  which was analyzed by scanning electron microscopy, microanalysis and atomic force microscopy. Our results showed that Ca/P ratio were 1.6 similar to those of biological hydroxiapatite when compared to the controls. Gene expression was assessed after 14



days of culture. Our finding revealed that  $\text{ZnAl}_2\text{O}_4$  promoted higher expression of type I collagen, bone sialoprotein, osteocalcin and alkaline phosphatase, suggesting that  $\text{ZnAl}_2\text{O}_4$  provides a microenvironment with an increased bioactivity, cell differentiation and holds a future potential use for the osteoinductive process in biomedical implants.

*Figure 1. AFM and SEM micrographs of A and C)  $\text{ZnAl}_2\text{O}_4$  nanostructured material, B and D) Mineralization tissue of HGF-CEMP1 cells deposited onto  $\text{ZnAl}_2\text{O}_4$  after 14 days of culture.*

## A Unique Strategy for Synthesis of CdS Nanocrystallites in Polymer Matrix

K. G. Kanade<sup>1</sup>, R. R. Hawaldar<sup>2</sup>, U. P. Mulik<sup>2</sup>, and D. P. Amalnerkar<sup>2\*</sup>

<sup>1</sup>*Department of Chemistry, Mahatma Phule College, Pimpri, Pune – 411 017.*

<sup>2</sup>*Centre for Materials for Electronics Technology (C-MET), Panchawati, Off Pashan Road,  
Pune – 411008, India.*

\*e-mail: dpa54@yahoo.co.in, Tel: + 91-20-25899273; Fax: + 91-20-25898085.

We describe a unique strategy for synthesis of nanosized chalcogenide semiconductors in polymer matrix by a novel polymer-inorganic solid-state reaction. In our previous study, the rationale of this strategy has been successfully established by the solid state reaction between CdI<sub>2</sub> and an intentionally chosen *engineering thermoplastic*, namely, polyphenylene sulphide (PPS). In the pursuit of this work, we explored the possibility of using other cadmium salts viz cadmium nitrate, cadmium chloride and cadmium acetate in place of cadmium iodide for the envisaged solid state reaction with PPS. All the reactions were carried out at the melting temperature of PPS (285°C) in 1:1 and 10:1 molar ratios of polymer to cadmium salt. The resultant products were characterised by XRD, SEM-EDAX and TEM-SAED. It is observed that only cadmium nitrate yielded CdS nanocrystallites (average size 15 nm) entrapped in modified polymer matrix in a competing behaviour with cadmium iodide when reacted in 10:1 molar ratio while (i) cadmium acetate leads to the formation of only cadmium oxide and (ii) cadmium chloride exhibits grossly incomplete solid state reaction yielding understated quantity of CdS when reacted with PPS.<sup>1</sup>

---

<sup>1</sup> “Novel polymer –inorganic solid-state reaction for the synthesis of CdS nanocrystallites” K.G. Kanade, R.R. Hawaldar, R. Pasricha, S. Radhakrishnan, T. Seth, U.P. Mulik, B.B. Kale & D.P. Amalnerkar, Materials Letters, 59/5, 554 (2005).

## Molecular Dynamics Study of the Interaction of Vanadium Oxides with Y-Zeolite Hydrogens Fixed

M. Arroyo<sup>1\*</sup>, E. Sansores<sup>1</sup>, R. Salcedo<sup>1</sup>, F. Alvarez<sup>2</sup>, and A. Montoya<sup>2</sup>

<sup>1</sup> *Instituto de Investigaciones en Materiales, UNAM, A.P. 70-360, Mexico DF, 04510.*

<sup>2</sup> *Instituto Mexicano del Petróleo, Eje Central Norte 152, Mexico DF, 07730.*

\*e-mail: marroyo@correo.unam.mx

The most of the chemical processes that take part in the refining oil industry are based on the use of catalysts. It is well known that vanadium oxides have a poisoning effect on most zeolites, the catalysts commonly contained in the Fluid Catalytic Cracking (FCC), reducing the activity and crystallinity of these materials. In this work we report a computational study about the reaction mechanism of vanadium oxides with a pore of Y-zeolite model, simulating the conditions of a FCC regeneration unit. In order to simulate the Y-zeolite we have taken a ring from a -1,1,1 plane that has 12 tetrahedral sites whose internal diameter is  $\sim 10$  Å. The external surface of the ring was saturated with 24 hydrogens. The saturation hydrogens are bonded to oxygens, keeping symmetry and with a O-H bond length of 1.02 Å. The hydrogen acid sites compensates the differences of charge due to the inclusion of aluminum in the silica network, in our model there are two acid sites located at opposite tetrahedral positions. The interaction was modeled by Molecular Dynamics (MD) calculations in an annealing process at 873 K using the code NWChem and introducing different vanadium oxide species, VO, V<sub>2</sub>O<sub>3</sub>, VO<sub>2</sub> and V<sub>2</sub>O<sub>5</sub>, at the center of the zeolite ring allowing a free interaction with the zeolite. A special border conditions was used: all H are fixed. Our results show the interaction of the vanadium monoxide with the zeolite model thought a bounding with an acid site by the vanadium atom. On the other hand, the V<sub>2</sub>O<sub>3</sub> molecule is unfolded and vanadium is bonded to oxygen of the alumina. These results are in agreement with different theoretical studies.

## Structural and Size effects of Metal Concentration and pH Conditions for the Synthesis of FeO<sub>x</sub> Nanoparticles by Biosynthesis

R. Herrera-Becerra,<sup>†</sup> C. Zorrilla<sup>†</sup>, and J. A. Ascencio<sup>‡\*</sup>

<sup>†</sup> *Dpto. Materia Condensada, Instituto de Física, Universidad Nacional Autónoma de México, A. P. 20-364, México, Distrito Federal, C.P. 01000, México.*

<sup>‡</sup> *Instituto Mexicano del Petróleo. Lázaro Cárdenas 152, Col San Bartolo Atepehuacan, México, Distrito Federal, C.P. 07730, México.*

\*e-mail: ascencio@imp.mx

Nanotechnology goals involve the improvement of methods to produce size controlled clusters, where the mechanisms become simpler and cleaner, because of the perspectives to increase the amount of required nanoparticles and the consequent pollutant contribution. The use of biosynthesis on the production of metal oxides nanoparticles has been recently reported. In that case and multiple reports of metal clusters, pH conditions has been determined as the main parameter to control size, while the kind of crystalline phase is also associated to this. The use of variation on metal ions concentration allowed a study of the effect of this against the pH conditions to produce small clusters and searching for magnetite type. The use of high resolution transmission electron microscopy (HRTEM) with digital processing and a comparison against HRTEM simulated images, allowed a structural determination and to associate these to the synthesis conditions.

Iron oxides have attracted great attention of basic research specialists because of their multivalent oxidation states, the big amount of possible adopted polymorphism, and especially at the nanometric scale, where its characteristic structural change. In this work, we are focused to determine the effect of both synthesis conditions in order to evaluate optimum mechanisms to produce a bigger amount of particles of iron oxide around 2-5 nm.

## Self-catalyzed Growth and Ultraviolet Photoresponse Properties of ZnO Nanowire Arrays

R. Ghosh, M. Dutta, and D. Basak\*

*Department of Solid State Physics, Indian Association for the Cultivation of Science, Jadavpur,  
Kolkata-700032, India.*

\*e-mail: sspdb@iacs.res.in

Since the first report of ultraviolet (UV) lasing from ZnO nanowires (NWs), many efforts have been devoted to the development of synthetic methodologies for one dimensional ZnO nanostructures<sup>1</sup>. Solution approach such as solvothermal process is appealing because of the low growth temperature and good potential for scale-up. We expand this synthetic method by growing self-catalyzed ZnO NW arrays over a ZnO seed layer grown by sol-gel technique. Two different concentrations of the sol were used to investigate the effect on the growth morphology. The structural studies show that the NWs have the hexagonal wurtzite phase of ZnO. The presence of an intense (002) peak reveals a texture effect of the NW arrays consistent with the c-axis orientation. The field emission scanning electron microscopy (FESEM) shows that the seed layer grown from the higher concentration sol produces more homogeneous and dense arrays of quasi-aligned ZnO NWs than those produced from the lower concentration one. The widths of the NW for 0.1 M and 0.03 M sol are in the range of 20-60 nm and about 135 nm respectively. An interesting difference in the growth feature has been observed. The NW tips are hexagonal for the higher concentration sol while mostly is trapezoidal for the lower concentration. A growth mechanism has been proposed through a model. The high resolution transmission electron microscopy (HRTEM) image indicates that each ZnO NW is hexagonal single crystal growing along [100] orientation. The photoresponse measurements show that the photocurrent from the ZnO NW arrays can reversibly be turned “on” and “off” by switching the illumination of UV light. The detailed results would be presented and discussed.

---

<sup>1</sup> M. H. Huang et al. Science **292**(2001) 1897. <sup>2</sup> R. Ghosh et al. J. Appl. Phys. **96** (2004) 2689.

## Nanostructured $\text{Cd}_{1-x}\text{Mn}_x\text{S}$ Films for Spintronics and Optoelectronic Device Applications: Synthesis and Characterization

D. Sreekantha Reddy<sup>a\*</sup>, D. Raja Reddy<sup>a</sup>, B. K. Reddy<sup>a</sup>, K. R. Gunasekhar<sup>b</sup>,  
and P. Sreedhara Reddy<sup>a</sup>

<sup>a</sup> Department of Physics, Sri Venkateswara University, Tirupati-517502, India

<sup>b</sup> Department of Instrumentation, Indian Institute of Science, Bangalore-560012, India

\*e-mail: dsreddy\_physics@rediffmail.com

Nanostructured  $\text{Cd}_{1-x}\text{Mn}_x\text{S}$  ( $x = 0.3$  and  $0.4$ ) films were prepared on glass substrates by thermal evaporation. All the films were deposited at 300 K and the films were annealed at 573 K in a high vacuum of  $10^{-6}$  m bar. The nanostructure films were characterized for composition, structure, microstructure, optical studies and magnetic properties. All the films exhibited wurtzite structure of the host material. SEM images of as-deposited films of all compositions had a smooth surface structure. AFM studies showed that all the films were in nanocrystalline form with the grain size varying in the range between 25 – 45 nm and root mean square surface roughness of the films below 2 nm.

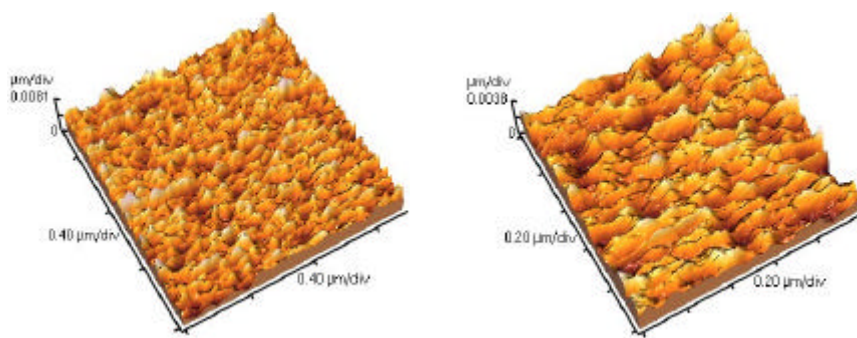


Figure 1. AFM images of (a)  $\text{Cd}_{0.7}\text{Mn}_{0.3}\text{S}$  films deposited at 300 K and (b)  $\text{Cd}_{0.7}\text{Mn}_{0.3}\text{S}$  films annealed at 573 K

II – VI compound semiconductor material have been extensively studied for a variety of application in optical coatings, solid state solar window layers, electro optic modulators, photo conductors, field effect transistors, optical sensors, photo catalysts, electroluminescence materials, phosphors, and other light emitting materials. In the recent trend DMS are also known as ‘spintronic’ materials as these offer spin as an additional handle to control current in addition to charge.



## **Effect of Iron Substitution on Microstructure and Optical Properties of Nanocrystalline $\text{CaTiO}_3$**

S. Mondal<sup>1</sup>, Manisha Pal<sup>2</sup>, U. Pal<sup>3</sup>, and M. Pal<sup>1\*</sup>

<sup>1</sup>*Department of Physics, The University of Burdwan, West-Bengal, 713 104, India.*

<sup>2</sup>*Department of Physics, Sarojini Naidu College, Kolkata, India.*

<sup>3</sup>*Instituto de Fisica, UNiversidad Autonoma de Puebla, 72570, Mexico.*

\*e-mail: mrinalp@yahoo.com

Nanocrystalline  $\text{CaTiO}_3$  doped with  $\text{Fe}_2\text{O}_3$  having different particle size have been prepared using a soft chemical route. The exothermic peak in DSC pattern revealed the phase transformation temperature, which changes with the concentration of iron. Surface morphology, crystal structure, optical and electrical properties of the nanostructures are investigated. X-ray diffraction study shows that the as-prepared powders are amorphous in nature and  $\text{CaTiO}_3$  phase formation starts at around 500 °C. Rietveld analysis revealed that the particle size of iron substituted  $\text{CaTiO}_3$  is in nanometer range, which is also reflected in their transmission electron micrographs. Optical bandgap of the nanostructures estimated from UV-vis spectra varies from 3.7 to 4.3 eV while the iron concentration varies from 0.05 to 0.2 mole %.

## SEM and AFM Characterization of MeV Si Ion-irradiation-induced Deformation of Colloidal Silica Particles

J.C. Cheang-Wong\*, U. Morales, E. Reséndiz, and A. López-Suárez

*Instituto de Física, Universidad Nacional Autónoma de México.*

*A.P. 20-364, Mexico, D.F. 01000, Mexico.*

\*e-mail: cheang@fisica.unam.mx

Colloidal silica particles are being intensively studied due to their potential applications in catalysis, intelligent materials, optoelectronic devices and coating technology. The properties of these SiO<sub>2</sub> particles depend on their size, size distribution and shape. It has been observed that amorphous glassy materials like silicon dioxide (in the form of films or colloidal particles) can undergo extreme deformations under exposure to high-energy ion beams<sup>1</sup>. Spherical submicrometer-sized silica particles were prepared from a reaction mixture containing tetraethoxysilane, ammonia and ethanol, and deposited onto silicon wafers. Monodisperse spherical particles were obtained with a narrow size distribution. The samples were then irradiated at room temperature with Si ions at different energies in the 4-8 MeV range and fluences up to  $5 \times 10^{15}$  Si/cm<sup>2</sup>, under an angle of 45° with respect to the sample surface.

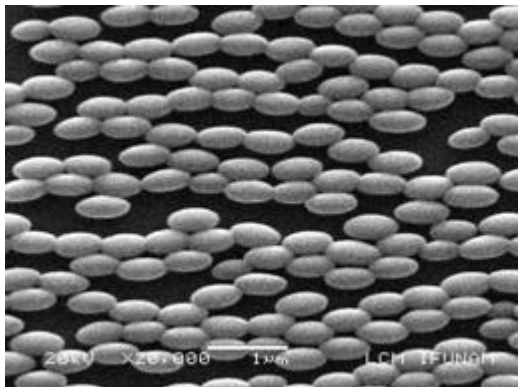


*Fig. 1. SEM image of 520 nm diameter silica particles after irradiation with 6 MeV Si ions at a fluence of  $4 \times 10^{15}$  ions/cm<sup>2</sup>. The image was taken in the direction perpendicular to the irradiation beam*

The size, size distribution and shape of the silica particles were determined using scanning electron and atomic force microscopes. After the Si irradiation the spherical silica particles turned into ellipsoidal particles, as a result of the increase of the particle dimension perpendicular to the ion beam and a decrease in the direction parallel to the ion beam. This effect increases with the ion energy and fluence, and depends on the electronic energy loss of the impinging ion.

<sup>1</sup> J.C. Cheang-Wong, U. Morales, A. Oliver, L. Rodríguez-Fernández, J. Rickards, "MeV ion beam deformation of colloidal silica particles". Nucl. Instr. and Meth. B 242 (2006) 452.

## Synthesis, Characterization and Deformation of Colloidal Titania Nanoparticles

Juan-Carlos Cheang-Wong\* and Ana Lilia Díaz

*Instituto de Física, Universidad Nacional Autónoma de México.*

*A.P. 20-364, Mexico, D.F. 01000, Mexico.*

\*e-mail: cheang@fisica.unam.mx

Titania ( $\text{TiO}_2$ ) powder is one of the most important particulate material used for many purposes such as pigment for paints, enamel or glazes of ceramics, solar cell, luminescent material, photocatalyst and for bactericidal action. Its properties depend strongly on its crystal structure, shape and size. Some of these properties can be perfectly controlled by appropriate synthesis conditions. On the other hand, it has been observed that the shape of silica nanoparticles can be modified by ion-irradiation-induced deformation.<sup>1</sup> For this work, spherical submicrometer-sized titania particles were prepared by the sol-gel method from hydrolysis and condensation of titanium alkoxide using different basic catalysts in ethanol/acetonitrile at different annealing temperatures. Subsequently, they were deposited onto silicon wafers and then irradiated at room temperature with Si ions at 4 MeV and fluences in the  $1 \times 10^{15}$ - $6 \times 10^{15}$   $\text{Si}/\text{cm}^2$  range, under an angle of  $45^\circ$  with respect to the sample surface.

The titania particles were characterized by scanning electron microscopy to determine size and shape and by X-ray diffraction to find their crystal structure. Our results showed that the shape deformation of the titania particles depends on the Si irradiation fluence.

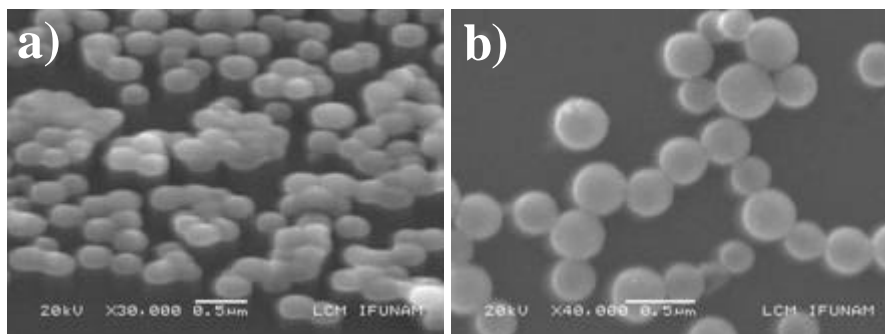


Figure 1. SEM images of titania particles: a) 370 nm diameter as-prepared particles, and b) 230 nm diameter particles after irradiation with 4 MeV Si ions at a fluence of  $1 \times 10^{15}$   $\text{ions}/\text{cm}^2$ . The image b) was taken in the direction perpendicular to the irradiation beam.

<sup>1</sup> J.C. Cheang-Wong, U. Morales, A. Oliver, L. Rodríguez-Fernández, J. Rickards, "MeV ion beam deformation of colloidal silica particles". Nucl. Instr. and Meth. B 242 (2006) 452.

## Effect of Al<sub>2</sub>O<sub>3</sub> Nanotubes on Pt/Al<sub>2</sub>O<sub>3</sub> Activity on CH<sub>4</sub> Abatement from Natural Gas Vehicles Exhaust

G. Corro<sup>1\*</sup>, C. Cano<sup>1</sup>, M.E. Manríquez<sup>1</sup>, and J.L.G. Fierro<sup>2</sup>

<sup>1</sup>*Instituto de Ciencias, Benemérita Universidad Autónoma de Puebla, 4 Sur 104, 72000, Puebla, Mexico.*

<sup>2</sup>*Instituto de Catálisis y Petroleoquímica, CSIC, Cantoblanco, 28049 Madrid, Spain.*

\*e-mail: cs0013802@siu.buap.mx

Methane emissions abatement from Natural Gas Vehicles exhaust was studied on platinum deposited on alumina ( $\gamma$ -Al<sub>2</sub>O<sub>3</sub>) nanotubes catalyst. The CH<sub>4</sub> abatement was studied by thermo programmed oxidation (CH<sub>4</sub>-O<sub>2</sub>).<sup>1</sup> Catalyst sulfation resulted in a promotional effect on Pt activity for this reaction. The CH<sub>4</sub>-O<sub>2</sub> evolutions as a function of temperature curves revealed that for the pre-sulfated Pt/ $\gamma$ -Al<sub>2</sub>O<sub>3</sub> catalyst, the chemical limiting step and the pore limiting steps were activated at lower temperatures. The results are explained on basis of XPS analysis that determined on pre-sulfated Pt/ $\gamma$ -Al<sub>2</sub>O<sub>3</sub> the presence of Pt on a higher oxidation state relative to unsulfated Pt/ $\gamma$ -Al<sub>2</sub>O<sub>3</sub>. On the other hand, SEM micrographs revealed that alumina nanotubes were shattered during sulfation resulting in a strong increase of platinum particles dispersion and in an increase of the accessibility of reactants (CH<sub>4</sub>) to the platinum active sites. This increase may result in the activation of the pore diffusion rate to lower temperatures.

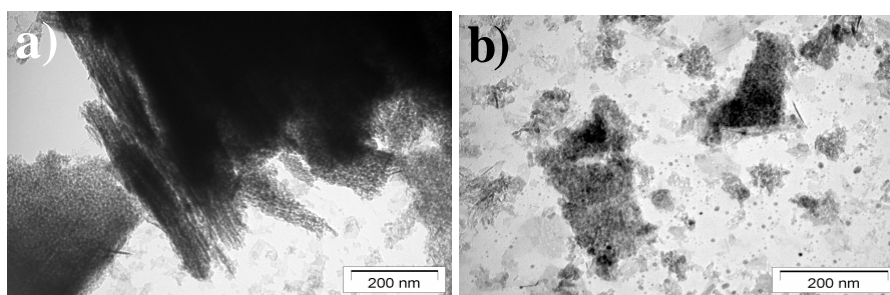


Figure 1. SEM micrographs of (a): unsulfated Pt/ $\gamma$ -Al<sub>2</sub>O<sub>3</sub> and (b): pre-sulfated Pt/ $\gamma$ -Al<sub>2</sub>O<sub>3</sub>.

The authors are pleased to acknowledge valuable support for this research from CONACYT-SEMARNAT (2002-COL-0212), Vicerrectoria de Investigación y Estudios de Posgrado (BUAP).

<sup>1</sup> G. Corro, JLG Fierro, O. Vazquez, Cat. Comm. 7 (2006) 436.

## **Nanostructuration of GaP and GaPO<sub>4</sub> by Using the Close-Spaced Vapor Transport Technique: Influence of the Carrying Gas**

F. Chávez<sup>1</sup>, C. Felipe<sup>1\*</sup>, E. Lima<sup>2</sup>, C. Ángeles-Chávez<sup>3</sup>, O. Goiz<sup>4</sup>,  
and R. Peña-Sierra<sup>4</sup>

<sup>1</sup>*Departamento de Fisicoquímica de Materiales, ICUAP, Benemérita Universidad Autónoma de Puebla, Puebla 72000, Mexico.*

<sup>2</sup>*Universidad Autónoma Metropolitana, Iztapalapa, Av. San Rafael Atlixco No. 186 Col. Vicentina, 09340 Mexico, D.F., Mexico.*

<sup>3</sup>*Instituto Mexicano del Petróleo, Programa de Ingeniería Molecular, Mexico, D.F. 07730, Mexico*

<sup>4</sup>*Departamento de Ingeniería Eléctrica, CINVESTAV, Instituto Politécnico Nacional, 07000 Mexico, D.F., Mexico.*

\*e-mail: carlos.felipe@icbuap.buap.mx

Starting from a powder gallium phosphide source, nanostructures of high-purity were growth on gallium arsenide substrate through the close-spaced vapor transport technique (CSVT). Morphology and structure of nanostructured products were characterized by means of SEM, EDS, XRD, and NMR techniques. The influence of the carrying gas was studied; H<sub>2</sub> and N<sub>2</sub> were considered. In the presence of a H<sub>2</sub> flow, GaP with a nanoflower-like morphology was obtained. Nanoflowers, in turn, are formed by numerous nanowires with diameters ranged between 80 and 300 nm. In contrast, the nanostructuration in nitrogen leads to the formation of GaPO<sub>4</sub> with a fibrous morphology. Indeed, several isolated filaments were detected by SEM.

It should be emphasized that growth of GaP and GaPO<sub>4</sub> on GaAs occurs without use of any catalyst. A mechanism of formation of structures is discussed, where the presence of the reductant agent and the residual water in the reactor emerges as two determinant factors for drives the chemicals reactions that take place.

## Cerium Effect in the Structural Properties of Nanosized Sol-Gel Prepared $\text{TiO}_2$

F. Galindo\* and R. Gómez

*Department of Chemistry, Universidad Autónoma Metropolitana-Iztapalapa, San Rafael Atlixco  
186, A. P. 55-534, Mexico City, D.F. 09340, Mexico.*

\*e-mail: cbi200280212@xanum.uam.mx

Sol-gel  $\text{TiO}_2$  and  $\text{Ce/TiO}_2$  materials (10 wt % Ce) were synthesized at pH3 using  $\text{HNO}_3$  as hydrolysis catalysts. Gels were annealed at 473, 673 and 873 K for 4h. X-ray diffraction was used to determine the mean crystallite size,  $\text{TiO}_2$  stoichiometry ( $\text{Ti}^{4+}$  vacancies) and Fourier electronic density map by Rietveld refinement. It has been found that more ordered  $\text{TiO}_2$  surfaces were formed at high annealed temperature, the fractal surface dimension diminishes from 2.73 to 2.5 for 473 and 873 K calcined  $\text{Ce/TiO}_2$ -10. The samples showed anatase as crystalline phase with a nanosized crystallite between 9.4 and 44.9 nm in depending of the annealing temperature. The plot of crystallite size as function of the number of  $\text{Ti}^{4+}$  vacancies showed a good correlation between them, as lowest is the crystallite size lowest is the number of  $\text{Ti}^{4+}$  vacancies. Strong modification in the electron density map of  $\text{TiO}_2$  was found in  $\text{Ce/TiO}_2$  materials. It is concluded that Ce favors the formation of nanosized  $\text{TiO}_2$  with high  $\text{Ti}^{4+}$  stoichiometric deficiency.

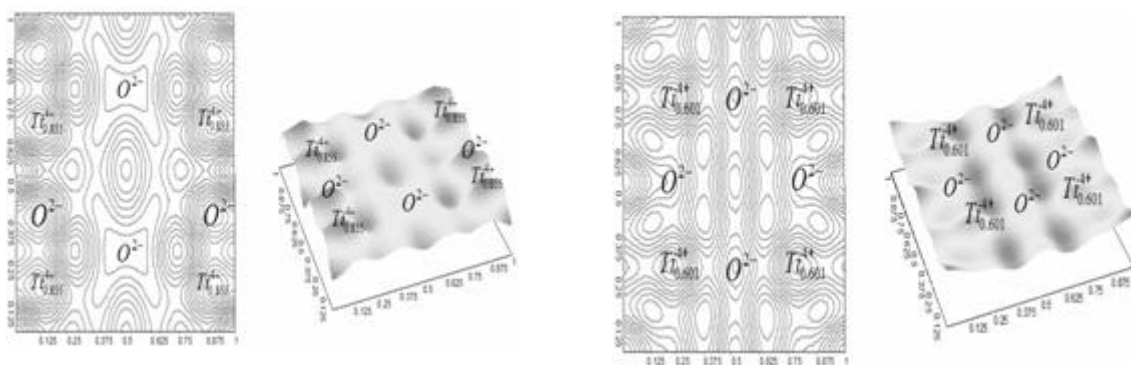


Figure 1. Electron density map: left  $\text{TiO}_2$ ; right  $\text{Ce/TiO}_2$ .

## **Synthesis of AlN Nanorods Using a Mecano-Thermal Process**

**E. García de León, R. Esparza, J. Verduzco, R. Torres, and G. Rosas<sup>\*</sup>**

Facultad de Química, CU, Universidad Nacional Autónoma de México.

México, DF. México.

Instituto de Investigaciones Metalúrgicas, UMSNH, Edificio U, Ciudad Universitaria, Morelia,

Mich. 58000, México.

\*e-mail: grtrejo@jupiter.umich.mx

We report the formation of AlN nanorods produced by high energy ball milling (HEBM) and subsequent annealing treatment of the milling powders. HEBM was carried out in a vibratory SPEX mill for 30 h., using vials and balls of Silicon Nitride. The annealing treatment was carried out at 600, 800 and 1100 °C for 5 and 10 mins. The characterization of the samples was performed by X-ray diffractometry and transmission electron microscopy. AlN nanorods could be obtained when the annealing temperature was 1100 °C. However, the formation of AlN nanorods was not observed for the annealing samples at 600 and 800 °C. TEM observations indicate that the synthesized AlN rods exhibit a well-crystallized structure with 25 nm in diameter and 100 nm in length.

## Effect of Annealing in Atomic Hydrogen or Nitrogen Atmospheres of SiO<sub>x</sub> Nanoclusters Obtained by HFCVD

G. García Salgado<sup>1\*</sup>, T. Díaz<sup>1</sup>, A. Coyopol<sup>1</sup>, E. Rosendo<sup>1</sup>,  
H. Juárez<sup>1</sup>, and A. I. Oliva<sup>2</sup>.

<sup>1</sup>*CIDS-ICUAP, Benemerita Universidad Autonoma de Puebla*

*14 sur y Av. Sn. Claudio, Edif. 137, Puebla, Pue. Mexico.*

<sup>2</sup>*Cinvestav IPN, Unidad Mérida. Km 6 Antigua Carretera a Progreso,*

*AP 73-Cordemex 97310 Mérida Yucatan Mexico.*

\*e-mail:godgarcia@yahoo.com

Nanoclusters of SiO<sub>x</sub> were obtained by Hot Filament Chemical Vapor deposition (HFCVD) using a quartz solid source and atomic hydrogen. The nanoclusters were characterized by PL, AFM, EDAX and FTIR. The FTIR and EDAX characterization shows clearly that the material is silicon oxide non-stoichiometric having a composition variable and dependent of the growth parameters; source-substrate distance and growth time. This parameters influence in the size average of spherical nanostructures observed by AFM. The nanoclusters of SiO<sub>x</sub> normally present PL with two peaks around 859 and 920 nm, the PL was enhanced when samples were annealed in an atomic hydrogen atmosphere and quenched when the same samples were annealed in an atomic nitrogen atmosphere. The PL was recovered when the sample was annealed again with the atomic hydrogen conditions. From these results we suppose that the PL produced in this material is due to deep level transitions associated with dangling bonds passivated with hydrogen on the surface of the SiO<sub>x</sub> nanocrystallites, when the hydrogen is substituted by nitrogen predominate the non radiative transitions given place to the quenched phenomenon.



## Photophysical Properties of Nanosized TiO<sub>2</sub>-Cr Sol-Gel: UV-VIS DRS and XPS Studies

J.A. Pedraza-Avella<sup>1</sup>, R. López<sup>2</sup>, F. Martínez-Ortega<sup>1</sup>, E. A. Páez-Mozo<sup>1</sup>,  
J. Navarrete<sup>3</sup>, and R. Gómez<sup>2,\*</sup>

<sup>1</sup> Centro de Investigaciones en Catálisis - CICAT, Universidad Industrial de Santander, Sede Guatigará, Km. 2 vía El Refugio, Piedecuesta, Santander, Colombia.

<sup>2</sup> Grupo ECOCATAL, Área de Catálisis, Departamento de Química, Universidad Autónoma Metropolitana-Iztapalapa, Av. San Rafael Atlixco 186, 09340 Mexico D.F., Mexico.

<sup>3</sup> Programa de Ingeniería Molecular, Instituto Mexicano del Petróleo, Eje Central Lázaro Cárdenas 152, 07730 Mexico D.F., Mexico.

e-mail: ross@xanum.uam.mx, gomr@xanum.uam.mx

Nanostructured TiO<sub>2</sub> is extensively studied as a very promising material for applications in sensors, photocatalysis, solar energy conversion and optical coatings<sup>1</sup>. However, its technological application has been limited by the need of ultraviolet radiation for its activation. In the last years there has been an increasing interest to synthesize TiO<sub>2</sub>-based materials which can operate with visible radiation<sup>2</sup>. In this work, samples of TiO<sub>2</sub>-Cr (0.1, 0.5, 1.0 and 5.0 wt. %) were prepared by the sol-gel method at pH = 3 (HNO<sub>3</sub>) using Cr(NO<sub>3</sub>)<sub>3</sub>·9H<sub>2</sub>O as dopant precursor. XRD patterns showed only anatase phase in all samples. Particle sizes were estimated by DLS and they were at the nanometer scale. Band-gap energies were calculated from their UV-VIS diffuse reflectance spectra and they indicate a red-shift in the visible region which depends on the dopant content. Cr<sup>3+</sup> and Cr<sup>6+</sup> species were observed by XPS, pointing out the occurrence of redox processes during the synthesis. Its implications in the resulting photophysical properties are discussed.

*We acknowledge the partial financial supports of UIS (DIEF Ciencias, Project 5125), COLCIENCIAS, UAM-I and CONACYT, as well as the doctoral scholarship given by COLCIENCIAS to J.A. Pedraza-Avella in 2003.*

---

<sup>1</sup> I.N. Kholmanov, E. Barborini, S. Vinati, P. Piseri, A. Podestà, C. Ducati, C. Lenardi and P. Milani, "The influence of the precursor clusters on the structural and morphological evolution of nanostructured TiO<sub>2</sub> under thermal annealing", *Nanotechnology* **14** (2003) 1168.

<sup>2</sup> K. Rajeshwar, C.R. Chenthamarakshan, S. Goeringer and M. Djukic, "Titania-based heterogeneous photocatalysis. Materials, mechanistic issues, and implications for environmental remediation", *Pure Appl. Chem.* **73** (2001) 1849.

**Influence of the cobalt concentration and the substrate temperature on the properties of cobalt-doped zinc oxide thin films deposited by pulsed spray pyrolysis**

A. Guillén-Santiago<sup>1\*</sup>, D. R. Acosta<sup>1</sup>, A. Maldonado<sup>2</sup>, and M. de la L. Olvera<sup>2</sup>

<sup>1</sup>*Instituto de Física, UNAM, Apdo. Postal 20-364, Mexico, D.F., 01000, Mexico.*

<sup>2</sup>*Departamento de Ingeniería Eléctrica, CINVESTAV-IPN, Apdo. Postal 14-740, 07000 Mexico DF, Mexico.*

\*e-mail: aguillen@fisica.unam.mx

Undoped and cobalt-doped zinc oxide (ZnO:Co) thin films were deposited onto Si substrates by the pulsed spray pyrolysis technique, using zinc acetate and cobalt chloride as precursors. Electrical, morphological and structural characteristics were analyzed as a function of the substrate temperatures and the [Co]/[Zn] at. % ratio. The substrates were heated at 450 and 500 °C and the cobalt concentration on solution was varied as a 3%, 8% and 16%. The results show that these parameters play an important role on the film properties measured. Resistivity on the order of  $5 \times 10^{-3} \Omega \text{ cm}$  and electronic mobility around of  $8 \text{ cm}^2/(\text{V}\cdot\text{s})$  values were found. X-ray diffraction analysis shows that all the films present a hexagonal wurtzite structure. The local concentration of Co in the films was estimated by energy dispersive X-ray analysis (EDX). The scanning electron microscopy (SEM) images show different morphologies of the films.

## Assisted – hydrothermal Synthesis and Characterization of Flowerlike ZnO Nanostructures

S. López – Romero<sup>1\*</sup>, P. Santiago<sup>2</sup>, and D. Mendoza<sup>1</sup>

<sup>1</sup>*Instituto de Investigaciones en Materiales, Universidad Nacional Autónoma de Mexico, Departamento de Materia Condensada y Criogenia, Apdo. Postal 70 – 360, Mexico D.F. , 04510, Coyoacán, Mexico.*

<sup>2</sup>*Instituto de Física, Universidad Nacional Autónoma de Mexico, Apdo Postal 20-364, 01000 Mexico D.F.*

\*e-mail sebas@servidor.unam.mx. Tel. (5) 5-6224732. Fax. (5) 5616-12-51

Flowerlike nanostructures formed by ZnO nanorods were synthesized and deposited on seeded silicon and glass ZnO substrates by an hexamethylenetetramine (HMTA) – assisted hydrothermal method at low temperature (90°C). The substrates were seeded with ZnO nanoparticles. The structure and morphology of the nanostructures ZnO flowerlike were studied by means of x-ray diffraction (XRD), high resolution transmission electron microscopy (HRTEM), and scanning electron microscopy (SEM). The remarkable influence of the dispersed ZnO nanoparticles seeded on the substrates surface to the formation of the flowerlike nanostructures is demonstrated for our case.

Figures 1(a) and (b) show the SEM images of the flowerlike ZnO nanostructures deposited on silicon and glass ZnO seeded substrates, respectively. They consisted of nanorods emerging from a common point in all directions.

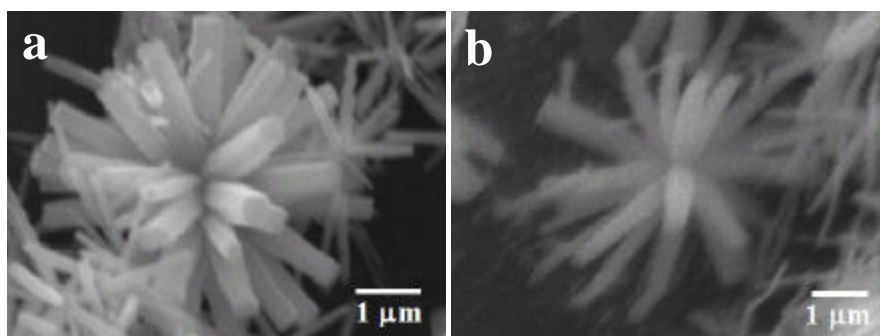


Figure 1 (a), (b) SEM images of ZnO flowerlike on ZnO seeded silicon and glass substrates respectively.

## **A Novel Approach for the Synthesis Vertical ZnO Nanorods on Glass Substrate by Simple Chemical Method**

P. Suresh Kumar<sup>1</sup>, M. Yogeswari<sup>1</sup>, D. Nataraj<sup>1</sup>, D. Mangalaraj<sup>1\*</sup>, and U. Pal<sup>2</sup>

<sup>1</sup>*Department of Physics, Thin Film Laboratory, Bharathiar University, Coimbatore 641046, India.*

<sup>2</sup>*Instituto de Física, Universidad Autónoma de Puebla, Apdo. Postal J-48, Puebla, Pue. 72570, Mexico.*

\*e-mail: dmraj800@yahoo.com

ZnO is a II-VI wide bandgap (3.37eV) semiconductor with excellent chemical, thermal and electrical properties. Semiconductor nanorods (NRs) have attracted much interest due to their potentials for diverse electronic and photonic applications. At present various chemical, electrochemical and physical deposition techniques have been employed to create oriented array of ZnO NRs. A novel aqueous solution method has been developed for growing well-aligned crystalline ZnO nanorods (NRs) on glass substrates. Successive ion layer adsorption and reaction (SILAR) method was used to grow ZnO as seed layer and subsequently a simple chemical growth method was used to grow vertical ZnO NRs. One-dimensional NR array of ZnO were obtained by using zinc acetate and hexamethylenetetramine in aqueous solution at different pH levels. The seed layer was found to influence the orientation, crystallinity and morphology of ZnO nanorods considerably. X-ray diffraction (XRD) analysis confirmed that the ZnO nanorods exhibit hexagonal wurtzite structure with orientation along C-axis. From the SEM analysis, we found that the diameter of ZnO NRs mainly depend on the concentration of reactants, reaction temperature and solution pH. The Raman spectrum confirmed two main peaks of ZnO at 437cm<sup>-1</sup> and 581cm<sup>-1</sup> due to E2 and E1 phonon vibrations.

---

<sup>1</sup> Quanchang Li, Vageesh Kumar, yan Li, *et. al.*, Chem. Mater. 2005, 17, 1001.

<sup>2</sup> Zhuo wang, Xue-feng qian *et al.*, Langmuir 2004, 20, 3441.

<sup>3</sup> X.D. Gao, X.M. Li *et al.*, Appl. Surf. Sci. 2004, 229, 275.

## **Characterization of Nanocrystalline ZnO Grown on Silicon Substrates by DC Reactive Magnetron Sputtering**

G. Juárez-Díaz<sup>a\*</sup>, A. Esparza-García<sup>c</sup>, M. Briseño-García<sup>c</sup>, H. Solache-Carranco<sup>a</sup>,  
G. Romero-Paredes R<sup>a</sup>., R. Peña-Sierra<sup>a</sup>, J. Martínez-Juárez<sup>b</sup>, and R. Galeazzi<sup>b</sup>

*<sup>a</sup>Depto. de Ingeniería Eléctrica, Sección de Electrónica del Estado Sólido, Centro de Investigación y de Estudios Avanzados del I.P.N., A.P. 14-7 40,07000, Mexico, D.F.*

*<sup>b</sup>Centro de Investigación en Dispositivos Semiconductores, BUAP, Puebla, Pue. 14 Sur y Av. San Claudio C.U., C.P. 72570. e-mail: javier.martinez@icbuap.buap.mx*

*<sup>c</sup>Centro de Ciencias Aplicadas y Desarrollo de Tecnología-UNAM. Apdo. Postal. 04510, Ciudad Universitaria. Mexico, D.F.*

\*e-mail: gabriel.juarez@icbuap.buap.mx

The aim of the work was to study the effect of postgrowth thermal annealing processes on the characteristics of the zinc oxide films grown on silicon substrates by dc reactive magnetron sputtering. The growth temperature of the ZnO thin films was fixed at 230°C and then the samples were annealed in dry air atmosphere at 800°C for an hour. The surface of the ZnO samples was observed with a scanning electron microscope and using an atomic force microscope. The structural properties were assessed by X-ray diffraction (XRD), Raman scattering, and photoluminescence (PL) measurements. The XRD studies and Raman studies revealed the ZnO films crystallize in the wurtzite structure with a certain amount of amorphous material in the as-grown films, after thermal treatment a preferential orientation along the c-axis is presented. The films are constituted by nanosized in spite of high temperature used in the annealing process. The most relevant result of this study was the excitonic structure of the room temperature photoluminescence (PL) at the ultraviolet (UV) band at 380 nm. This result demonstrates that the thermal annealing processes at 800°C produces high quality nanocrystallites. The PL response also shows a broad defect-related green band at 516 nm.

## Effects of Morphology on the Electronic Properties of Hydrogenated Silicon Carbide Nanowires

A. Miranda\*, J. L. Cuevas, and M. Cruz-Irisson

*Instituto Politécnico Nacional*

*Sección de Estudios de Posgrado e Investigación, ESIME-Culhuacan*

*Av. Santa Ana 1000, 04430 D.F. Mexico.*

\*e-mail: amirandad9700@ipn.mx

One-dimensional nanostructures deserve special attention, as they are expected to play a crucial role as building blocks of future molecular electronics applications. Silicon carbide nanowires have the considerable advantage over silicon nanowires of a much higher electrical conductance and an excellent mechanical stability, making them extremely interesting as scanning microscope tips, for instance. In this work we study the electronic band structure of hydrogenated silicon carbide by changing the mean diameter, and morphology using a semiempirical  $sp^3s^*$  tight-binding approach and compared with *ab-initio* methods. Variation in hydrogen concentration is used to explore the sensing capabilities of different surface morphologies. The gap broadening of the H-passivated wires is expected to depend on the diameter thickness. In the limit of very large diameter the quantum confinement not play any role and the electronic features of the {100} facets will approach that the corresponding infinite (100) surfaces, which are semiconducting.

## **Incorporation of Cu and Mn ions in TiO<sub>2</sub> nanoparticles through Sol-gel process**

J. A. Moreno Rodríguez<sup>1\*</sup>, E. Sánchez Mora<sup>2</sup>, L. R. Genis Najera<sup>1</sup>, A. M. Cervantes Tavera<sup>1</sup>, and L. A. Moreno Rodríguez<sup>3</sup>

1. *Facultad de Ciencias Químicas, Benemérita Universidad Autónoma de Puebla.*

*Blvd. 14 sur y Esq. San Claudio, Ciudad Universitaria, Col. San Manuel.*

*Puebla, Pue, Mexico. C. P. 72570. TEL. (01 222) 229 55 00 Ext. 7542.*

2. *Instituto de Física, Benemérita Universidad Autónoma de Puebla.*

*Apto. Postal J-48, Puebla, Pue. 72570, Mexico*

3. *Emiliano Zapata. Benemérita Universidad Autónoma de Puebla.*

*4 Norte Esquina 2 oriente. Col. Centro Histórico.*

*Puebla, Pue. Mexico*

\*e-mail: albinomx@yahoo.com

The basic powder nanomaterials (pH9) of titanium oxide (TiO<sub>2</sub>) and titanium oxide-doped with bimetallic ions of copper (II) oxide and manganese (II) oxide (Cu-Mn/TiO<sub>2</sub>) were prepared by the sol-gel method, using copper (II) chloride (CuCl<sub>2</sub>) to 35 wt % and manganese (II) chloride tetrahydrate (MnCl<sub>2</sub>·4H<sub>2</sub>O) to 15 wt % and titanium (IV) butoxide (Ti (But)<sub>4</sub>) as precursors of TiO<sub>2</sub> and Cu-Mn/TiO<sub>2</sub> nanomaterials. They were added to a homogeneous solution of distilled water (H<sub>2</sub>O), absolute ethanol (ETOH) and ammonium hydroxide (NH<sub>4</sub>OH). Both nanomaterials, TiO<sub>2</sub> pH9 and Cu-Mn/TiO<sub>2</sub> pH9 were dried to 70°C and later calcined at 200°C, 400°C, 600°C and 800°C. The nanostructure and the phases compositions of these nanomaterials were characterized with X-Ray Powder Diffraction (XRD) and Transmission Electron Microscopy (TEM). The spectroscopic characterizations were also done with UV-Vis diffuse reflectance spectroscopy and infrared spectroscopy with Fourier Transformer (FTIR). The studies of XRD for the nanomaterials of TiO<sub>2</sub> pH9 and Cu-Mn/TiO<sub>2</sub> pH9 when increasing the temperature of calcination from 400°C to 600°C, show the transition of the phase anatase to rutile, while the incorporation of the ions Cu<sup>2+</sup> and Mn<sup>2+</sup> to the network of TiO<sub>2</sub>, probably it does not influence in the crystallographic phases transition of TiO<sub>2</sub>. The TEM images, show a evolution in the

nanomaterials crystallinity and the size of nanoparticle nanomaterials until arriving at the material condensation at 800°C. The nanoparticles shows a form of agglomerate and spherical aggregates from 70°C to 400°C, with an approximated particle size of 10 nm (to 70°C) and 50 nm (to 400°C), later appears the Cu-Mn/TiO<sub>2</sub> pH9 materials crystallinity to 600°C with an approximated particle size of 100 nm and finally the nanomaterials condensation appears to 800°C with an approximated particle size of 600 nm. Contrary, the TiO<sub>2</sub> nanomaterials do not show a marcable particles crystallinity with the temperature increase from 70°C to 800°C. They show a particle size from 10 nm (at 70°C) to 50 nm (at 800°C). The FTIR sprectra shows a total deshydroxilation for TiO<sub>2</sub> pH9 and Cu-Mn/TiO<sub>2</sub> pH9 nanomaterials and the presence of two different hydroxide groups chemically connected to the nanomaterials; the groups terminal hydroxile and groups bridge hydroxile bridge to a temperature at 800°C. The UV-Vis spectra, shows significant absorption bands in the visible region for the Cu-Mn/TiO<sub>2</sub> pH9 materials from 70°C to 800°C and for the TiO<sub>2</sub> are located just in the ultraviolet region.



## **Nano-composite of $\text{Pb}(\text{Zr,Ti})\text{O}_3$ - $\text{CoFe}_2\text{O}_4$ Multiferroic Thin Films by Pulsed Laser Deposition**

N. Ortega<sup>1\*</sup>, P. Bhattacharya<sup>1</sup>, R.S. Katiyar<sup>1</sup>, P. Dutta<sup>2</sup>, M.S. Seehra<sup>2</sup>  
I. Takeuchi<sup>3</sup>, and S.B. Majumder<sup>4</sup>

<sup>1</sup>*Department of Physics, University of Puerto Rico, San Juan, PR 00931-3343.*

<sup>2</sup>*Department of Physics, West Virginia University, Morgantown, WV 26506, USA.*

<sup>3</sup>*Small Smart Systems Center, University of Maryland, College Park, Maryland 20742, USA*

<sup>4</sup>*Materials Science Center, Indian Institute of Technology, Kharagpur 721 302, India.*

\*e-mail: norapatricia50@gmail.com

In recent years, multiferroic materials display simultaneous magnetic, electric and ferroelasticity ordering, have drawn increasing interest due to their multi-functionalities for a variety of device applications. Only few single phase materials exhibit this kind of properties, therefore intense research activity is being pursued towards the development of new materials with strong magneto-electric (ME) coupling. In this work, we have fabricated ferroelectric (FE)  $\text{Pb}(\text{Zr,Ti})\text{O}_3$  (PZT) and ferromagnetic (FM)  $\text{CoFe}_2\text{O}_4$  (CFO) multilayers thin films with 3, 5, and 9 layers of the configuration PZT/CFO (PC) and CFO/PZT (CP) by pulsed laser deposition technique. The x-ray diffraction and Raman spectra of these multilayers revealed that the perovskite PZT and the spinel (CFO) were grown as two separate phases. The TEM and XPS depth profile of the films showed that the layer structure was not clear, more inter-diffusion of the CFO and PZT forming nano-composites was observed when both the number of layers and annealing time were increased. The dielectric constant ( $\epsilon_r$ ) of PC multilayers showed strong frequency dispersion. Similar behavior of  $\epsilon_r$  of CP multilayers structure was observed. Reversing the multilayer configuration from CP to PC resulted in increasing the remanent polarization. The observed dielectric relaxation has been explained by Maxwell-Wagner type contributions at the interface between insulating PZT and semi-insulating CFO regions. The ME effect of the multilayer films will be discussed.

*This work was supported in parts by DoD-W911NF-06-1-0030 and W911NF-06-1-0183 grants. One of us (N. Ortega) is thank full for the NSF-EPSCOR Fellowship.*

## Mechanical Properties of Boron Nitride Nanotubes

Ramón Elizarrarás<sup>1, 2</sup> and Luis A. Pérez<sup>1\*</sup>

<sup>1</sup>*Instituto de Física, Universidad Nacional Autónoma de México, Apartado Postal 20-364, C.P. 04510, México D.F., México.*

<sup>1</sup>*Instituto Tecnológico de Tlalnepantla, Av. Instituto Tecnológico s/n Col. la Comunidad, C. P. 54070, Tlalnepantla, Estado de México, México.*

\*e-mail: lperez@fisica.unam.mx

We report an *ab initio* study of the structural and mechanical properties of single-walled boron nitride nanotubes (BNT) with different radii and chiralities. The calculations on BNT were carried out using density functional theory within the generalized gradient approximation, as implemented in the *SIESTA* code. The Young modulus and the Poisson ratio were calculated as a function of the diameter and chirality of the nanotubes, and they show a slight dependence on the nanotube radius. The results obtained were compared with those of continuum elastic theory.

*This work was partially supported by CONACYT 43414-F and by UNAM under grants IN116605 and IN104402.*

## High Pressure Regime of Plasma Enhanced Deposition of Nanocrystalline Silicon-Germanium

L. Sanchez<sup>1\*</sup>, A. Kosarev<sup>1</sup>, and A. Torres<sup>1</sup>

<sup>1</sup>National Institute for Astrophysics, Optics and Electronics, Puebla, 72000, Mexico.

\*e-mail: lmorales@inaoep.mx

Nanocrystalline materials (nc-materials) are poly-crystals that are characterized by a grain size in the range of 1-100 nm. The unique microstructures of nc-materials suggest that these materials have the potential of exhibiting exceptional mechanical, optical and electrical properties. As a consequence, they have been attracting wide attention in materials research. Recently, silicon films deposited by plasma enhanced chemical vapor deposition (PECVD) under conditions close to those for powder-particle formation have revealed interesting new optoelectronic properties.<sup>1</sup> These films are nano-structured, some of them containing ordered silicon crystals with nanometer sizes (1-2 nm).<sup>2</sup> The synthesis of nc-Si by PE CVD has advantages in term of simplicity, cost, and bulk production. This new class of silicon thin films has been fabricated using a wide range of plasma conditions. However, there is no study about the synthesis of SiGe films under the powder regime. Therefore, in this work we focused on study of deposition conditions for the production of nano-structured SiGe films.

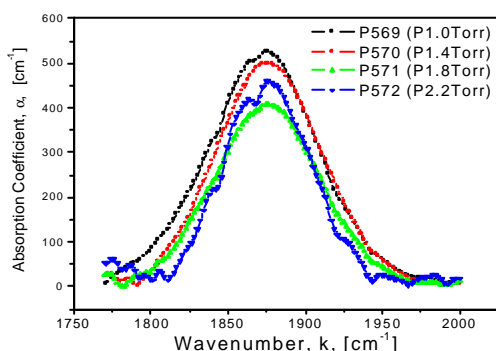


Figure 1. Absorption coefficients at different wavenumbers at the 4 different pressures can be observed from the graphic

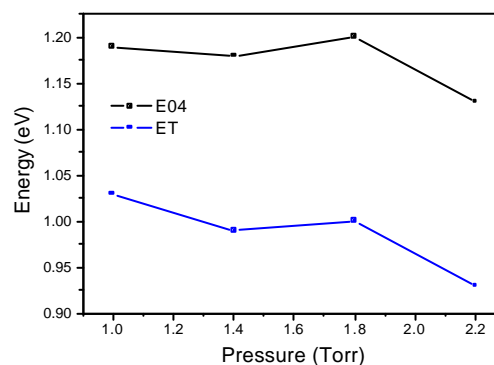


Figure 2. Tauc energy,  $E_T$ , and  $E_{04}$  energy as function of pressure.

<sup>1</sup> Pere Roca i Cabarrocas<sup>‡</sup>, Anna Fontcuberta i Morral, Sarra Lebib, and Yves Poissant *Pure Appl. Chem.*, Vol. 74, No. 3, pp. 359–367, 2002.

<sup>2</sup> A. Hadjadj, L. Boufendi, S. Huet, S. Schelz, P. Roca i Cabarrocas, H. Estrade-zwarckopf, and B. Rousseau, *J. Vac. Sci. Technol. A*, **18**(2), 529 (2000).

FTIR measurements were used to determine germanium and hydrogen bond concentrations in the films. In Figure 1, is shown the spectra from  $1750\text{ cm}^{-1}$  to  $2000\text{ cm}^{-1}$  that corresponds to the Ge-H bonds for the SiGe films deposited at the four different pressures. The behavior in figure 1 suggests that the concentration of the Ge-H bonds reduces as the pressure increases. From figure 1 can be observed that the width of the curve reduces with pressure. As consequence, the structure of the film becomes with less surrounding neighborhoods meaning that the structure of the film is changing. In this work, in order to characterize optical properties we have used the following parameters:  $E_{04}$  energy corresponding to  $\alpha=10^4\text{ cm}^{-1}$  and the Tauc optical gap,  $E_T$ . In figure 2 is shown the energy  $E_{04}$  and the Tauc optical gap,  $E_T$ , as function of deposition pressure. The optical gap reduces as the pressure increases.

## Mathematical Approach to Obtain the Atoms in Excess on Crystalline Column-Domains Observed in a Complex $\text{Nb}_{16}\text{W}_{18}\text{O}_{94}$ Structure Using HAADF-STEM: A Binary Approximation

L. Rendón and P. Santiago\*

<sup>1</sup>*Departamento de Materia Condensada, Instituto de Física, Universidad Nacional Autónoma de México, Coyoacán, 04510, A.P. 20-364, 01000, Mexico City, Mexico.*

\*e-mail: paty@fisica.unam.mx

The observation of atomic column-domains, produced by non-uniformity intercalation of W and Nb atoms along the [001] projection is reported. An ultra thin sample of the complex oxide  $\text{Nb}_{16}\text{W}_{18}\text{O}_{94}$  was observed using a high-angle annular dark field detector. An empirical calculation was developed to quantify the number of W atomic sites in excess at a specific column using a binary approximation in the ternary system  $\text{Nb}_{16}\text{W}_{18}\text{O}_{94}$ . This theoretical calculation is based on the fact that the contrast of the incoherent images obtained by HAADF strongly depends on the square of the atomic number (Z-contrast) and this effect generates column domains in the HAADF image recorder. The study was developed along the [001] zone axis projection. Some atomic columns observed by STEM-HAADF technique showed an excess of W atoms, this effect is directly related to the intensity distribution in the image generated by the HAADF scintillation detector.

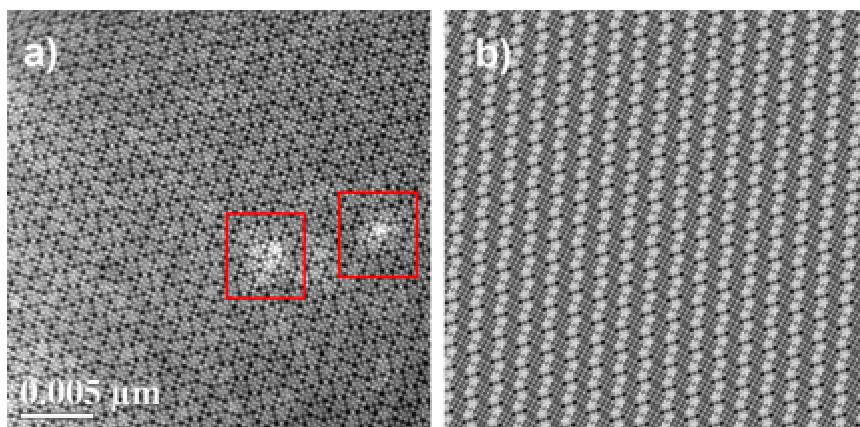


FIG. 1. a) HAADF image showing atomic column-domains in a single crystal  $\text{Nb}_{16}\text{W}_{18}\text{O}_{94}$  octahedral structure. b) HAADF of ordered domains of  $\text{Nb}_{12}\text{O}_{29}$  (square structure) and a  $\text{W}_x\text{O}_y$  compound.

We kindly acknowledge to Instituto de Física at UNAM for allowing the use of their microscopy facilities and CUDI project for financial support.

## Cooperative Pair Driven Quenching of $\text{Yb}^{3+}$ Emission in Nanocrystalline $\text{ZrO}_2:\text{Yb}^{3+}$

O. Meza,<sup>1</sup> L.A. Diaz-Torres,<sup>1,\*</sup> P. Salas,<sup>2</sup> E. De la Rosa,<sup>1</sup>

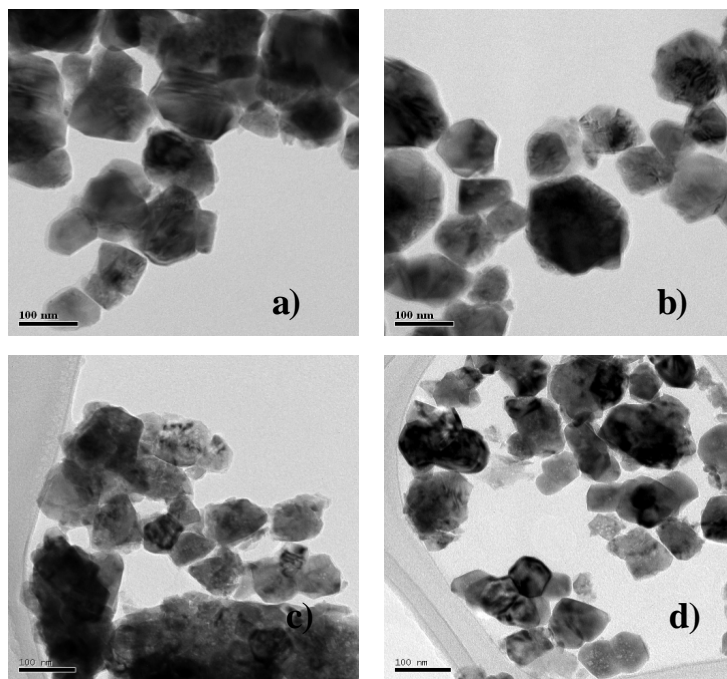
C. Angeles-Chavez,<sup>2</sup> and D. Solis<sup>1</sup>

<sup>1</sup> Centro de Investigaciones en Optica A.C. Departamento de Fotonica, 37150 León, Gto., Mexico.

<sup>2</sup> Instituto Mexicano del Petróleo, Programa de Simulación Molecular, 07730 Mexico, D.F., Mexico.

\*e-mail: ditlacio@cio.mx

The concentration luminescence quenching of the IR emission of  $\text{Yb}^{3+}$  in nanocrystalline  $\text{ZrO}_2$  is studied. It is found that the quenching is dominated by cooperative energy transfer processes from isolated  $\text{Yb}^{3+}$  ions to Yb-Yb pairs (Yb dimers). The Yb dimer concentration depends on the crystallite



TEM Images of  $\text{ZrO}_2:\text{Yb}^{3+}$  for different Yb concentrations:  
a) 0.5% b) 2% c) 4% d) 8% of Yb

phase and size, which on time depends on Yb concentration. An extended energy transfer model was developed to predict the IR and cooperative visible fluorescence emissions by taking in to account the crystalline phase, the nanocrystal size, and the geometrical construction of Yb dimers. Our model succeeds to fit simultaneously both experimental VIS and NIR emissions, and the corresponding interaction parameters are reported.

This work was partly supported by CONACYT through grants 46971-F and 43168-F. O. Meza and D. Solis acknowledge CONACYT by a PhD scholarship at Centro de Investigaciones en Optica A.C

## Atomic Force Microscopy (AFM) and Ellipsometry Study on Low Roughness (100) Silicon Surfaces

M. A. Vásquez-A.<sup>1\*</sup> G. Águila Rodríguez<sup>1</sup>, G. García-Salgado<sup>2</sup>,

G. Romero-Paredes R.<sup>1</sup>, and R. Peña-Sierra<sup>1</sup>

<sup>1</sup>*Departamento de Ingeniería Eléctrica, SEES, CINVESTAV-IPN*

*Av. IPN 2805, Col. Zacatenco, 07000 Mexico D. F., Mexico.*

<sup>2</sup>*Centro de Investigación en Dispositivos Semiconductores, BUAP, Puebla, Pue.*

*14 Sur y Av. San Claudio C.U., 72570 Mexico.*

\*e-mail: mava\_vasquez@yahoo.com

The research on microelectronics and nanotechnology makes use of silicon (Si) either as substrate or as a part of the compounds or alloys constituting the nanosized features <sup>1</sup>. In spite of the high volume data about silicon oxide (SiO<sub>2</sub>), the mechanisms involved in the growth of ultrathin SiO<sub>2</sub> films are even controversial <sup>2</sup>. The formation of SiO<sub>2</sub> films at lower temperatures is an intrinsic process and usually produces defective SiO<sub>2</sub>/Si interfaces<sup>3</sup>. The existence of native oxide films can produce deviations on the related refractive index values or can introduce strains on the growth films when used as substrate.

In this work the characterization of specially prepared low roughness Si surfaces are reported. The results are compared with surfaces after the typical RCA cleaning process. Two specially prepared Si surfaces were studied, one annealed under pure H<sub>2</sub> gas for 3 min. at 1000°C and the other under N<sub>2</sub> gas for a relatively longer time at 750°C. Results showed that both surfaces had distinct roughness, but the sample annealed under H<sub>2</sub> gas resulted with the lowest roughness. The influence of the native SiO<sub>2</sub>, considered as ultrathin SiO<sub>2</sub> film, in non-processed surfaces is discussed. AFM and Ellipsometry measurements were done on the different surfaces. The origins of the roughness are explained as a deviation from an singular surface. At the initial stage of the Si surface oxidation, the influence of the SiO and SiO<sub>2</sub> species are considered.

<sup>1</sup> R Bennowitz, J N Crain, A Kirakosian, J-L Lin, J L McChesney, D Y Petrovykh and F J Himpsel., "Atomic scale memory at a silicon surface", *Nanotechnology* **13**(2002)499-502.

<sup>2</sup> E. Tradif, A. Chabli, A. Danel, N. Rochat, and M. Veillerot, "Thermal evolution of Chemical Oxides and (100) silicon at 300°C in ambient air as seen by Attenuated Total Reflection Infrared Spectroscopy", *J. Electrochem. Society*, **150**(2003)G333-G338.

<sup>3</sup> A.H. Carim and R. Sinclair, "The evolution of Si/SiO<sub>2</sub> interface roughness", *J. Electrochem. Society*, **134**(1987)741-46.

## Silver Doped-TiO<sub>2</sub> Crystalline Nanocomposites for Slurry Photo- Decomposition of 2, 4 D

O. Vázquez-Cuchillo<sup>2,3\*</sup>, V. Rodríguez-González<sup>1</sup>, F. M. Morán-Pineda<sup>1</sup>,  
J. Hernández-Fernandez<sup>1</sup>, and R. Gómez<sup>2</sup>

<sup>1</sup>*Instituto Mexicano del Petróleo, Dirección de Investigación y Postgrado / Eje Central 152, C.P.  
07730 Mexico D. F. Mexico.*

<sup>2</sup>*Universidad Autónoma Metropolitana-I, Depto. de Química/Av. San Rafael Atlixco No 186,  
Mexico 09340, D.F. Mexico.*

<sup>3</sup>*Universidad Autónoma de Puebla, Facultad de Ingeniería Química 4 sur 104 Puebla, Pue.  
72000, Mexico.*

\*e-mail: ovazcu@siu.buap.mx

The present communication describes an innovative nanosemiconductor system, TiO<sub>2</sub>-Ag for UV photoassisted aqueous decomposition of 2,4-Dichlorophenoxyacetic acid (2,4-D). The doped composites have been synthesized by controlled sol-gel method using titanium alkoxide, silver acetylacetonate (Ac) and silver nitrate (NO<sub>3</sub>). Nanocrystalline anatase phase and Eg shift to the visible region was observed in doped samples. It is believed that when silver nitrate was used for doping TiO<sub>2</sub> some Ag<sup>1+</sup> could be inserted in to TiO<sub>2</sub> bulk creating titanium stoichiometric deficiency. The semiconductors materials exhibit enhanced photoactivity when compared with commercial TiO<sub>2</sub> P-25. The relative enhancement in the 2,4-D decomposition after 180 min of photodegradation follows the order TiO<sub>2</sub>-Ag (NO<sub>3</sub>) > TiO<sub>2</sub> > TiO<sub>2</sub>-Ag (Ac) > P-25. It was assumed that the combined effect generated between (Ti<sup>4+</sup>) vacancies and titania crystallite size is the responsible of the enhancement in the 2,4-D photodegradation.

*We would like to acknowledge the technical support of R. Velazquez Lara*



### **Preparation and Photocatalytic Activity of TiO<sub>2</sub> Clusters**

N. Huanosta P<sup>1</sup>., A. Viveros. R<sup>1</sup>., J.J. Sánchez-Mondragón<sup>2</sup>., C. Velásquez<sup>1</sup>,  
and A. Campero<sup>1</sup>

<sup>1</sup>*Universidad Autónoma Metropolitana-I, Department of Chemistry*

*P. O. Box 55-534, Mexico D. F. 09340.*

<sup>2</sup>*Photonics Laboratory, Optics Dept. INAOE, Puebla, Pue. 72000 Mexico.*

TiO<sub>2</sub> was prepared by hydrolysis condensation process titanium isopropoxide. The Transmission Electronic Microscopy (TEM) shows the product possessed, Absorbance spectra, FTIR spectra and are showed and photocatalytic activity of cumulus of TiO<sub>2</sub> could efficiently degrade methyl orange under irradiation UV light (366nm) and showed a stronger photocatalytic activity (time 19hs).

PI31

### **Synthesis and characterization of TiO<sub>2</sub> nanospheres and TiO<sub>2</sub> nanospheres with silver metallic, Obtained by the Sol-Gel Method.**

N. Huanosta P<sup>1</sup>., A. Viveros. R<sup>1</sup>., J. Sánchez-Mondragón<sup>2</sup>., C. Velásquez<sup>1</sup>,  
and A. Campero<sup>1</sup>

<sup>1</sup>*Universidad Autónoma Metropolitana-I, Department of Chemistry*

*P. O. Box 55-534, Mexico D. F. 09340.*

<sup>2</sup>*Photonics Laboratory, Optics Dept. INAOE, Puebla, Pue. 72000 Mexico.*

In this work, we present synthesis and characterization of TiO<sub>2</sub> nanospheres, pure and coated with metallic silver. The preparation was sol-gel method are showed for each of 3 cases in the present paper. Transmission Electronic Microscopy (TEM), showed size silver nanospheres varying in the range of 2-10 nm, TiO<sub>2</sub> nanospheres in the range of 720 -920 nm and the TiO<sub>2</sub>/Ag<sup>0</sup> about 0.6-2 μm. By FT-IR spectrums shows vibrations of O-H and Ti-O (3340 and 1650 cm<sup>-1</sup>), the UV-Vis of TiO<sub>2</sub>/Ag<sup>0</sup> shows a adsorption at 420 nm.

## Mechanochemically Synthesized CdS Nanoparticles Using a High-energy Mill

S. Velumani<sup>1\*</sup>, Erika Dutková<sup>2</sup>, Parviz Pourghahramani<sup>2</sup>, and Peter Baláž<sup>2</sup>

<sup>1</sup> *Department of Physics, Tecnológico de Monterrey, E.Garza Sada # 2501, Monterrey, CP 64849, Mexico* <sup>2</sup> *Institute of Geotechnics, Slovak Academy of Sciences, 043 53 Košice, Slovakia.*

<sup>3</sup> *Division of Mineral Processing, Luleå University of Technology, SE-971 87 Luleå, Sweden.*

\*e-mail:velu@itesm.mx

This paper describes the structural and surface properties of cadmium sulphide nanoparticles synthesized in a planetary mill. CdS nanoparticles were prepared by the mechanochemical route from cadmium acetate and sodium sulphide precursors. The structure of the as-prepared products was characterized by X-ray powder diffraction which reveals the crystalline nature of CdS nanoparticles. Cubic  $\beta$ -CdS (hawleyite) is the only product of mechanochemical synthesis. SEM, TEM and low temperature nitrogen sorption were used to analyze the particle size and morphology as well as surface composition. The SEM measurements show the aggregates of small nanocrystals in which particle sizes approximately of 2 nm were calculated by application of Williamson-Hall as well as Warren-Averbach method. The TEM confirms the aggregate formation of CdS nanoparticles due to the extremely small particle size and tendency to lower high surface energy. The optical properties of CdS nanoparticles were studied by UV-VIS spectroscopy. UV-VIS spectrum shows an obvious blue shift, which is the result of the quantum size effect. The main advantages of mechanochemical synthesis in the production of CdS nanoparticles is in the formation of uniform crystallites and particles with large surface area in comparison with CdS prepared by chemical route. The cadmium sulphide nanoparticles are obtained in the simple step, making the process attractive for industrial applications.

## **Characterization of Two Dimensional CdTe Nanostructures Prepared by Electrodeposition Technique**

S. Velumani<sup>1\*</sup>, J.L. Garza-Cantú<sup>1</sup>, G. Martínez<sup>1</sup>, C. Ángeles-Chávez<sup>2</sup>,  
and J.A.Chavez<sup>3</sup>

<sup>1</sup>*Department of Physics, TEC de Monterrey-Campus Monterrey, E.Garza Sada # 2501,  
Monterrey, Nuevo Leon, C.P.64849, Mexico.*

<sup>2</sup>*SIPPI, Instituto Mexicano del Petróleo, Eje Central, D.F.Mexico*

<sup>3</sup>*IIM-UNAM, Circuito interior, D.F.Mexico.*

\*e-mail: velu@itesm.mx

Two dimensional nanostructures of CdTe thin films were prepared by electrodeposition technique. Depositions were performed at constant temperature, concentration and time at different voltages. For all the deposited films the composition was found to be almost uniform with 50% cadmium and 50% telluride and a trend of decrease in the cadmium was observed with decrease in the deposition potential. SEM and AFM analysis showed that particle size increased as potential increased from -635mV to -595mV, while XRD analysis showed almost a uniform average particle size for all deposited films. SEM images showed a uniform deposition all over substrate while AFM revealed that in small scale, size distribution was very broad. Roughness didn't follow the same pattern, it had a maximum at -615mV, and it was explained as a consequence of Stranski-Krastanov growth. An optimum potential was found to be -615 mV, where a minimum grain size and maximum roughness were observed.

## **Synthesis and Characterization of ZrO<sub>2</sub> Nanospheres Obtained by the Sol-Gel Method**

A. Viveros. R<sup>1</sup>., N. Huanosta P<sup>1</sup>., J. Sánchez-Mondragón<sup>2</sup>., C. Velásquez<sup>1</sup>,  
and A. Campero<sup>1</sup>

<sup>1</sup>*Universidad Autónoma Metropolitana-I, Department of Chemistry*

*P. O. Box 55-534, Mexico D. F. 09340.*

<sup>2</sup>*Photonics Laboratory, Optics Dept. INAOE, Puebla, Pue. 72000 Mexico.*

In this work, we present synthesis and characterization of, ZrO<sub>2</sub> prepared by the hydrolysis condensation process of the zirconium (IV) butoxide, the TEM characterization shows nanospheres with diameter average 43.5 nm. The FT-IR spectra show vibrations of O-H and Ti-O (3340 and 1023, 472 cm<sup>-1</sup>).

## **Synthesis of Hybrid Coating of Polymethylmethacrylate-Silica and their Characterization by Nanoindentation**

J.L. Almaral-Sanchez<sup>1</sup>, E. Rubio-Rosas<sup>2,3\*</sup>, V. Rodríguez-Lugo<sup>2</sup>,  
and R. Ramirez-Bon<sup>4</sup>

<sup>1</sup> *Universidad Autónoma de Sinaloa, Fuente de Poseidon y Prol. Angel Flores, S.N., C.P. 81223.  
Los Mochis Sin., Mexico.*

<sup>2</sup> *Centro Universitario de Vinculación, Benemérita Universidad Autónoma de Puebla.  
Prolongación 24 Sur. Col. San Manuel. C. P. 72570. Puebla, Pue. Mexico.*

<sup>3</sup> *Facultad de Ingeniería Química, Benemérita Universidad Autónoma de Puebla.*

<sup>4</sup> *Centro de Investigación y Estudios Avanzados del Instituto Politécnico Nacional (IPN) Unidad  
Queretaro Apdo. Postal 1-798, 7600. Queretaro, Qro., Mexico.*

\*e-mail: efrain.rubio@cuv.buap.mx

Hybrid coatings combine the flexibility and easy processing of polymers with hardness of inorganic materials and have been successfully applied on glass, metal and polymeric substrates. In general, these hybrid coatings are transparent, show a good adhesion, and enhance the scratch and abrasion resistant of a polymeric substrate. On the other hand, sol-gel process is known to be very attractive to design organic-inorganic hybrid materials. Moreover, this process allows the easy deposition of thin films directly from the solution by techniques such as dip coating, spin-coating or spray-coating. In this work, hybrid silica- polymethylmethacrylate coatings were prepared from methyl methacrylate, water based colloidal silica and a coupling agent. The hybrids coatings were chemically and physically characterized using, FTIR spectroscopy, scanning electron microscopy, and two different depth sensing indentation systems. From the indentation measurements we found that the mechanical properties of the hybrid coatings were improved in comparison with those of conventional acrylics. Hardness of the hybrid coatings was from three times to more than one order of magnitude higher than the acrylic hardness, depending on the molar ratio.

## **Cobalt Oxide Films Obtained by Pulsed-Injection Chemical Vapor Deposition**

**E. Rubio**<sup>1,2\*</sup>, L.M. Apátiga<sup>3</sup>, V. Rodríguez Lugo<sup>1</sup> and V.M. Castaño<sup>3</sup>

<sup>1</sup> *Centro Universitario de Vinculación, Benemérita Universidad Autónoma de Puebla.*

*Prolongación 24 Sur. Col. San Manuel. C. P. 72570. Puebla, Pue. Mexico.*

<sup>2</sup> *Facultad de Ingeniería Química, Benemérita Universidad Autónoma de Puebla.*

<sup>3</sup> *Centro de Física Aplicada y Tecnología Avanzada, UNAM, A.P. 1-1010, C.P. 76001, Querétaro, Qro., Mexico.*

\*e-mail: efrain.rubio@cuv.buap.mx

Cobalt oxide films were deposited by pulsed-injection Chemical Vapor Deposition from a metalorganic precursor (MOCVD). By using cobalt (II) acetylacetonate as the metalorganic precursor, oxygen as the reactant gas and argon as the carrier gas, cobalt oxide films were deposited on Si (100) wafers at 650 °C. The pulsed-injection MOCVD reactor is based in a principle of formation from metalorganic precursor in vapor phase allowing the formation of oxide layers and multilayers by using small micro-doses of precursors mixed in an organic solvent. The precise micro-doses of such solution are injected through a computer-driven system into the evaporation zone, where they instantly evaporate (flash evaporation), so there is no time for chemical changes of the precursor. The resulting vapor mixture is transported by a carrier gas into the high temperature reaction chamber, where the reactant gas flows and the decomposition reaction and film growth on the hot substrate occurs. The X-ray diffraction (XRD) patterns displays a clear preference for the (311) orientation, which is a characteristic reflection in the crystalline Co<sub>3</sub>O<sub>4</sub> phase, meanwhile the Atomic Force Microscopy (AFM) studies show a film surface formed densely, uniformly and homogeneously along the Si substrate. All films were black-grayish in color, pin-hole free, and strongly adherent to the substrate surface.

## Synthesis of Size Selective SiO<sub>2</sub> Colloidal Spheres

D. Cornejo-Monroy<sup>1</sup>, J. F. Sánchez-Ramírez<sup>1\*</sup>, E. Espíndola<sup>2</sup>, and U. Pal<sup>3</sup>

<sup>1</sup>*CICATA-IPN, Legaria # 694, Col. Irrigación, 11500 Mexico D.F., Mexico.*

<sup>2</sup>*Escuela Nacional de Ciencias Biológicas, Instituto Politécnico Nacional.*

<sup>3</sup>*Instituto de Física, Universidad Autónoma de Puebla, Apdo. Postal J-48, Puebla, Pue. 72570, Mexico.*

\* e-mail: jfsanchez@ipn.mx

Size selective colloidal SiO<sub>2</sub> spheres were prepared through hydrolysis of tetraethyl orthosilicate (TEOS) in methanol - buthanol (4:1) solvent. Controlling the concentration of ammonium hydroxide in the reaction mixture, SiO<sub>2</sub> spheres of 400 - 25 nm sizes could be synthesized. Transmission electron microscopy (TEM) observation revealed that the SiO<sub>2</sub> spheres are monodispersed. The results indicate that a higher concentration of ammonium hydroxide restricts the formation of higher number of nuclei and consequently forming bigger particles. Fourier transform infrared (FTIR) spectra of the samples confirmed the composition of the samples as SiO<sub>2</sub>.

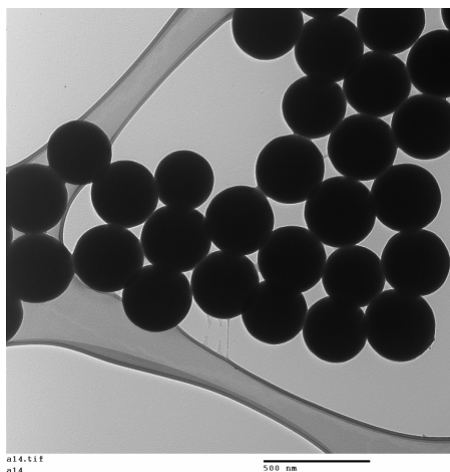


**Figure 1.** TEM image of SiO<sub>2</sub> particles of 317 nm average size.

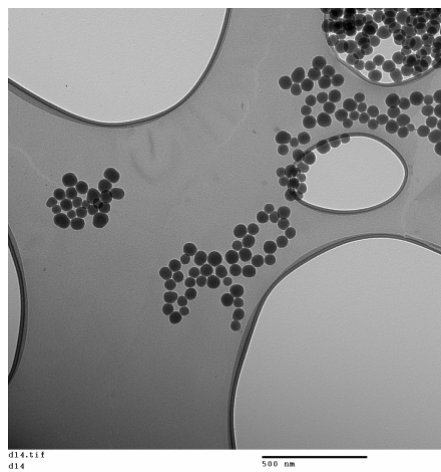


**Figure 2.** TEM image of SiO<sub>2</sub> particles of 54 nm average size.

*The authors are thankful to the Mexican Agencies, CONACYT, CGPI-IPN for financial supports.*

## Synthesis and Characterization of $\text{Mg}(\text{OH})_2$ Nanoparticles under Mild Reaction Conditions

Yolia León-Paredes,<sup>1</sup> Alicia Díaz<sup>2</sup>, Silvia Castillo-Blum<sup>1</sup>, and David Díaz<sup>1\*</sup>,

<sup>1</sup> *Facultad de Química. Universidad Nacional Autónoma de México. México D. F., CP 04510, México.*

<sup>2</sup> *Facultad de Química. Universidad de La Habana, CP 10400, C. Habana. Cuba.*

\*e-mail: david@servidor.unam.mx

Magnesium hydroxide (brucite) is a common precursor for the preparation of MgO (periclase). MgO is an important material used in heterogeneous catalysis for the organophosphorous compounds degradation. One of the reported methods for obtaining metal oxides is based on the

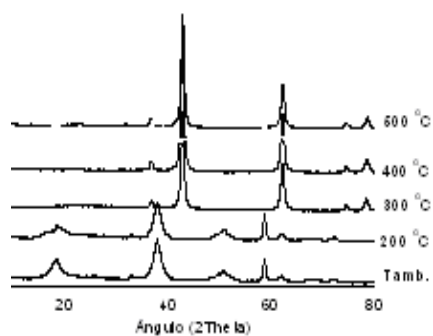


Figure 1

sol-gel technique<sup>1</sup>. In many cases this method requires a hypercritical drying procedure and employs hazardous metal-organic precursors. Here we present an easy  $\text{Mg}(\text{OH})_2$  nanoparticles synthesis method, *via* the spontaneous hydrolysis of ~~the~~ magnesium acetate ~~salt~~, in DMSO and DMF<sup>2</sup>. Different reaction conditions to prepare nanostructured  $\text{Mg}(\text{OH})_2$  were investigated. When  $\text{Mg}(\text{OH})_2$  DMSO colloidal dispersions are irradiated at

280 nm, an intensive emission band, centered at 330 nm is observed. Different spectroscopic techniques, such as FTIR, electronic emission and XRD were used for the  $\text{Mg}(\text{OH})_2$  colloids characterization. The XRD patterns of  $\text{Mg}(\text{OH})_2$  at room temperature and after heating it at different temperatures are shown in Figure 1. The corresponding average particle size for  $\text{Mg}(\text{OH})_2$  is close to 15 nm.

<sup>1</sup> V. Štengl, S. Bakardjieva, M. Maríková, P. Bezdička, J. Šubrt, *Magnesium oxide nanoparticles prepared by ultrasound enhanced hydrolysis of Mg-alkoxides*, Materials Letters 57 (2003) 3998.

<sup>2</sup> G. Rodríguez-Gattorno, P. Santiago-Jacinto, L. Rendon-Vázquez, J. Nemeth, I. Dekany, and D. Díaz\*, *Novel Synthesis Pathway of ZnO Nanoparticles from the Spontaneous Hydrolysis of Zinc Carboxylate Salts*, J. Phys. Chem. B. 107, (2003) 12597.



## Characterization of $\text{Al}_x\text{Ga}_{1-x}\text{Sb}$ Structures Grown by Liquid Phase Epitaxy

J. Martínez-Juárez<sup>a\*</sup>, G. Juárez-Díaz<sup>b</sup>, F. De Anda<sup>c</sup>, A. M. Jiménez-Fuentes<sup>a</sup>,  
G. García<sup>a</sup>, and D. Hernández de la Luz<sup>a</sup>

<sup>a</sup>*Centro de Investigación en Dispositivos Semiconductores, BUAP, Puebla, Pue. 14 Sur y Av. San Claudio C.U., C.P. 72570.*

<sup>b</sup>*Depto. de Ingeniería Eléctrica, Sección de Electrónica del Estado Sólido, Centro de Investigación y de Estudios Avanzados del I.P.N., A.P. 14-740, 07000 Mexico D.F., Mexico.*

<sup>c</sup>*IICO-UASLP Av. Karakorum 1470, Lomas Cuarta Sección, SLP, C.P. 78210.*

\*e-mail: javier.martinez@icbuap.buap.mx

$\text{Al}_x\text{Ga}_{1-x}\text{Sb}$  films p-type and n-type were grown on GaSb substrates n-type by Liquid Phase Epitaxy (LPE) with a temperature of 400 °C, with them structures type p-AlGaSb/n-AlGaSb/Substrate were fabricated. The composition of p-type film was varied from 5 to 20 % in aluminum content while the composition of n-type film was keeping constant. The thickness of the obtained films were 4 and 6  $\mu\text{m}$ , respectively. Photoluminescence (PL) and High Resolution X-Ray Diffraction(HRXRD) measurements were realized to determine the real composition of the films as well as the structure quality, the PL spectra shows the band to band transitions of structures material also excitonic and band to impurity level transitions. In addition, were made electrical measurements to determine the effect of p-type film composition on electrical performance of the structure.

## **Analysis of the Propagation of Low Dimensional Optical Wave**

A. Luis-Ramos\*, J.L. Lampallas, and L.C. Gómez-Pavón

*Benemérita Universidad Autónoma de Puebla*

*Facultad de Ciencias de la Electrónica*

*Av. San Claudio y 18 Sur (CU) Edificio 181-220. Col. San Manuel, 72570, Puebla, Pue.*

*Mexico.*

\*e-mail: [aluis@ece.buap.mx](mailto:aluis@ece.buap.mx)

The smallest diameter of an optical beam is of the order of a wavelength due to diffraction even in a waveguide. Having a way to decrease the smallest beam diameter without a diffractive limit, it is a contribution to optical devices and optical measurements in the nanometer range.

Optical waves with one or two dimension can be very useful to create nano-waveguides which could be used in the fabrication of optical circuits with nanometer-scale devices, these nano-optical circuits are needed to satisfy the increasing demands for capacity of the optical communication industry. Another important potential application of 1D optical waveguides in the future could be as a high-efficiency optical probe with high resolution.

In this work we present a theoretical and computational analysis of propagation of low dimensional optical waves using symbolic computational support (MAPLE). Also we laid the foundations for late studies for more complex structures.

## Synthesis of True Au-Ag Alloy Nanoclusters with Controlled Composition

L. Nolasco-Hernández<sup>1,2</sup>, J. F. Sánchez-Ramírez<sup>1\*</sup>, J. A. Pescador-Rojas<sup>1</sup>, U. Pal<sup>2</sup>,  
and P. Santiago<sup>3</sup>

<sup>1</sup> CICATA-IPN, Legaría 694, Col. Irrigación, 11500 Mexico D.F., Mexico.

<sup>2</sup> Instituto de Física, Universidad Autónoma de Puebla, Apdo. Postal J-48, Puebla, Pue. 72570, Mexico.

<sup>3</sup> Instituto de Física, Universidad Nacional Autónoma de México, A.P. 20-365, C.P. 01000, Mexico.

\*e-mail: jfsanchez@ipn.mx

Colloidal  $\text{Au}_x\text{Ag}_{1-x}$  solid solution alloy nanoclusters of different compositions ( $0.1 \leq x \leq 0.9$ ) were synthesized through citrate reduction technique without using any other protective or capping agent. Optical absorption of the alloy nanoclusters was studied both theoretically and experimentally. The position of the surface plasmon resonance (SPR) absorption band of the nanoclusters could be tuned from 419 nm to 521 nm through the variation of their composition. Considering effective dielectric constant of the alloy, optical absorption spectra for the nanoclusters were calculated using Mie theory, and compared with the experimentally obtained spectra. Theoretically obtained optical spectra resembled well with the experimental spectra. High resolution transmission electron microscopy (HRTEM) and high angle annular dark field (HAADF) imaging revealed the true alloy structure of the nanoparticles. Mechanism of formation of homogeneous alloy structures with precise tuning their SPR band is discussed.

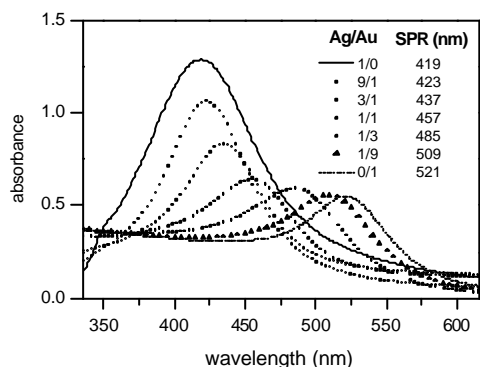


**Figure 1.** Absorption spectra of the bimetallic colloidal dispersions of Au-Ag with different molar ratios, prepared by reducing the metal ion solutions of total concentration 1.32 mM (solubility product  $< 6.9 \times 10^{-12}$ )

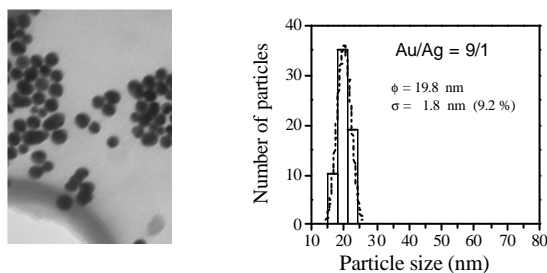


**Figure 2.** Transmission electron micrographs and particle size of bimetallic nanoparticles: Au/Ag = 9/1.

The authors are thankful to the Mexican Agencies, CONACYT, CGPI-IPN for financial supports

## Effect of pH-Adjusted on the Formation and Structure of Gold Nanoparticles

R. Esparza<sup>1,\*</sup>, G. Rosas<sup>1</sup>, M. López-Fuentes<sup>2</sup>, U. Pal<sup>2</sup>, and R. Pérez<sup>3</sup>

<sup>1</sup>*Instituto de Investigaciones Metalúrgicas, UMSNH, Edificio U, Ciudad Universitaria, Morelia, Mich. 58000, Mexico.*

<sup>2</sup>*Instituto de Física, Universidad Autónoma de Puebla, Apdo. Postal J-48, Puebla, Pue. 72570, Mexico.*

<sup>3</sup>*Instituto de Ciencias Físicas, Universidad Nacional Autónoma de Mexico, P. O. Box 48-3, Cuernavaca, Mor. Mexico.*

\*e-mail: roesparza@gmail.com

Nowadays, the attention of many scientists is focused on the development of new methods for synthesis and stabilization of metal nanoparticles. Moreover, special attention is paid to monodispersed particles with a great degree of control over size, structure and composition. Chemical reduction is used most extensively in the liquid phase, including aqueous and nonaqueous media. The wide application of this method stems from its simplicity and availability. In this work, we presented the synthesis of gold particles by the technique of chemical reduction. Particles with different pH reaction mixtures have been synthesized. The structure, morphology and compositions of the nanoparticles were obtained using high resolution electron microscopy. Depending of the pH reaction mixtures different nanometric sizes and consequently different atomic structural configurations of the particles are obtained. The nanoparticles synthesized were approximately 2 - 10 nm in size. The main structures produced were fcc-like and decahedral, when a low final pH and high final pH reaction mixtures was used, respectively.

## Synthesis of Monodispersed Au-Pd Bimetallic Nanoparticles of Core-Shell and Alloy Structures

L. Ruiz Peralta, U. Pal, and P. Santiago

*Instituto de Física, Benemérita Universidad Autónoma de Puebla, Adpo. J-48,*

*CP 72570, Puebla, Pue., Mexico.*

e-mail: mruizp@sirio.ifuap.buap.mx

Monodispersed bimetallic Au-Pd nanoparticles of core-shell and alloy structures were synthesized in water without using any polymer protector. Using sodium citrate and ascorbic acid as reducing agents, stable monometallic Au and Pd seeds of different sizes could be prepared by controlling the concentration of metal ions in the reaction mixtures. While for core-shell structures, successive reduction technique with pre-prepared monometallic seed was used, for bimetallic alloy structures, both the metal ions were reduced simultaneously. It is seen that due to very different reduction potential of Au and Pd ions, the synthesis parameters have to be controlled critically to prepare their alloy or core-shell structures through citrate reduction process.

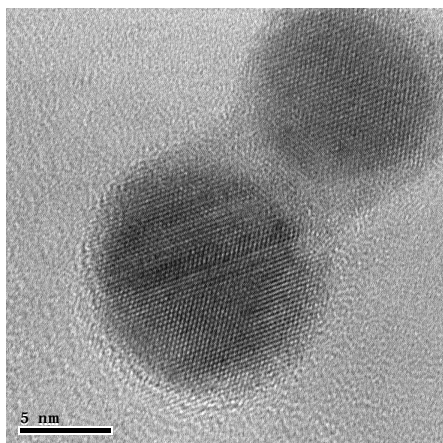


**Fig. 1.** A typical HREM image of Au-core/Pd-shell nanoparticles

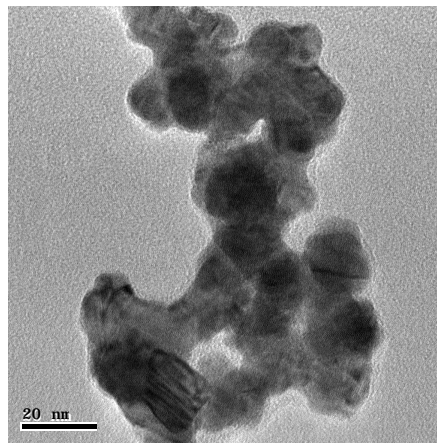


**Fig. 2.** Typical TEM image of Au-Pd (1:1) alloy nanoparticles.

*The work was partially supported by CONACyT, Mexico (Grant # 46269) and VIEP, BUAP. LR. Peralta acknowledges CONACyT, Mexico for extending fellowship.*

## Obtención de Nanopartículas de Au-Pd por Deposición Física de Plasma

M. Rosario Mendieta-Anzúrez<sup>1</sup> and García Bórquez<sup>1</sup>

<sup>1</sup>*Ciencia de los Materiales, ESFM-IPN, U.P. “Adolfo López Mateos”*

*C.P. 07738, Mexico D.F.*

e-mail: mabdel\_ross@[yahoo.com.mx](mailto:mabdel_ross@yahoo.com.mx)

La deposición física de vapor son procesos de deposición atomística, en la cual el material es vaporizado de una fuente sólida o líquida en forma de átomos o moléculas y es transportada en forma de vapor a través de vacío o plasma hacia el sustrato, donde se condensa. Se puede obtener deposición molecular o particulada. La razón de deposición se encuentra en el orden de 1-10 nm por segundo. Las nanopartículas metálicas con tamaños inferiores a los 10 nm han demostrado efectividad como catalizadores, pueden ser aprovechadas en diversas áreas<sup>1</sup> y para la protección ambiental<sup>2</sup>.

La obtención de nanopartículas ha abierto un campo de investigación muy amplio que podemos dividir esencialmente en dos métodos de deposición: químico y físico. Entre los métodos químicos tenemos: “Spray” Pirólisis, Chemical Vapor Deposition (CVD)<sup>3</sup> y Chemical Liquid Deposition (CLD)<sup>4</sup>, entre otros. Sin embargo cada uno de estos métodos presenta diferentes variables como: presión de la cámara, presión de vacío, temperatura del sustrato, morfología del sustrato, distancia del blanco a la muestra y tiempo de deposición.

Las nanopartículas de Au-Pd estudiadas en este trabajo, fueron obtenidas mediante deposición de plasma. Por microscopía electrónica de transmisión se observa que el tamaño de partícula es menor a los 10 nm y la distancia entre ellas oscila entre 5 y 15 nm. La mayoría tiene forma facetada y solo algunas se encuentran aglomeradas.

---

<sup>1</sup> Sergio Mejía Rosales, et. al. “*Dinámica molecular de nanopartículas de oro-paladio*”. Ciencia UANL Vol. IX, No. 1 (2006).

<sup>2</sup> Comisión Europea. Oficina de Publicación Oficial de las Comunidades Europeas. “*La nanotecnología innovaciones para el mundo del mañana*”. 56 p. (2004).

<sup>3</sup> Donald M. Mattox. “*Handbook of Physical Vapor Deposition (PVD) Processing*”. Noyes Publication (1998).

<sup>4</sup> Galo Cardenas T., Rodrigo Segura D. “*Synthesis and properties of Au-Pd bimetallic colloids*”. Materials Research Bulletin 35 (2000) 1369–1379.

## Grain Size Homogeneity in Metallic-oxides Prepared by Sol-Gel Acrylamide Polimerization

B. Salas<sup>1</sup>, S. Rodríguez<sup>1</sup>, A. Ordoñez<sup>1</sup>, G. Herrera<sup>2</sup>, and E. Chavira<sup>1</sup>

<sup>1</sup>*Instituto de Investigaciones en Materiales, Universidad Nacional Autónoma de Mexico AP 70-360, 04510 Mexico D. F.*

<sup>2</sup>*Instituto de Ciencias Nucleares, Universidad Nacional Autónoma de Mexico AP 70-360, 04510 Mexico D. F.*

e-mail: guillermo.herrera@nucleares.unam.mx

The most important contribution of sol-gel acrylamide polimerization<sup>1</sup> as a synthesis method is to get an excellent homogenization of grain size in comparison with the traditional sol-gel route. We followed the evolution of grain size in isolated systems such as  $YVO_4$  (JCPDS 72-0274),  $LaVO_4$ ,  $Y_2Ti_2O_7$  (JCPDS 42-0413) and  $La_2Ti_2O_7$  (JCPDS 70-1690) under several heat treatments, also magnetic materials such as  $Sr_2Fe(Mo_{1-x}Re_x)O_{6\pm z}$  (JCPDS 39-0954) where  $x = 0.2-0.8$  and  $SrMoO_3$  (JCPDS 85-0586). By thermogravimetric and differential thermal analysis (TGA and DTA) we determined the temperature where start the formation of nanocrystals, also we can determine the range of temperatures of the denaturalization of organic part (400-600 °C). X-Ray Diffraction patterns (XRD) for those compounds are in agreement with the respective phase reported in the standard XRD cards. Infrared spectroscopy was used to evaluate the organic residues at the end of synthesis step. Atomic force microscopy images of gel reveals small grains with sizes between 4-12 nm. Scanning electron microscopy (SEM) micrographs in powders showed small and uniform grains with sizes between 20-60 nm. In xerogel of  $Sr_2Fe(Mo_{1-x}Re_x)O_{6\pm z}$  the porosity varies between 2-20 μm. The results of the quantitative electron dispersive X-ray (EDX) analysis indicate that the measured atomic percentage is in agreement with the compound stoichiometry. Xerogel and powders were analyzed by transmission electron microscopy (TEM). TEM results are in agreement with XRD.

*We acknowledge the partial financial supports of UNAM-PAPITT (IN102203) and CONACyT.*

---

<sup>1</sup> A. Sin and P. Odier. "Gelation by Acrylamide, a Quasi-Universal Medium for the Synthesis of Fine Oxide Powders for Electroceramic Applications". Adv. Mater. 12, 9, (2000) 649-652.

## Platinum Nanoparticles Synthesized into Alumina Template

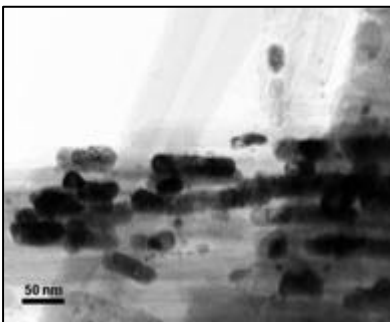
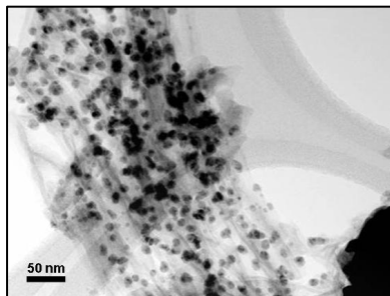
C. Reza-San Germán<sup>1</sup>, P. Santiago<sup>2</sup>, and M. A. Valenzuela<sup>1</sup>

<sup>1</sup>*Instituto Politécnico Nacional-ESIQIE, Lab. Catálisis, Edif. Z, 1er Piso, Sec. 6, Mexico, 07738, Mexico.*

<sup>2</sup>*Instituto de Física, Universidad Nacional Autónoma de Mexico, Apdo. Postal 20-365, Mexico D.F., Mexico.*

e-mail: creza@ipn.mx

A method for preparing Pt-inserted alumina template was reported. By suction of Platinum Acetylacetonate- dimethyl formamidesolution into the nanochannels first and annealed with a N<sub>2</sub>/H<sub>2</sub> flow at 400 to 600°C for 1 h afterwards, Pt nanoparticles formed in the nanotubes. The size and morphology of Pt nanoparticles are controlled by the dimensions of nanotubes, precursor concentration, time of reaction and gas flow. Some of them are spherical, some are nanorods. SEM and TEM results revealed this difference. The nanoporous alumina templates have been produced by anodization of aluminum<sup>1</sup>. Nanoparticles and nanorods with diameters ranging from



10 to 50 nm and lengths in nanorods of ~50 μm can be produced. When changing some synthesis conditions we could vary the crystal growth and therefore dependent upon particle size and morphology<sup>2,3,4</sup>. Also we suggest that particle size and morphology will be dependent of phase transition. This difference allows us to prepare nanoparticles and nanorods by porous alumina template. It will be shown that this fabrication method yields extremely high quality crystalline nanostructures.

**Fig.1.** Nanoparticles(a) and nanorods(b) synthesized by mold method

We would like to acknowledge CUDI Mexico for support this project through the inter-institutional IMP-IFUNAM project and the Catalysis and Materials Laboratory (IPN-ESIQIE).

<sup>1</sup> C. Zelenski and P. Dorhout. J. Am. Chem. Soc., 120, 734 (1998).

<sup>2</sup> Carl C. Koch, Nanostructured Materials, 2<sup>nd</sup> edition, Ed. William Andrew (2007).

<sup>3</sup> Tapesha Yadav, Patent Application Publication, US2006/0248982 A1, (2006)

<sup>4</sup> Xinqi Ma, Caixia Feng, Zhensheng Jin, Xinyong Guo, Jianjun Yang and Zhijun Zhang, Journal of Nanoparticle Research 7: 681–683, (2005)



## **Influence of Oxygen on the Optical Properties of Gold Nanoparticles**

**V. M. Renteña-Tapia<sup>1</sup> and J. García-Macedo<sup>1</sup>**

<sup>1</sup> *Departamento de Estado Sólido. Instituto de Física, Universidad Nacional Autónoma de México, Apartado Postal 20-364, 01000, México, D. F.*

e-mail: gamaj@fisica.unam.mx

Gold nanoparticles in sol-gel silica films were annealed in hydrogen atmosphere and subsequently in oxygen atmosphere. The optical properties of these metallic nanoparticles were measured by UV-vis spectroscopy. The experimental optical spectra of the samples prepared in a reducing atmosphere exhibited a surface plasmon resonance located at 531 nm, typical of gold nanoparticles in silica films. On the opposite side, the gold nanoparticles in an oxidizing atmosphere exhibited a strong diminution of the surface plasmon resonance. These optical properties were explained due to the complete oxidation of gold nanoparticles to gold ions yield in an oxygen atmosphere. The experimental observations were modeled by means of the Gans theory. So, this study shows that the interaction between oxygen and the metallic surface of the nanoparticles sensitively alters the optical properties of the sol-gel films.

*The authors wish to thank to Conacyt (Mexico) Project 43226 and Conacyt postdoctoral fellowships and DGAPA UNAM IN 111902.*

## In-situ Formation of Ag & Ag<sub>2</sub>S Nanoparticles in Polymer Matrix by Novel Polymer-Inorganic Solid State Reaction

Sujata Waghmare<sup>1</sup>, Ranjit Hawaldar<sup>2</sup>, N. Koteswara Rao<sup>3</sup>, Uttam Mulik<sup>2</sup>,  
and Dinesh Amalnerkar<sup>2\*</sup>

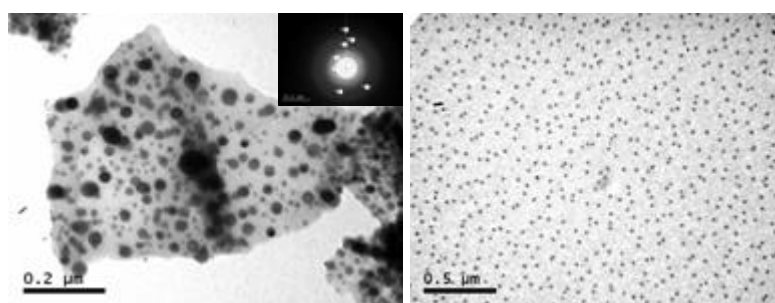
<sup>1</sup>*Abasaheb Garware College, Karve Road, Pune-411004, India.*

<sup>2</sup>*Center for Materials for Electronics Technology, Panchawati, Off Pashan Road Pune-411008, India.*

<sup>3</sup>*National Chemical Laboratory, Pune-411008, India.*

\*e-mail: dpa54@yahoo.co.in

We herein report the feasibility of polymer-inorganic solid-state reaction route for the insitu generation of Ag & Ag<sub>2</sub>S nanostructures in polymer network wherein the engineering thermoplastic polymer polyphenylene sulphide (PPS) itself acts as a chalcogen source as well as a stabilizing matrix. Typical solid-state reaction was accomplished by simply heating the physical admixture of the 2 reactants i.e AgNO<sub>3</sub> and PPS in unimolar ratio at the crystalline melting temperature (285 °C) of PPS. The resultant product was characterized by X-Ray Diffractometry (XRD), Scanning Electron Microscopy (SEM) and Transmission Electron Microscopy (TEM) with selected area electron diffraction (SAED). The TEM-SAED analysis reveals the formation of nanosized Ag<sub>2</sub>S with average particle size around 70 nm. However, XRD studies indicate the



formation of cubic Ag in addition to monoclinic Ag<sub>2</sub>S in cyclized PPS matrix. The prima facie observations indicate the apparent formation of crystalline silver in the bulk (as inferred

from sharp peaks pertaining to Ag in XRD pattern) while that of nanocrystalline Ag<sub>2</sub>S confined to surface (as implied by TEM-SAED analysis).

<sup>1</sup> "Novel polymer –inorganic solid-state reaction for the synthesis of CdS nanocrystallites" K.G. Kanade, R.R. Hawaldar, R. Pasricha, S. Radhakrishnan, T. Seth, U.P. Mulik, B.B. Kale & D.P. Amalnerkar, *Materials Letters*, 59/5, 554 (2005).

<sup>2</sup> "Nano-CdS by polymer –inorganic solid-state reaction: Visible light pristine photocatalyst for Hydrogen generation", K.G. Kanade, Jin-Ook Baeg, U.P. Mulik, D.P. Amalnerkar, B.B. Kale, *Materials Research Bulletin*, 41/12, 2219 (2006).

## Optical and Surface Morphology Characterization of Nanometric Palladium Films on Silicon Substrates Annealed in Hydrogen Atmosphere

C. López-Rodríguez<sup>1,2</sup>, M. Galván-Arellano<sup>1</sup>, R. Peña-Sierra<sup>1</sup>, G. Romero-Paredes<sup>1</sup>,  
and A. Morales-Hernández<sup>3</sup>

<sup>1</sup> *Departamento de Ingeniería Eléctrica, Sección de Electrónica del Estado Sólido (SEES) Centro de Investigación y Estudios Avanzados del I.P.N.(CINVESTAV) Av. I.P.N. 2508, Apartado Postal 14-740, 07000, Mexico D.F. Tel. (01) 50613777, <sup>2</sup> Escuela Superior de Computo (ESCOM), I.P.N. Mexico D.F., Tel. (01) 57296000 Ext. 52022, <sup>3</sup> Unidad Profesional Interdisciplinaria en Ingeniería y Tecnología Avanzada (UPIITA) I.P.N. Mexico D.F., Tel. (01) 57296000 Ext. 56846.*

e-mail: vancla01@hotmail.com, agusmora@hotmail.com

Palladium-hydrogen systems have been extensively studied since the discovery in 1886 by Graham<sup>1</sup> of the ability of Pd to absorb relatively large amounts of hydrogen (H<sub>2</sub>)<sup>2</sup>. The Pd either as nanoparticles or continuous films is very attractive for H<sub>2</sub> storage and some other important technological applications. The joining of the Pd capability of absorbing huge quantities of H<sub>2</sub> with the advanced silicon (Si) integrated circuits technology is a very important task<sup>3</sup>. In this work the ability of Pd films deposited on Si substrates towards H<sub>2</sub> absorption was studied. The influence of the hydrogen (H<sub>2</sub>) loading on nanometric Pd films over their optical properties and surface characteristics was studied. The Pd films were grown on (100) silicon substrates by the electroless method<sup>4</sup> where the use of an electrolytic bath containing HF guarantees a free oxide Pd/Si interface. The H<sub>2</sub> loading was realized by annealing of the Pd films in a pure H<sub>2</sub> atmosphere at 585 torr over the temperature range of 200 to 500 °C. The initial thickness of the Pd films was chosen under 40 nm to observe incomplete covering effects. The deviation on the Pd films thickness and the refractive index was measured by the multiple angle ellipsometry technique. The value of the refractive index was used as indication of the H<sub>2</sub> loading. The refractive index is related to the existence of the phases  $\alpha$  and  $\beta$  in the Pd-H system. The surface characteristics of the Pd films were studied by Atomic Force Microscopy measurements.

---

<sup>1</sup> Graham, T., 1869, Proc.. Roy. Soc., 17, 212.

<sup>2</sup> Alefeld, G., and Völkl, J. 1978, Hydrogen in Metals I and II, vols. 28 and 29, series Topics in Applied Physics (Berlin: Springer-Verlag).

<sup>3</sup> Seals, L., Gole, J. L., and Tse, L. A., "Rapid, reversible sensitive porous silicon gas sensors", Journal of Applied Physics, 91, 4, 2519-2523, 15 feb. 2002.

<sup>4</sup> López, C., Pedrero, L., Peña, R., and Romero, G., Study of the optical properties of nanometric Palladium Films grown on silicon substrates by electroless", Proceedings of 2<sup>nd</sup> International Conference on Electrical and Electronics Engineering (ICEEE) and XI Conference on Electrical Engineering (CIE 2005), 428-421, Mexico City, Mexico September 7-9, 2005.

## **Analysis of Ag Nanoparticles Synthesized by Bioreduction. Searching Candidates of Active Nanocomposites for Gas Separation**

L. Tavera-Davila,<sup>1,2</sup> G. Canizal,<sup>3</sup> M. Balcazar,<sup>4</sup> R. Herrera-Becerra<sup>5</sup>,  
and J. A. Ascencio<sup>1,2\*</sup>

<sup>1</sup> *Facultad de Química. Universidad Autónoma del Estado de Mexico. Paseo Colón Esq. Con Paseo Tollocan, Toluca, Estado de Mexico. C.P. 50160. Mexico.*

<sup>2</sup> *Instituto Mexicano del Petróleo. Lázaro Cárdenas 152, Col San Bartolo Atepehuacan. Mexico Distrito Federal, C.P. 07730, Mexico.*

<sup>3</sup> *CECD, IPN, Allende No. 38, Centro, Mexico D.F. 06010, Mexico.*

<sup>4</sup> *ININ. Carr. Mex-Tol, s/n Ocoyoacac, Mexico. C.P.*

<sup>5</sup> *IFUNAM, A. P. 20-364, Mexico, Distrito Federal., C.P. 05500, Mexico.*

\*e-mail; ascencio@imp.mx

Ag metal nanoparticles were biosynthesized with the control of pH conditions as the main variable to generate the most of the particles (big density) and the small dispersion in size and structure. The structural characterizations were performed by high resolution transmission electron microscope and energy dispersive spectroscopy. The size distribution, clusters density, structures and elemental distribution were studied for the synthesized samples. Molecular simulation methods based on quantum mechanics have been applied to acquire the further information on their structural stability, electronic properties etc. The results show that the particle size for the pH=10 was the optimum, with a distribution around 4 nm and the most dense samples. By the analysis of the HRTEM images, it is identified fcc-like clusters with multiple planar defects, which may be produced after coalescence of smaller particles for most of the pH conditions.

The structure of these particles eventually produce hcp-like structure which denotes a extra energy presence during the synthesis process for most of the samples, however for pH=10, the structure tend to be of the minimum energy configuration and the maximum production, which was expected to be used in the development of gas separation membranes.

## Combustion of Toluene on Pt/Al<sub>2</sub>O<sub>3</sub> - La Catalysts

J. M. Padilla<sup>1</sup> and G. Del Angel<sup>1</sup>

<sup>1</sup>*Universidad Autónoma Metropolitana- Iztapalapa. Departamento de Química, Área de Catálisis. Av. San Rafael Atlixco No 186, C.P. 09340, AP. 55-534. Mexico D. F. Mexico.*

e-mail; jmpf33@hotmail.com. gdam@xanum.uam.mx.

The catalytic oxidation of Toluene on Pt(0.5 wt%)/ $\gamma$ -Al<sub>2</sub>O<sub>3</sub>-La catalysts with 0.5, 1, 10 and 20 wt% La was investigated. The alumina-La supports were prepared by adding a La-nitrate precursor to the Aluminium boehmite. The supports were characterized by, Xray diffraction (XRD), RMN (Al<sup>27</sup> RMN-MAS), FTIR-CO adsorption and BET areas. It was observed a crystalline loss with the La content; also it was observed characteristic peaks of La<sub>2</sub>O<sub>3</sub>, Al<sub>2</sub>O<sub>3</sub> and LaAlO<sub>3</sub> were the first is probably very disperse on the supports<sup>1</sup>. RMN study showed an increase in the aluminum on tetrahedral sites and a decrease in the octahedral sites due to a structural replace of the  $\gamma$ -Al<sub>2</sub>O<sub>3</sub>. The profiles of TPD-NH<sub>3</sub> showed a decrease in the acid sites. The BET areas showed that for the  $\gamma$ -alumina with 20 wt% La, the effect of the incorporate La, is more important since the distortion of the structure leads to a reduction of the surface area. The diameter of the pore remains constant, probably to that La in excess segregates and it is deposited in the pores of large diameter. Desorption at temperature programme. By FTIR-CO adsorption, it was found that the dispersion of nanoparticles Pt on the supports. The combustion of toluene (1400 ppm) in air was carried out at atmospheric pressure<sup>2</sup>. Two behaviours were observed: for the catalysts with low La content (0.5 %) and without La, the combustion occurs in a broad temperature range 100-397 °C, meanwhile, catalysts with high La content (1, 10, 20 %), the toluene combustion occurs in the range 100-305 °C.

*We acknowledge to CONACyT for the support provided under projet C01-46689.*

---

<sup>1</sup> H. Chaper, E.B.M. Doesburg, L.L. Van Reijen., "The Influence of Lanthanum Oxide on the Thermal Stability of Gamma Alumina Catalyst". Appl. Catal. **7**, (1983), 211-220

<sup>2</sup> P. Papaefthimiou, T. Ioannides, X.E. Verykios. "Combustion of non- halogenated volatile organic compounds over group VIII metal catalysts." Appl.Catal. B. **13**, (1997), 75-92

## Synthesis and Characterization of Nanoparticles of Gold Supported on TiO<sub>2</sub> and TiO<sub>2</sub>-Ce

C. Guzmán<sup>1</sup>, G. del Ángel<sup>1,\*</sup>, R. Gómez<sup>1</sup>, F. Galindo<sup>1</sup>, R. Zanella<sup>2</sup>, and G. Torres<sup>3</sup>

1.- Universidad Autónoma Metropolitana-Iztapalapa. Departamento de Química, Área de Catálisis, C.P. 09340, AP. 55-534. Mexico D. F. Mexico.

2.- Centro de Ciencias Aplicadas y Desarrollo Tecnológico, UNAM, C.P. 04510, AP. 70-186, Mexico D.F. Mexico.

3.- Universidad Juárez Autónoma de Tabasco, DACB, CP86690, AP. 24, Cuanduan Tabasco, Mexico.

\*e-mail: gdam@xanum.uam.mx

The catalytic activity is sensitive to the method of preparation and thermal treatments as calcination and reduction<sup>1,2,3</sup>. We present here the synthesis and characterization of Au/TiO<sub>2</sub>-Ce catalysts prepared by deposition-precipitation method from a gold salt in presence of urea. The supports TiO<sub>2</sub> and TiO<sub>2</sub>-Ce (2.5, 5, 7.5, 10 wt % Ce) were prepared by sol-gel method with a solution of nitrate of cerium. The supports were characterized by different techniques. The specific surface areas BET method showed that the addition of CeO<sub>2</sub> to TiO<sub>2</sub> produced an increase in the specific area and in the pore diameter. X-ray diffraction (XRD) patterns presented only peaks corresponding to anatase phase. Cerianite phase was not detected (CeO<sub>2</sub>). The XRD spectra for Au/TiO<sub>2</sub> and Au/TiO<sub>2</sub>-Ce catalysts showed only traces of Au corresponding to Au<sup>0</sup>. The Au metallic contents in these catalysts were determined by inductive coupled plasma (ICP); all samples gave around of 2.0 wt %. The average size of gold particles obtained by transmission electron microscopy (TEM) was 5-3 nm. We observed that gold particle size decrease as increases the content of Ce. Additionally we used these catalysts in catalytic wet oxidation (CWAO) of Methyl Ter-butyl Ether (MTBE) with great results, obtained conversions until 78% and 97 % of selectivity to CO<sub>2</sub>.

*We Acknowledgments to CONACYT for the support provided under Project SEP-CONACYT 2004-COI-46689 and C. Guzmán Thanks to CONACYT for the support provided.*

---

<sup>1</sup> F. Porta, L. Prati, M. Rossi, S. Coluccia, G. Mantra, *Catal. Today*, **61**, 165, (2003).

<sup>2</sup> R. Zanella, S. Giorgio, C. R. Henry and C. Louis, *J. of Catal*, **222**, 357, (2004)

<sup>3</sup> R. Zanella, L. Dennaioy, C. Louis., *Appl. Catal A: Gen*, **291**, 62 (2005).

## Synthesis of Nanocomposites of Ag Nanoparticles on Mesoporous SiO<sub>2</sub>

M. E. Díaz Mora<sup>1</sup>, E. Rubio Rosas<sup>1,2\*</sup>, V. Rodríguez Lugo<sup>1</sup>,  
and M. Espinosa-Pesqueira<sup>3</sup>

<sup>1</sup> Centro Universitario de Vinculación, Benemérita Universidad Autónoma de Puebla.

Prolongación 24 Sur. Col. San Manuel. C. P. 72570. Puebla, Pue. Mexico.

<sup>2</sup> Facultad de Ingeniería Química, Benemérita Universidad Autónoma de Puebla.

<sup>3</sup> Instituto Nacional de Investigaciones Nucleares. Carretera Mexico-Toluca S/N,  
(Km. 36.5), La Marquesa, Ocoyoacac, Mexico C.P. 52750.

\*e-mail: efrain.rubio@cuv.buap.mx

The development of materials in the nanotechnology area, it has transformed into one of the primary disciplines among scientists and industries of the whole planet. The properties of the porous materials depend on the nature of the material, pore geometry, porosity and diameter. The mesoporous material occupies a primordial place in this new vision of the modern technology, since it has been reported in the past few years, the multiple applications with special interest in the development of inorganic mesoporous material. Inside the nanoscaled materials they are important the nanocomposites, and more often the nanocomposites have superior properties compared to the composites at conventional scale, and they can be synthesized using surprisingly simple and economic methods. Hence, it has been important the development of nanocomposites like in this case mesoporous SiO<sub>2</sub> impregnated with Ag nanoparticles (2 %wt), where we can take the advantage of the arrangement of the SiO<sub>2</sub> mesopores to dispersed the metallic Ag nanoparticle which is indeed the catalyst. This nanocomposite was made to be applied in the N<sub>2</sub>O reduction in

the presence H<sub>2</sub>. As we know N<sub>2</sub>O are combustion products and have an important environment impact. The characterization was made by SEM, EDS, TEM and XRD, The catalytic conversion of N<sub>2</sub>O was performed on a Rig-100.

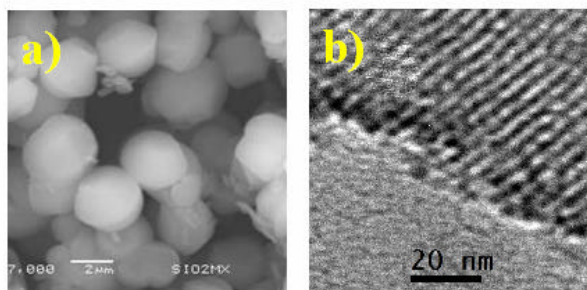


Fig. 1 SEM and TEM micrograph of mesoporous silica

## **Análisis nanoestructural de la capa de alúmina crecida sobre una aleación de FeCrAl**

**J. I. Guzmán-Castañeda, and A. García-Bórquez**

*ESFM-IPN, Dep. Ciencia de Materiales, Ed. 9-UPALM, 07738 Mexico, D.F.*

e-mails: jigc\_x@yahoo.com.mx ; borquez@esfm.ipn.mx

Entre las diversas aplicaciones de la alúmina, una muy novedosa y actual es su empleo en la fabricación de monolitos para los convertidores catalíticos<sup>1</sup>. Su papel en ellos es muy indispensable por el área de contacto que ofrece a los gases y los puntos de anclaje para la fase activa del catalizador reductor. Es por ello que se requiere una alúmina con una gran área superficial. Además la porosidad de este compuesto depende de la fase polimórfica, enumerándolas de mayor a menor porosidad, tenemos las fases  $\gamma$ ,  $\delta$ ,  $\theta$  y  $\alpha$ <sup>2</sup>. Por otro lado, en la búsqueda de nuevos materiales para la fabricación de monolitos más duraderos y reciclables, hemos experimentado con aleaciones de FeCrAl conteniendo diferentes concentraciones de Cr y Al. De esta manera, el objetivo de este trabajo es inducir el crecimiento de alúmina porosa y con una superficie nanoestructurada en la aleación de Fe22%wtCr5%wtAl.

Para lograr este objetivo muestras de FeCrAl en forma de placa fueron sometidas a una erosión mecánica severa y posteriormente a un proceso de oxidación, a 900 °C por 24 horas en atmósfera de aire. Las micrografías por SEM de la superficie oxidada, muestran el crecimiento de plaquetas de tamaño nanométrico conocidas como “whiskers”, y las micrografías de la sección transversal muestra que el grosor de la capa formada oscila entre 2 y 3 micras. Los análisis de EDXS realizados en la sección transversal muestran variaciones en la concentración de Al y O en la capa y de Al en el sustrato a profundidades de hasta 7 micras con enriquecimiento en la superficie, lo que indica que la formación de la capa de alúmina, se realiza por mecanismos difusivos de este elemento hacia la superficie. Finalmente DRX detecta además de la fase  $\alpha$  del hierro (sustrato), varios picos correspondientes a las fases  $\delta$ ,  $\theta$  y  $\alpha$  de la alúmina. Con todo esto concluimos que en la superficie de la aleación se presentan características nanoestructuradas y una fase de alúmina de porosidad adecuada para aplicaciones catalíticas mencionadas anteriormente.

*Este trabajo fue apoyado por el proyecto CGPI 20060720 del IPN \*Becario PIF.*

---

<sup>1</sup> R. W. Cahn, P. Haasen, Mat. Science and Technology, Vol. 11 Structure and Properties of Ceramics, USA 1994, pp 520-530.

<sup>2</sup> G. Brown The X- Ray Identification and Crystal Structure of Clay Minerals London 1961, pp(360-372).



## **Polymer Nanofibers Containing Gold Nanoparticles: Synthesis and Characterization**

J. A. Pescador Rojas<sup>1</sup>, A. G. Juárez Gracia<sup>1</sup>, J. G. Mendoza Álvarez<sup>2</sup>,  
J. L. Herrera Pérez<sup>1</sup>, and J. F. Sánchez-Ramírez<sup>1,2\*</sup>

<sup>1</sup>CICATA-IPN, Legaria # 694, Col. Irrigación, 11500 Mexico D.F., Mexico.

<sup>2</sup>Department of Physics, Cinvestav-IPN, Apartado Postal 14-740, Mexico, DF, 07000, Mexico.

\* e-mail: jfsanchez@ipn.mx

Gold nanoparticles prepared through reduction of HAuCl<sub>4</sub> by citrate under refluxing conditions in polyvinyl pyrrolidone (PVP) ethylene glycol solution were dispersed into PVP nanofibre film by electrospinning. The optical properties of Au nanoparticles in PVP were measured by UV-Vis spectroscopy. The presence of face-centred cubic crystalline gold embedded in PVP nanofibre film was indicated by the x-ray diffractometer pattern. The morphology and distribution of gold nanoparticles in PVP nanofibres were observed by transmission electron microscopy and scanning electron microscopy. The interaction between PVP and Au nanoparticles was confirmed by x-ray photoelectron spectrum.

*The authors are thankful to the Mexican Agencies, CONACYT, CGPI-IPN for financial supports.*

## Proton Charge Transport in Nafion Nanochannels

E. Valenzuela<sup>1\*</sup>, S.A. Gamboa<sup>2</sup>, J.P Sebastian<sup>1,2</sup>, J. Moreira<sup>1</sup>, J. Pantoja<sup>1</sup>, G. Ibañez<sup>1</sup>, R. Trujillo<sup>1</sup>, A. Reyes<sup>1</sup>, B. Campillo<sup>3</sup>, and S. Serna<sup>4</sup>

<sup>1</sup>*Universidad Politécnica de Chiapas, Cuerpo Académico de Energía y Sustentabilidad, Eduardo J. Selvas S/N, Col. Magisterial, 29010, Tuxtla Gutiérrez, Chiapas.*

<sup>2</sup>*Centro de Investigación en Energía-UNAM, 62580 Temixco, Morelos, Mexico.*

<sup>3</sup>*Facultad de Química e Instituto de Ciencias Físicas-UNAM, Cd. Universitaria, 04510, Mexico D.F.*

<sup>4</sup>*Centro de Investigación en Ingeniería y Ciencias Aplicadas-UAEM, Av. Universidad 1001, 62251, Cuernavaca, Morelos, Mexico.*

\*e-mail: edgarvm@gmail.com

The actual trends in electrolytes points to solid ionic carriers, the solid electrolytes are easier to store and handle, and it doesn't have leakage problems as the liquid compounds. The Nafion perfluorinated membranes are one of the best electrolytes used in Polymeric Membrane Fuel Cell (PMFC). Despite the Nafion has been extensively used and studied, there are still parts of the conduction process that are not well understood. According to the SAXS images and the simulations of Nafion, the membrane is a nanometric multichannel material composed by three main regions, i) a hydrophobic phase made of Polytetrafluoroethylene, ii) a hydrophilic phase directly related to the proton charge transport and iii) an interphase zone. When the Nafion is properly hydrated the water confined in the nano channels of the structure of the Nafion, reduces the bond energy strength between hydrogen and oxygen due it is confinement in nano spaces. This phenomenon along with the presence of  $\text{SO}_3^-$  anions, results on the high ionic conductive characteristic of Nafion. In this work a novel method to study the proton conduction process in Nafion nano channels is presented, and experimental results that not only validate the experimental design, but contribute with new findings related to the proton charge transport in nano confined water wires.

## **Extracción de Características de Nanoestructuras Metálicas con Técnicas de Reconocimiento de Patrones y Visión por Computadora**

**J.A. Lombardero Chartuni<sup>1,2\*</sup>, E. Juárez-Ruiz<sup>3</sup>, J. C. Moctezuma<sup>3</sup>, U. Pal<sup>4</sup>, J.A. Ascencio<sup>5</sup>**

<sup>1</sup> *Universidad Popular Autónoma del Estado de Puebla, Posg. en Ing. Mecatrónica,  
21 sur 1103, Col. Santiago, Puebla, Pue. CP 72000 Mexico.*

<sup>2</sup> *Universidad del Desarrollo del Estado de Puebla, 2 Sur 2303, Puebla, 72000, Mexico.*

<sup>3</sup> *Fac. Cs. Elec., BUAP, 18 Sur y Sn Claudio, CU, Pue. 72570, Mexico.*

<sup>4</sup> *Inst. Física, Universidad Autónoma de Puebla, PO Box J-48, Puebla 72570, Mexico.*

<sup>5</sup> *Ductos, Corrosión y Materiales, Instituto Mexicano del Petróleo, Lázaro Cárdenas 152, Col  
San Bartolo Atepehuacan Mexico, Distrito Federal 07730, Mexico.*

\*e-mails: jlombard@ece.buap.mx; jorge\_lombardero@yahoo.com.mx

La interpretación directa y la extracción de información de cualquier imagen obtenida por HREM es difícil debido al contraste generado por diferentes procesos y particularmente por la calidad de la imagen, por tanto, no resulta fácil su interpretación, por ello se hace necesaria la implementación de técnicas de caracterización por métodos computacionales. Se observa que existe mucho traslape entre estos campos de la ciencia y la tecnología, y su aplicación al estudio de los materiales nanoestructurados resulta una verdadera necesidad, donde su integración permite una aplicación práctica en la ciencia de materiales sin extraviarse en formalismos teóricos. En este trabajo, a través de técnicas del reconocimiento de patrones y de la visión por computadora, es decir, del procesamiento y análisis de la imagen digital, se desarrolla una herramienta de software de apoyo -en su segunda etapa- al trabajo del nanotecnólogo y del microscopista, que le permita realizar más eficientemente la caracterización de tamaños de nanoestructuras metálicas de forma rápida y segura, con un sistema robusto y confiable, ya que, en esta fase se ha logrado desarrollar el programa ejecutable en el marco de la hoy llamada microscopía computacional que marca la entrada del desarrollo de este sistema para la determinación semiautomatizada y de la extracción flexible de forma que implica encontrar su posición, orientación, tamaño o estructura con un sistema adaptable.

---

<sup>1</sup> A.B. Flores, L.A. Robles, M.O. Arias, J.A. Ascencio, Small Metal Nanoparticle Recognition Using Digital Image Analysis And High Resolution Electron Microscopy

<sup>2</sup> Ascencio JA. PhD Thesis Disertation. ININ-UAEM, Mexico; 2000 [3] Yacamán M. J. Reyes G. J. 1995, Microscopía Electrónica, FCE, Mexico.

## Diagrama de Fase de Nanopartículas Metálicas de AuCu

C. Fernández Navarro<sup>1\*</sup>, S. Mejía Rosales<sup>1</sup>, E. Pérez Tijerina<sup>1</sup>,  
y M. José Yacaman<sup>2</sup>

<sup>1</sup>*Facultad de Ciencias Físico Matemáticas, Universidad Autónoma de Nuevo León  
San Nicolás de los Garza, Nuevo León, 66450, Mexico.*

<sup>2</sup>*Department of Chemical Engineering, The University of Texas at Austin,  
Austin Tx. 78712 USA.*

e-mail: cfernandez@fcfm.uanl.mx

Las aleaciones de metales nobles son los sistemas más estudiados experimentalmente. La reducción en la escala proporciona a los materiales nuevas propiedades que son significativamente diferentes de las propiedades del bulto. Los diagramas de fase binarios son una herramienta utilizada para materiales en el bulto, pero los diagramas de fase para materiales de tamaño nanométrico son aún estudio de muchos investigadores.

En años recientes las aleaciones de metales nobles han sido estudiadas teóricamente por medio de las simulaciones computacionales, las cuales hacen uso de potenciales interatómicos para representar de la manera más exacta las interacciones de las partículas del sistema.

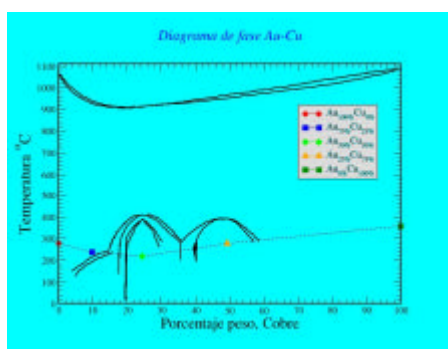


Fig.1. Comparación diagrama de fase para AuCu en bulto( línea continua) y nanopartícula cuboctaedral de 561 átomos.

Hemos desarrollado simulaciones de dinámica molecular a nanopartículas cuboctaedrales de Au Cu en las concentraciones: Au, Au<sub>3</sub>Cu, AuCu, AuCu<sub>3</sub> y Cu; y en los tamaños de 561, 1451, 3871, 6525 y 10179 átomos. . El objetivo es determinar las temperaturas de fundido para cada sistema, que es dependiente del tamaño de la partícula, y obtener el diagrama de fase; compararlo con el diagrama de fase para el bulto y observar las diferencias existentes debido al cambio de tamaño de las partículas.

Agradecemos al CONACYT el apoyo financiero otorgado para el proyecto NL-2004-C05-60 y a The University of Texas at Austin por el tiempo de computo otorgado.

## Adsorption of Molecular Hydrogen in a Graphene-Carbon Nanotube System

J. S. Arellano

*Area de Física Atómica Molecular Aplicada, División de Ciencias Básicas e Ingeniería, UAM-Azcapotzalco. Av. San Pablo No. 180. Mexico 02200, D.F. Mexico.*

e-mail: jsap@correo.azc.uam.mx

It is simulated an isolated system formed by a fragment of a (6,6) carbon nanotube and a portion of a graphene layer. The purpose of the work is to investigate how is adsorbed the hydrogen molecule in different sites of this system and compare with the way in which only one hydrogen molecule is adsorbed upon a lonely graphene layer or with the different ways in which the hydrogen molecule can be adsorbed inside or outside the (6,6) carbon nanotube. To do the calculations it has been used a plane wave code as FHI98MD. This is based in density functional theory, and pseudopotentials for the atomic species, carbon and hydrogen atoms. A side of 25 a.u. has been used for the cubic supercell containing the composed system. In a first approach the graphene layer is oriented in a tangential way to the carbon wall nanotube, but separated one from another at least a distance of 5 a.u. A distance close to this was obtained as the equilibrium one for the adsorption of the hydrogen molecule above the hexagonal cavity for the graphene layer and upon the center of the hexagonal cavity of the carbon nanotube wall. With these now we compare if it is possible that in the region close to the middle point between the wall and the graphene layer the hydrogen molecule can be adsorbed with a greater binding energy that in any other case. In particular it will be compared with the favorable configuration when the molecule is at the center of the carbon nanotube.

## **Inestabilidades Vibracionales, Transición de Fase y Esfuerzo Ideal en el Cúmulo de $\text{Ti}_{13}$**

M. Salazar-Villanueva,<sup>1\*</sup> A. Bautista Hernández,<sup>1,2</sup> y J. A. Ascencio<sup>3</sup>

<sup>1</sup>*Instituto de Física, Universidad Autónoma de Puebla, Apdo. Postal J-48, Puebla, Pue., 72570,*

<sup>2</sup>*Facultad de Ingeniería, Universidad Autónoma de Puebla.*

<sup>3</sup>*Ductos, Corrosion y Materiales. Instituto Mexicano del Petróleo, Eje Central Lazaro Cardenas  
152. San Bartolo Atepehuacán, Mexico, Distrito Federal, 07730, Mexico.*

e-mail: msalazar@sirio.ifuap.buap.mx

Recientemente se ha iniciado el estudio del esfuerzo ideal en nanomateriales. En el caso de cúmulos el esfuerzo ideal máximo se calcula en el punto de inflexión de la curva de energía vs. deformación. En este trabajo se obtiene el diagrama carga deformación del cúmulo icosaedral de titanio  $\text{Ti}_{13}$ , se aplica deformación axial a lo largo de la dirección  $\mathbf{e}_{yy}$  y se obtiene la variación de la energía total respecto a la deformación aplicada usando la Teoría del Funcional de la Densidad (DFT). Se encuentra una transición de fase al aplicarse tensión axial, por lo que se reporta un cambio de simetría  $I_h$  a  $D_{5h}$ . Para probar la estabilidad vibracional del cúmulo, se obtuvieron las frecuencias como función de la deformación. Para el tratamiento de los términos de correlación e intercambio se consideró la aproximación GGA bajo la parametrización propuesta por Perdew y Wang.

## Density Functional Study of the Structural Properties of Copper Iodide: LDA vs GGA Calculations

H. Hernández Cocoltzi<sup>1\*</sup>, Gregorio H. Cocoltzi<sup>2</sup>, N. Takeuchi<sup>2</sup>, J. F. Rivas-Silva<sup>2</sup>,  
and A. Flores<sup>2</sup>

<sup>1</sup>*Colegio de Ingeniería en Materiales-Facultad de Ingeniería Química*

*Benemérita Universidad Autónoma de Puebla*

*Av. San Claudio y 18 Sur. C. U. Edificio 149, 72570. Puebla, Mexico.*

<sup>2</sup>*Instituto de Física, Universidad Autónoma de Puebla, Apartado Postal J-48, Puebla 72570, Mexico.*

\*e-mail: heribert@sirio.ifuap.buap.mx

We perform first principles total energy calculations to investigate the atomic structure of copper iodide in the sodium chloride, cesium chloride, zincblende and wurtzite structures. Calculations are done within the density functional theory. We employ the full potential linearized augmented plane wave method as implemented in the wien2k code. The exchange and correlation potential energies are treated in the generalized gradient approximation (GGA), and the local density approximation (LDA). Optical absorption experiments and x-ray diffraction measurements showed that zincblende is the ground state of CuI. Our calculations find that in the GGA formalism the lowest minimum corresponds to wurtzite, and in the LDA the lowest minimum corresponds to zincblende. Our results show that the energy difference between the wurzite and the zincblende structures, as calculated within the GGA formalism is 9 meV, and within the LDA formalism, is 75 meV. These results may suggest a coexistence of both wurzite and zincblende structures in the ground state of CuI. Structural parameters are correctly reproduced by the GGA calculations. We obtain that under the application of external pressure the atomic configuration may transform into the NaCl structure. At higher pressures it is possible to have a phase transition to the CsCl geometry.

*Acknowledgement. This work was partially supported by Conacyt under Grants 48549 and 43830-F, SEP-PROMEP under Grant UADY-PTC-054, and DGAPA under Grant IN101103-3. The work of GHC was partially supported by VIEP-BUAP under grant 31/EXC/06-G.*

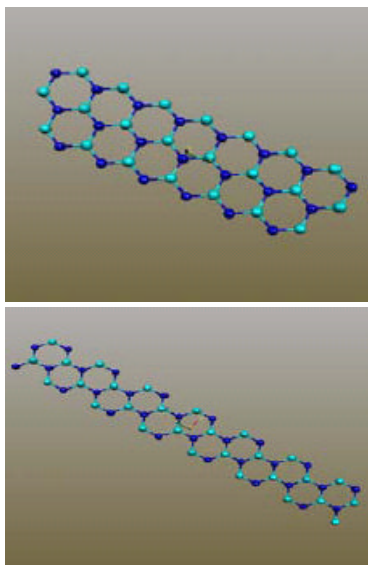
## DFT Theory Based Analysis of the Electronic Properties of Boron-Nitrogen Sheets

E. Chigo-Anota\*, H. Hernández Cocolletzi, M. López Fuentes,  
and A. Rodríguez Juárez

*Colegio de Ingeniería en Materiales-Facultad de Ingeniería Química Benemérita Universidad  
Autónoma de Puebla, Av. San Claudio y 18 Sur. C. U. Edificio 149, 72570. Puebla, Mexico.*

\*e-mail: aechigoa@sirio.ifuap.buap.mx

In this work the electronic properties of boron nitride sheet are investigated. Our studies include the (7,0) and (7,7)<sup>1</sup> quiralitys of the sheet and we use the density functional theory (DFT) as implemented in GAUSSIAN98 package. The hybrid functionals B3PW91 and B3LYP are considered for the exchange-correlation term and STO-3G and 3-21G bases are used.



Positive frequencies criterion is used to obtain the optimal geometric structure. Reactivity parameters and molecular density of states are calculated to investigate its electronic behavior.

Preliminary results indicate that the sheet has low chemical reactivity compared with the corresponding free atoms and it behaves as semiconductor, contrary to the graphene sheet, which is metallic<sup>2</sup>.

*Figure1. Boron-nitrogen sheets within the quirality (7,0) and (7,7).*

\* We acknowledge the financial support of VIEP-BUAP and FI-BUAP (Grants No. 02/ING/06-G, 06/ING/06-G and research internal project 2006-2007).

<sup>1</sup> A. Rodríguez Juárez and E. Chigo Anota, Análisis ab-initio de las propiedades fisicoquímicas de hojas de Boro-nitrógeno con quirality (7,0) y (7,7). **Primer Simposium de Ingeniería en Materiales-FIQ-BUAP**, November 2006.

A. Rodríguez Juárez and E. Chigo Anota, Cálculo de las propiedades electrónicas de hojas de boro-nitrógeno. **II Foro de Estudiantes de Ingeniería 2007-FIQ-BUAP**, April (2007).

A. Rodríguez Juárez, Tesis de licenciatura en desarrollo en el CIMAT-FIQ-BUAP (2007).

<sup>2</sup> E. Chigo Anota, et al, **XXVI Congreso Nacional de la Sociedad Mexicana de Ciencia y Tecnología de Superficies y Materiales, CAS-1** September (2006).



## Cálculo del Módulo de Young de Superficies de Metales *fcc*

A. Bautista-Hernández<sup>1,2\*</sup>, J. H. Camacho-García<sup>1</sup>, and U. Pal<sup>1</sup>

<sup>1</sup>*Instituto de Física, Universidad Autónoma de Puebla, Apdo. Postal J-48, Puebla, Pue., 72570, Mexico.*

<sup>2</sup>*Facultad de Ingeniería, Universidad Autónoma de Puebla, Apdo. Postal J-39, Puebla, Pue., 72570, Mexico.*

e-mail: abautist@sirio.ifuap.buap.mx

Mediante el estudio de los módulos elásticos de cristales se puede conocer su resistencia mecánica ideal y estabilidad elástica bajo la aplicación de un esfuerzo. Recientemente, se han calculado los módulos de Young de superficies de  $\text{ZnO}$ <sup>1</sup> y  $\text{Cu}$ <sup>2</sup> y se ha podido establecer que dichos valores, en las direcciones  $\langle 0001 \rangle$  y  $\langle 001 \rangle$ , son superiores a los valores del bulto. Sin embargo, existen pocos trabajos en donde se realicen estudios sistemáticos de una familia de elementos tales como los metales de transición, importantes en aplicaciones tecnológicas. En este trabajo se presenta el cálculo del módulo de Young en superficies de 10 metales de transición en fase *fcc* (Al, Ni, Cu, Rh, Pd, Ag, Ir, Pt, Au y Pb) mediante cálculos semiempíricos. Para modelar la energía de interacción entre los átomos de los metales, se emplean los potenciales de Sutton-Chen<sup>3</sup>. Para validar el uso de estos potenciales calculamos parámetros de red, constantes elásticas y relaciones de dispersión para estos cristales en bulto, obteniendo un buen acuerdo con datos experimentales. Se construyeron superceldas en la dirección  $\langle 001 \rangle$  y se optimizaron sus parámetros de red. Posteriormente se realizaron deformaciones sucesivas para obtener el módulo de Young a partir del ajuste de las curvas energía-deformación usando la expresión:  $Y = (1/\Omega) d^2E/d\varepsilon^2$ , donde  $\Omega$  es el volumen de la supercelda,  $E$  es la energía total y  $\varepsilon$  es la deformación. Nuestros resultados indican que los módulos de Young de las superficies con menores números de monocapas son aproximadamente 1.5 más grandes que sus valores de bulto y disminuyen hasta llegar a un valor constante cercano al valor del bulto cuando se tienen 40 monocapas en promedio.

*Trabajo apoyado por Proyectos VIEP-BUAP # 10/ING/06-G y # 27/EXC/06-1.*

<sup>1</sup> L. Zhang and H. Huang, Appl. Phys. Lett. **89** (2006) 183111.

<sup>2</sup> L. Zhang and H. Huang, Appl. Phys. Lett. **89** (2006) 183111.

<sup>3</sup> A. P. Sutton and J. Chen, Philos. Mag. Lett. **61** (1990) 139.

## **Ab-Initio Simulation of the Structural and Electronic Properties of Aluminosilicate and Aluminogermanate Nanotubes with Imogolite-Like Structure**

Fernando Álvarez Ramírez

*Programa de Ingeniería Molecular, Instituto Mexicano del Petróleo, Eje Central Lázaro Cárdenas 152, Colonia San Bartolo Atepehuacan, Mexico D.F., 07730.*

A theoretical study of imogolite-like single wall nanotubes as a function of silicon and germanium content and their tubular radius is presented mapping of silicon/germanium content properties in models that contain from 9 gibbsite-like units ( $N_u = 9$ ) to 13 gibbsite-like units ( $N_u = 13$ ) with a silicon/germanium content ( $X = \text{Si}/(\text{Si} + \text{Al})$ ) of 0, 0.20, 0.40, 0.60, 0.80, and 1.00. The imogolite nanotubes were built setting periodic boundary conditions to DFT geometry-optimized models along both radial and axial directions in order to obtain the stable structure. The DFT calculations were carried out on the  $\Gamma$  point and for various  $k$  points, using the GGA-PW91 functional, finding an optimal unit cell length of 8.72 Å along the axial direction. The structural properties were analyzed through the evolution of the X-ray diffraction pattern as a function of both  $N_u$  and  $X$ . A linear correlation between the tube radius and the position of the first two peaks on the X-ray diffraction is found. The imogolite surface charge was mapped with the Hirshfeld charge showing the characteristic acid tendency experimentally reported. The reactivity of imogolite-like structures was studied employing the total density of states and the band gap evolution as a function of  $N_u$  and  $X$  showing an increasing behavior with  $X$ . Finally the local reactivity was analyzed by looking at the local density of states in models with  $X=0.0$  and  $X=1.0$  with  $N_u = 10$ .

## Methanofullerenes: IR Spectrum and Electronic Properties by DFT

A. Tlahuice-Flores<sup>†</sup>, E. G. Pérez-Tijerina, and S. J. Mejía-Rosales

*Facultad de Ciencias Físico-Matemáticas, Universidad Autónoma de Nuevo León,*

*San Nicolás de los Garza, N.L. 66450 Mexico.*

<sup>†</sup>e-mail: atlahuice@cfm.unal.mx

Methanofullerenes are a family where the C<sub>61</sub>H<sub>2</sub> [6,6] isomer is the parent<sup>1</sup>. Until now, almost all existent IR spectrums for fullerenes derivatives are experimental, because this kind of calculations is extremely time-consuming. However, all of these calculations can be speeded by exploiting the symmetry of the structure.

The importance of sustituent attached to the like-cyclopropane carbon in the methanofullerenes is due to the Gap modification. The raising of the LUMO orbital is a necessary condition to the application of the fullerene derivatives in photovoltaic devices<sup>2</sup>. Fullerenes derivatives act like electron-acceptors and their LUMO orbital is the place where the electrons from the electro-donating sustituent are added in an organic solar cell.

DFT calculations of some methanofullerenes, PCBM included, were done using the B3LYP/6-31g(d) and the PW91/dnd methods. Here we present the structural and electronic properties result of these calculations.

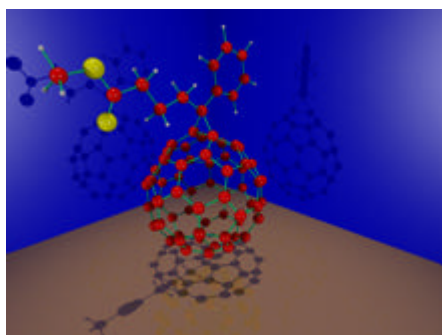


Figure 1. Optimized PCBM, C<sub>s</sub> symmetry using DMol<sup>3</sup>.

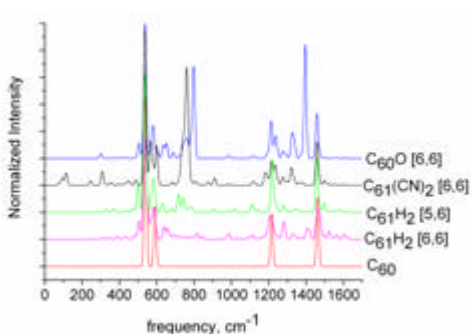


Figure 2. Calculated IR spectra

We acknowledge PROMEP, for the support through the grant No. PROMEP/103.5/05/2236 and from UANL through PAICYT, project CA1267-06; from CONACYT, project 43772 (Ciencia Básica), and finally, from Consejo Estatal de Ciencia y Tecnología del Estado de Nuevo León.

<sup>1</sup> T. Akasaka, M. T. H. Liu, Y. Niino, Y. Maeda, T. Wakahara, M. Okamura, K. Kobayashi, and S. Nagase. *J. Am. Chem. Soc.* **122**, 7134-7135 (2000).

<sup>2</sup> Xiaoni Yang et al., Nanoscale morphology of high-performance polymer solar cells, *Nanoletters* **5**, 579-583 (2005).

## Synthesis and Characterization of Nanogels and Microgels from Cellulose Derivatives and Polyacrylates

C. Castro Guerrero<sup>1</sup>, A. Morales Cepeda<sup>1\*</sup>, and O. Kharissova<sup>2</sup>

<sup>1</sup>*División de Estudios de Posgrado e Investigación, Instituto Tecnológico de Ciudad Madero, Juventino Rosas y Jesús Urueta, Col. Los Mangos, C. P. 89440., Cd. Madero, Tam., Mexico.*

<sup>2</sup>*Facultad de Ciencias Físico-Matemáticas, Universidad Autónoma de Nuevo León, Pedro de Alba s/n, Cd. Universitaria, San Nicolás de los Garza, N. L., Mexico.*

\*e-mail: acepeda71@yahoo.com

Nanostructures from cellulose derivatives, especially from hydroxypropyl cellulose (HPC) have been widely studied before. Gels from HPC and PAA have been done and they were subjected to characterization, the scope is to reach nanostructures and to make a chemical crosslinking between raw materials. The reaction is made in a nitrogen atmosphere at 40°C with initiators and crosslinkers. It is being studied the effect on the size of particles of reactant variation, crosslinker concentration and pH. Many changes of color (from blue-colorless to white) are seen while working with HPC, possibly due to changes of mesophases, which are mainly isotropic and anisotropic. At alkaline pH a yellow color is seen in the samples with HPC or HEC. FTIR analysis shows that main functional groups are present in the gels and that pH does not change chemical composition, but affects density of crosslinking. Some AFM analysis has been done and shows the formation of lamellae through the surface of the samples distances from 125 to 400 nm and heights from 10 to 45 nm, depending on the concentration of reactants and crosslinker.

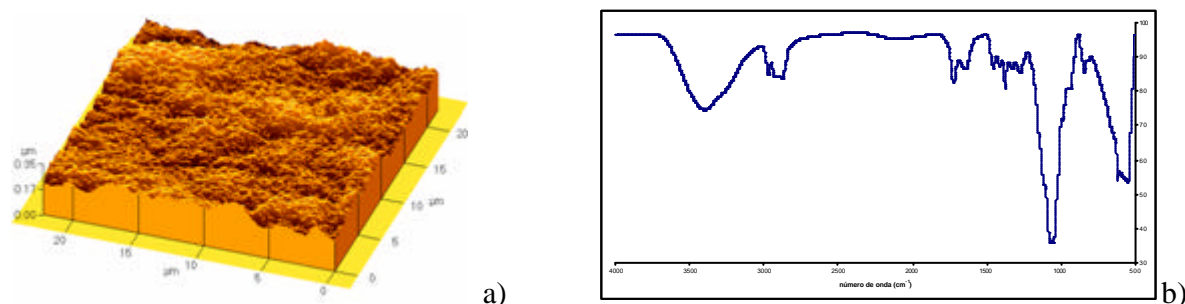


Figure 1.- a) AFM image of HPC/PAA 50/50, b) FTIR spectrum of the same sample.

We acknowledge the partial financial of CONACyT, Mexico, through the grant # 181581.

## **Influencia de Adición de Compuestos Orgánicos Sobre las Estructuras Cristalinas $C_3S$ Y $C_2S$ del Cemento Pórtland**

**F. Jiménez Álvarez, L. Téllez-Jurado, y H. Balmori Ramírez**

*Depto. Ing. en Metalurgia y Materiales, ESIQIE-IPN, Zacatenco, 07738, Mexico D. F., Mexico.*

e-mail: francisco@icqlatino.zzn.com

La adición de compuestos orgánicos al cemento Pórtland ordinario mejoran las propiedades mecánicas de este último. Lo anterior se debe a que los compuestos orgánicos interactúan con los componentes del cemento, principalmente con el hidróxido de calcio proveniente de reacciones de hidratación. Se han reportado mediante la termogravimetría la formación de complejos carbonatados ( $Ca-O-CH_2\sim R$ ) los cuales son producto de la reacción entre el  $Ca^{2+}$  del hidróxido de calcio con los compuestos orgánicos. En el presente trabajo se investigaron dichos complejos mediante DRX y FT-IR. Los compuestos orgánicos consisten de una mezcla de alcoholes, alquenos y alcanos de cadenas cortas de carbonos 9 a 22 provenientes de la despolimerización de envases de polietileno de desecho. La adición de esta mezcla de compuestos orgánicos en el cemento se llevó a cabo en diferentes proporciones en el momento de llevar a cabo la reacción de hidratación. Los análisis se realizaron a los 28 días después de que solidificaron las muestras. Por DRX se observó que existe efecto de la adición de estos compuestos orgánicos en la estructura del cemento. Sin embargo, por la técnica de FT-IR no queda claramente evidenciada la interacción entre el compuesto orgánico y el cemento.

## Modificación de la Superficie de la Aleación Ni22%at.Si; Irradiada con Iones Ni de 3.66 MeV a 650 °C

C. A. Camacho Olguín\*, A. García Borquez, G. Rueda y A. Ávila García

*Departamento de Materiales, E.S.F.M, Instituto Politécnico Nacional, Zacatenco, 07738 Mexico D.F., Mexico.*

*Departamento de Ing. Eléctrica, CINVESTAV, Ticomán, 07738 Mexico D.F., Mexico.*

\*e-mail: Cachisolguín@hotmail.com

Como resultado de irradiar la superficie de la aleación concentrada Ni22%@Si con iones de Ni de 3.66 MeV a 650 °C, hemos detectado la presencia de nanopicos, conglomerados de ranuras y cráteres<sup>1</sup>, cuya formación es atribuida a diferentes mecanismos de erosión atómica. Para caracterizar estos cambios hemos usado microscopia óptica y microscopios de fuerza atómica; sea concluido que dichas modificaciones a la microestructura superficial depende principalmente de las características microestructurales desarrolladas por la aleación durante su solidificación.

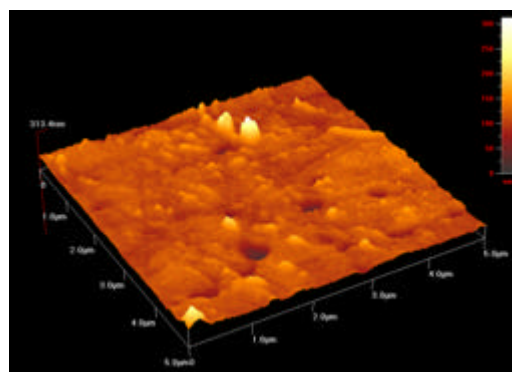
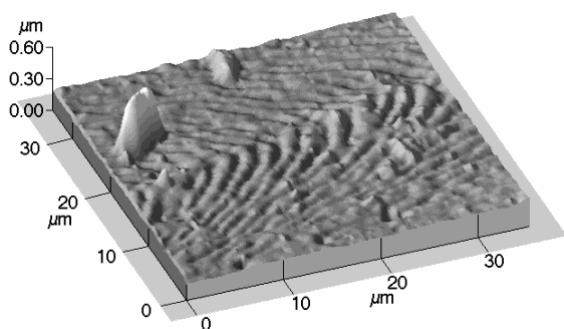


Figura 1. Nanopicos formados en la superficie irradiada.

Agradecemos al Instituto Politécnico Nacional por su apoyo; proyecto PIFI 20070836.

<sup>1</sup> Orlando Auciello and Roger Kelly, Ion Bombardment Modification of Surfaces, Elsevier 1984.

## Synthesis and Characterization of Ag nanoparticles Doped with Ion-exchange Compounds

J. García-Serrano<sup>1\*</sup>, A. M. Herrera<sup>1</sup>, M. Ocampo-Fernández<sup>2</sup>, and U. Pal<sup>3</sup>

<sup>1</sup> *Centro de Investigaciones en Materiales y Metalurgia, Universidad Autónoma del Estado de Hidalgo, Carretera Pachuca Tulancingo Km 4.5, Pachuca, Hidalgo, Mexico.*

<sup>2</sup> *Posgrado en Ciencia de Materiales, Universidad Autónoma del Estado de Hidalgo, Carretera Pachuca Tulancingo Km 4.5, Pachuca, Hidalgo, Mexico.*

<sup>3</sup> *Instituto de Física, Universidad Autónoma de Puebla, Apdo. Postal J-48, Puebla, Pue. 72570, Mexico.*

\*e-mail: jserrano@uaeh.reduaeh.mx

Recently, H. Behar-Levy and D. Avnir<sup>1</sup> introduced a new family of functional materials namely organically doped metals. These new materials have attractive properties useful for catalytic applications with superior performance<sup>2</sup>. In this work, we report the synthesis of Ag nanoparticles doped with ion-exchange monomers and polymers. The preparation of Ag nanoparticles involved the chemical reduction of silver ions with metallic zinc powder in the presence of the organic dopants. The doped Ag particles did not oxidize and maintain their characteristic metal color and shine. Scanning electron microscopy (SEM), energy dispersive spectroscopy (EDS), UV-Visible spectroscopy, thermogravimetric analysis (TGA) and infrared (IR) spectroscopy techniques were used to characterize the doped Ag nanoparticles.

*The work was partially supported by VIEP-BUAP, Mexico (Grant # 27/EXC/06-1)*

---

<sup>1</sup> H. Behar-levy, D. Avnir. *Chem. Mater.* **14** (2002) 1736

<sup>2</sup> H. Behar-levy, D. Avnir. *Adv. Funct. Mater.* **15** (2005) 1141.

## Síntesis y Caracterización Microestructural de Magemita

M. Magdalena Martínez Mondragón<sup>1</sup> y R. Hernández Reyes<sup>2</sup>

<sup>1</sup>*División de Materiales Avanzados, IPICYT.*

<sup>2</sup>*Departamento de Materia Condensada, IFUNAM.*

magdalena@ipicyt.edu.mx, robertoh@fisica.unam.mx

Entre los materiales magnéticos los óxidos de hierro ocupan un lugar especial ya que se pueden obtener de manera relativamente fácil, presentan una gama amplia de fases y se puede transitar entre dichas fases mediante tratamientos relativamente simples. Estas características han hecho que dichos materiales sean utilizados tanto solos como en combinación con metales y otros óxidos y en una gran gama de aplicaciones de entre las cuales destaca su uso como medio de grabado magnético.

Por otro lado la tendencia actual a desarrollar grabado magnético cada vez de mayor densidad hace necesario que se refinen los métodos de síntesis de dichos materiales a fin de lograr tamaños de partícula más finos y que se evalúen las propiedades de los granos y sus agregados conforme disminuye dicho tamaño de partícula.

En este trabajo reportamos la síntesis y caracterización microestructural de magemita. La síntesis fue llevada a cabo siguiendo el procedimiento de reacción y precipitación de Ozaki y Matijevic<sup>1</sup>.

Los materiales obtenidos fueron caracterizados por difracción de rayos X, microscopia electrónica de barrido y microscopia electrónica de transmisión convencional. La caracterización por rayos X fue llevada a cabo en un difractómetro D8 Advance Bruker axs, la microscopia electrónica de barrido en un microscopio JEOL JSM 5600LV y la microscopia electrónica de transmisión en un microscopio JEOL JEM 100CX.

Los resultados muestra que la fase obtenida es magemita y que esta constituida por cristales aciculares con longitud promedio de 1  $\mu$ m y ancho promedio de 30 nm

*Los autores queremos agradecer su valiosa colaboración Técnica al M en C Manuel Aguilar y al Sr. José Angel Flores.*

---

<sup>1</sup> Ozaki M. and Matijevic E. 1985 J. Colloid Interface Sci. **107** 199



## Rh Very Small Nanoparticles Shapes DFT Calculations

V. Bertin<sup>1</sup>, R. Avilés<sup>2</sup>, E. Poulain<sup>2</sup>, H. Luna-García<sup>2</sup>, O. Olvera<sup>3</sup>,  
and R. López-Rendon<sup>1</sup>

<sup>1</sup>*UAM-I, Av. San Rafael Atlixco N° 186, Col. Vicentina, C.P. 09340, Mexico D.F., Mexico.*

<sup>2</sup>*UAM-A, Av. San Pablo N° 180, Col. Reynosa-Tamaulipas, C.P. 02200, Mexico D.F., Mexico.*

<sup>3</sup>*UAEH, Campus Tepeji, Av. Del Maestro s/n, Col. Noxtongo, C.P. 42850, Edo. Hidalgo, Mexico*

e-mail: neya@xanum.uam.mx

Theoretical studies of transition metal nanoparticles have attracted recently much attention due to its important role in catalysis. Here we present a comparative study of the smallest Rh nanoparticles, Rh<sub>4</sub>, Rh<sub>5</sub> and Rh<sub>6</sub>, is presented, with the view of determine their ground states characteristics, namely: shape, energy and spin. The density functional (DFT) formalism is employed by means of the Gaussian 2003 program. Full geometry optimization was applied in all of the cases considered. Three different functionals were employed with the purpose to find best convergence of the program and the correct spin of the particles considered: the classic B3LYP and also the most used nowadays: BP86 and BPW91. The Rh-Rh initial distances are set to those of the Rh (111) plane. No planar shape was examined because the natural shapes of nanoparticles are three dimensional with tendency to a spherical shape. The Rh<sub>4</sub> shape was the tetragonal pyramid. For Rh<sub>5</sub> two different shapes were studied, the triangular dipyramid and the pyramid of square base. These two forms are almost degenerated in energy, so for small geometry changes easily can be interchanged. The Rh<sub>6</sub> is an octahedron. In all cases, the two lowest spin were considered, i.e. singlet and triplet for Rh<sub>4</sub> and Rh<sub>6</sub> and doublet and quadruplet for Rh<sub>5</sub>. The best results for spin and energies were obtained using the BP86 functional. The results of spin values obtained were very well approximations to the expected values.

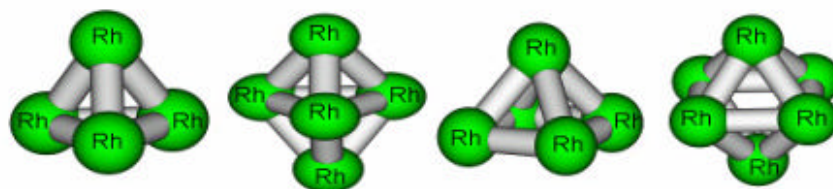


Fig 1. Rh nanocluster shapes.

## Photonic Band Structure in Pascal-type Quasiperiodic Multilayers with Left-handed Materials

Xóchitl I. Saldaña<sup>1\*</sup> and D. A. Contreras-Solorio<sup>2</sup>

<sup>1</sup> *Instituto de Física, Benemérita Universidad Autónoma de Puebla, Apdo. Postal J-48, C.P. 72570, Puebla, Pue., Mexico.*

<sup>2</sup> *Escuela de Física de la UAZ, Apdo. Postal C-580, C.P. 98060, Zacatecas, Zac., Mexico.*

\*e-mail: xochitl@sirio.ifuap.buap.mx

Using a transfer matrix method we investigate some properties of the photonic band structure of one-dimensional quasiperiodic multilayers<sup>1</sup> formed with  $2^P$  bilayer units composed of a right-handed material with constant width and a left-handed material whose width varies following a quasiperiodic Pascal's sequence given by  $dp(x) = d1 + D \times P$ ,  $d1$  is a chosen width  $D$  is a constant increment and  $P$  represents the quasiperiodic sequence. We assume that the dielectric permittivity and magnetic permeability are constant in each layer<sup>2</sup>. The band structure of these multilayers presents structures not present when the layers are only right-handed materials.

*We acknowledge the partial financial support of VIEP-BUAP through grant 37/EXC/06-G.*

---

<sup>1</sup> Xóchitl I. Saldaña, D. A. Contreras-Solorio and Elias López-Cruz "Self-similar Optical Properties in Pascal-type Quasiperiodic Dielectric Multilayers", sent to Revista Mexicana de Física, 2007.

<sup>2</sup> D. Bria, B. Djafari-Rouhani, A. Akjouj, L. Dobrzynski, J. P. Vigneron, E. H. El Boudouti and A. Nougouai, "Band structure and omnidirectional photonic band gap in lamellar structures with left-handed materials" Phys. Rev. E **69** (2004) 066613.

## **Effect of Nanoparticles of $\text{Al}_2\text{O}_3$ in the Conductive Process Al Doped ZnO Thin Films, Obtained by the Sol-Gel Technique**

D. C. Altamirano Juárez

*Universidad de la Sierra Sur, Guillermo Rojas Mijangos s/n, Col. Ciudad Universitaria. C. P. 70805; Miahuatlán de Porfirio Díaz, Oaxaca, Mexico.*  
e-mail: djuarez@unsis.edu.mx, delcris\_1@yahoo.com

The Sol-Gel technique allows to obtain polycrystalline films very thin, evenness and of homogeneous composition of almost any material on a glass splint, starting from precursor solutions. The thickness obtained by layer can be as thin as  $0.08\mu$  and to contain structures so small of some dozens of nanometer. ZnO:Al thin films were obtained by this technique and like evidence of the formation  $\text{Al}_2\text{O}_3$  nanoparticles important changes are obtained at structural level, it allowing to explain the increment of the conductivity and to propose the involved processes of carriers transport.

## Silicoaluminophosphate (SAPO) Catalysts with Controlled Nanopore Size

I. Ramírez-Sánchez<sup>1</sup>, T. Castrejón-Rosales<sup>1</sup>, Antonio S. Araujo<sup>2</sup>,  
R. García-Alamilla<sup>3</sup>, G. Sandoval-Robles<sup>3</sup>, R. Salgado-Delgado<sup>1</sup>,  
E. García-Hernández<sup>1</sup>, B. Garza-Montoya<sup>1</sup>, and A. Álvarez-Castillo<sup>1\*</sup>

<sup>1</sup>*Instituto Tecnológico de Zacatepec División de Estudios de Posgrado e Investigación y Departamento de Ingeniería Química y Bioquímica, , Calzada Instituto Tecnológico 27, Col. Ampliación Plan de Ayala, Zacatepec Morelos, Mexico, C.P. 62780;* <sup>2</sup>*Universidade de Rio Grande do Norte (URGN), Departamento de Engenharia Química, 59078-970, NATAL RN, CP 1662, BRASIL,* <sup>3</sup>*Instituto Tecnológico de Ciudad Madero, 1º. de Mayo y Sor Juana I. de la Cruz s/No., C.P. 89440, Cd. Madero Tamaulipas, MEXICO.*

\*e-mail: nuabli@yahoo.com.mx

Polyolefins is one of the most used plastic in society, because its production reaches around 60 % of the plastic wastes. Besides, this kind of plastic are not easily biodegradable due to their chemical structure. Therefore, many efforts have been done to produce catalyst, in order to thermally degrade this type of plastics. In this contribution the synthesis and characterization of Brösted-Lewis catalysts, of the Silicoaluminophosphate (SAPO) family, with controlled pore size are presented. Catalysts were synthesized using hydrothermal method using surfactants of quaternary ammonium salts with different lengths to get different pore sizes. Catalysts were characterized by BET technique to evaluate the pore size and their distribution. Simultaneous Differential Thermal Analysis and thermogravimetric analysis (TGA-DTA) were performed to evaluate complete burning of organic templates (Ammonium salts) with temperature and the transformation to a desirable catalyst structure. Besides, acidity of the catalysts was determined in order to compare our catalyst with published results. It was found that effectively pore size was controlled by the templating agent size.

## **Incorporation of Yb Atoms in TiO<sub>2</sub> Nanoparticles through Room Temperature Chemical Synthesis**

**Mou Pal<sup>1</sup>, Rutilo Silva<sup>2</sup>, E. Aparicio Ceja<sup>3</sup>, P. Santiago<sup>4</sup>, and U. Pal<sup>2\*</sup>**

<sup>1</sup> *Posgrado en Ingeniería y Ciencias Aplicadas, UAEM-CIICAP, Av. Universidad 1001, Col. Chamilpa, 62210-Cuernavaca, Morelos, Mexico. E-mail: mou\_pl@yahoo.com*

<sup>2</sup> *Instituto de Física, Universidad Autónoma de Puebla, Apdo. Postal J-48, Puebla, Pue. 72570, Mexico. \* e-mail: upal@sirio.ifuap.buap.mx*

<sup>3</sup> *Centro de Ciencias de materiales Condensada, Universidad Autonoma Nacional de Mexico, Apdo. Postal 2861, ensenada, BC 22800, Mexico.*

<sup>4</sup> *Instituto de Física, Universidad Nacional Autónoma de Mexico, Apartado Postal 20-364, 01000 Mexico D.F., Mexico.*

Spherical shaped titanium dioxide (TiO<sub>2</sub>) nanoparticles of 35-50 nm size range, doped with different nominal concentrations of ytterbium (Yb) have been synthesized through controlled hydrolysis of titanium tetrabutoxide at room temperature. All the nanoparticles were of rutile phase and their crystallinity decreased with the increase of Yb concentration. Optical absorption spectra of the doped samples revealed the presence of Yb in atomic state. Diffused reflectance spectroscopy (DRS) was used to study the effect of Yb doping concentration on the bandgap energy of the TiO<sub>2</sub>. Effect of Yb doping on the characteristic absorption band of Ti-O-Ti has been studied by Fourier transform infrared (FTIR) spectroscopy. Distribution of Yb atoms and its effect on the lattice deformation of TiO<sub>2</sub> nanoparticles were studied by high resolution transmission electron microscopy (HRTEM), high angle annular dark field imaging (HAADF), and x-ray diffraction (XRD) techniques.

*We acknowledge the partial financial supports of CONACyT, Mexico and UC-MEXUS-CONACyT through the grants # 46269 and #. CN-05-215*

## Synthesis of Au/Pd Nanoparticles with High Size-Control

E. Pérez-Tijerina<sup>1\*</sup>, M. Gracia Pinilla<sup>1</sup>, S. Mejía-Rosales<sup>1</sup>, U. Ortiz-Méndez<sup>2</sup>,  
A. Torres<sup>2</sup>, and M. José-Yacamán<sup>3</sup>

*1. Laboratorio de Nanociencias y Nanotecnología, Facultad de Ciencias Físico-Matemáticas, Universidad Autónoma de Nuevo León, San Nicolás de los Garza, Nuevo León, Mexico, 66450.*

*2. Facultad de Ingeniería Mecánica y Eléctrica, Universidad Autónoma de Nuevo León, San Nicolás de los Garza, Nuevo León, Mexico, 66450.*

*3. Texas Materials Institute and Chemical Engineering Department, The University of Texas at Austin, Austin, Texas 78712, USA.*

\*e-mail: egperez@cfm.uanl.mx

By technique of Inert Gas Condensation, is possible to synthesize Au/Pd nanoparticles, using a dc magnetron sputtering in an inert gas atmosphere. The size of the nanoparticles was controlled through the variation of (i) gas flow (Ar and He), (ii) partial pressure ( $1-2 \times 10^{-4}$  torr), (iii) magnetron power (that works on the range of 32-130W), and (iv) zone condensation length (that can be varied from 50mm to 130mm). The nanoparticles were deposited onto quartz substrates and copper grids/holey carbon. The chemical composition was analyzed by X-ray microanalysis, the structure and size of the Au/Pd nanoparticles were determined by mass spectroscopy, and confirmed by atomic force microscopy and electron transmission microscopy measurements. From these measurements we confirmed that with this technique we are able to produce particles of 1, 3, and 5 nm on size. Finally the STEM-HAADF micrographs show no evidence of a core-shell structure, in contrast to what is observed in the case of nanoparticles prepared by chemical synthesis.

Figure 1. Mass spectrometer profile (line, before of filter nanoparticles) and HAADF (filled, after of filter nanoparticles) size distribution function.

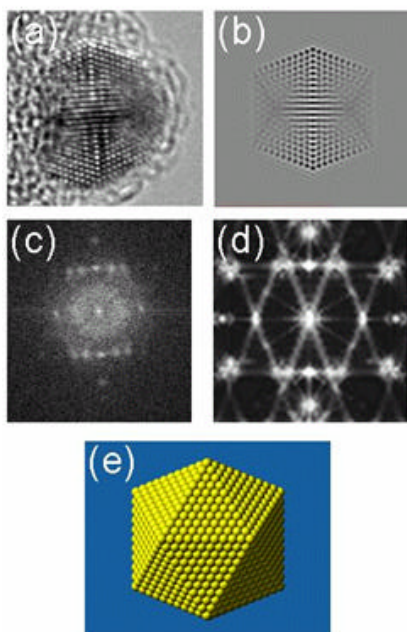
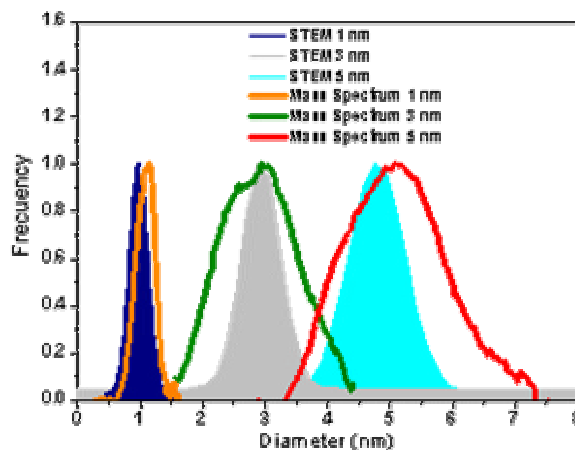


Figure 2. a) HRTEM AuPd Nps, b) HRTEM simulation model of nanoparticles, c) FFT pattern experimental Nps, d) FFT pattern of simulation model and e) Model of icosahedral nanoparticles

This work was supported by the International Center for Nanotechnology and Advanced Materials of The University of Texas at Austin (ICNAM), the Council for Science and Technology of the State of Nuevo León, Mexico, and the National Council for Science and Technology, Mexico (CONACYT), grants (43772 & 207569) and NL-2004-C05-060

## **Comparative Studies of Nanostructured Indium Oxide Thin Films: Pure and Doped with Tin and Tungsten Atoms Respectively**

Dwight R. Acosta and Arturo I. Martínez\*

*Instituto de Física, UNAM; A.P. 20-364, 01000 MEXICO D.F., Mexico.*

*\*Instituto Politécnico Nacional, Saltillo, Coahuila, Mexico.*

The nanostructured Transparent Conductive Oxides (TCO) receive considerable attention given its increasing important technological and industrial applications: solar cells, displays, smart windows, etc. Indium oxides thin films are commonly used as components in many opto-electronic devices like the mentioned in previous lines. In this work, Indium Oxide ( $\text{In}_2\text{O}_3$ ) thin films pure and doped with tin and tungsten atoms respectively, were synthesized by the pneumatic and pulsed spray pyrolysis technique at different deposition conditions in order to obtain materials with improved optical and electronic properties. The effects of parameter synthesis in structural, electrical and optical properties were studied systematically for all the samples using X-ray diffraction, electron and atomic force microscopy, optical absorption and Hall and van der Pauw electrical measurements. The crystallographic  $\text{In}_2\text{O}_3$  structure remains basically the same for pure and doped compounds as revealed from X-ray and electron diffraction patterns analysis. The effects of adding impurity atoms in the electronic structure and in the corresponding valences states of the  $\text{In}_2\text{O}_3$  compound were studied using the XPS technique. For  $\text{In}_2\text{O}_3$  thin films produced with optimized deposition parameters, the band gap energy derived from optical absorption experiments and using the Moss-Burstein approximation, was found to be of 3.7 eV. For  $\text{In}_2\text{O}_3\text{:Sn}$  deposited at the same substrate temperature ( $T_s = 475^\circ\text{C}$ ) an increase up to 3.81 eV. was observed. This behavior is a consequence of a better occupation of the lower levels in the conduction band with free electrons coming from donor atoms. The modification of electronic and /or band structure of the  $\text{In}_2\text{O}_3$  compound when doped with Sn (ITO) and W (IWO) atoms respectively was followed by XPS observations: The maximum of band energy for  $\text{In}_2\text{O}_3$  is found at 8.16 eV and when this material is doped with W and Sn, the maximum is displaced to 7.91 and 7.64 eV respectively. The lowest resistivity values for  $\text{In}_2\text{O}_3$  films were close to  $5 \times 10^{-3} \text{ } \Omega\text{-cm}$ , with  $T_s = 450^\circ$ , for ITO and IWO thin films the lowest resistivity values were  $5 \times 10^{-4}$  and  $9 \times 10^{-4} \text{ } \Omega\text{-cm}$  respectively. The grain size distributions detected for each sample, were correlated when possible with variations in electrical behavior. The nanostructure nature of  $\text{In}_2\text{O}_3$  compounds in thin films configurations and deposited by spray pyrolysis presented in this work were confirmed for all the cases from high resolution electron microscopy (HREM) observations.



## Forma Geométrica y Crecimiento de Nanoestructuras Metálicas

E. Juárez-Ruiz<sup>a,b</sup>, J. A. Lombardero-Chartuní<sup>a,c</sup>, L.C. Gómez-Pavón<sup>b</sup>,  
J. A. Ascencio<sup>d</sup>, and U. Paí<sup>e</sup>

<sup>a</sup> *Universidad Popular Autónoma del Estado de Puebla, 21 sur 1103, Col. Santiago, Puebla, Pue. CP72000, Mexico.*

<sup>b</sup> *Facultad de Ciencias de la Electrónica, Universidad Autónoma de Puebla, 18 Sur y San Claudio, CU, Puebla, Puebla 72570, Mexico.*

<sup>c</sup> *Universidad la Salle Benavente, 25 Ote. 9, Col. El Carmen, Puebla, 72000, Mexico.*

<sup>d</sup> *Ductos, Corrosión y Materiales, Instituto Mexicano del Petróleo, Lázaro Cárdenas 152, Col. San Bartolo Atepehuacan, Mexico, DF, 07730, Mexico.*

<sup>e</sup> *Instituto de Física, Universidad Autónoma de Puebla, PO Box J-48, Puebla 72570, Mexico.*  
e.mail: estela\_juarez2000@hotmail.com

Un esquema de clasificación de clusters es categorizarlos en clases de acuerdo a su nucleación y forma de crecimiento. Una de ellas es el crecimiento a través de capas. Los clusters primarios son los poliedros más simples, tales como tetraedros o icosaedros. Estos clusters sirven como cubiertas de nucleación para el siguiente estado de crecimiento el cual produce los así llamados clusters secundarios. El crecimiento capa por capa o cubierta por cubierta da origen a clusters poliedrales, los cuales pueden tener la misma forma o la de su poliedro dual.

En este trabajo se hace un análisis del déficit angular en los poliedros arquimedianos. En particular de los duales del cuboctaedro e icosaedro truncado. Describimos un modelo de crecimiento basado en este análisis y algunas propiedades derivadas de consideraciones geométricas y topológicas relacionadas a la estructura del espacio de configuración local de átomos y moléculas.

---

<sup>1</sup> Boon K. Teo and Hong Zhang, Magic Numbers in Clusters: Nucleation and Growth Sequences, Bonding, Principles and Packing Patterns, edited by Daniel L. Feldheim, and Colby A. Foss, Jr. Marcel Dekker, Inc. pp. 55-87, 2002.

<sup>2</sup> J. M. Montejano-Carrizales et al, Crystallography and Shape of Nanoparticles and Clusters, Enciclopedia of Nanosciences and Nanotechnology, edited by H. S. Nalwa, Vol. 2, pp 237-282, 2004.

<sup>3</sup> R. Kerner, The Role of Topology in Growth and Agglomeration, 61-90, Springer Berlag, 2006.

## Theoretical Examination of Sulfur Poisoning in PEM Fuel Cell Catalysts

### $\text{Pd}_{70}\text{Co}_{20}\text{X}_{10}$ (X : Au, Mo, Ni)

Mauricio Garza Castañón<sup>1</sup>, S.Velumani<sup>2\*</sup>, Marco A. Jiménez<sup>1</sup>,  
and Oxana Vasilievna Kharissova<sup>1</sup>

<sup>1</sup> *Facultad de Ciencias Físico-Matemáticas, UANL, Monterrey, Mexico.*

*Pedro de Alba S/N, Ciudad Universitaria, C.P. 66450, San Nicolás de los Garza, N.L. Mexico.*

<sup>2</sup> *Tecnológico de Monterrey – Campus Monterrey, E Garza Sada #2501, Monterrey, N.L. Mexico.*

\*e-mail. velu@itesm.mx

In this theoretical analysis, we intend to report some results obtained by computer modeling and simulation using ab-initio techniques for the sulfur adsorption on the (110) plane of the PdCoX (X: Au, Mo, Ni) trimetallic compound. The use of computational ab-initio and molecular dynamics techniques have been widely accepted as one way to have prior information about specific properties of the compounds under study, giving very valuable information about thermodynamics, reactivity, structure, optical properties, etc. Sulfur poisoning on catalysts is mainly due to the use of hydrocarbon compounds as fuels of hydrogen for the fuel cells. These hydrocarbons might contain sulfur that can attack the catalyst surface reducing its overall efficiency and lifetime. PdCoAu and PdCoMo have already been reported by us using similar ab-initio technique to be good catalysts and have good CO-tolerance, hence now we are reporting on the Sulphur poisoning. A CASTEP calculation is used to show change in chemisorption energy for a Sulphur molecule in the trimetallic (110) plane, and compared with that of pure Pt.

## Electronic and Vibrational Properties of Porous Silicon

Miguel Cruz<sup>a</sup> and Chumin Wang<sup>b</sup>

<sup>a</sup>*Instituto Politécnico Nacional, ESIME-Culhuacán, Av. Santa Ana 1000, 04430, D.F., México*

<sup>b</sup>*Instituto de Investigaciones en Materiales, Universidad Nacional Autónoma de México, A.P. 70-360, 04510, D.F., México*

\*e-mail: irisson@servidor.unam.mx

Porous silicon is a structurally complex material, in which effects of the pore topology on its physical properties are even controversial. In this work, we use the Born potential and the Green's function, both applied to a supercell model, in order to analyze the Raman response and the phonon band structure of porous silicon<sup>1</sup>. Also, the electronic band structure and dielectric function of ordered porous Si are studied by means of a  $sp^3s^*$  tight-binding supercell model<sup>2</sup>, in which periodical pores are produced by removing columns of atoms along [001] direction from a crystalline Si structure and the pore surfaces are passivated by hydrogen atoms. An advantage of this model is the interconnection between silicon nanocrystals and then, all the states are delocalized. However, the results of both electronic and vibrational properties show clear quantum confinement effects. The tight-binding results are compared with *ab-initio* calculations performed in small supercell systems<sup>3</sup>. The results also show a shift of the main Raman peak towards lower frequencies, in agreement with experimental data.

---

<sup>1</sup> P. Alfaro, M. Cruz, and C. Wang, *IEEE Trans. Nanotech.* **5**, 466 (2006).

<sup>2</sup> M. Cruz, M.R. Beltrán, C. Wang, J. Tagüña-Martínez, and Y.G. Rubo, *Phys. Rev. B* **59**, 15381 (1999).

<sup>3</sup> Y. Bonder and C. Wang, *J. Appl. Phys.* **100**, 044319 (2006).

## **Comparación de Métodos Numéricos en la Búsqueda de Geometrías Óptimas en Nanopartículas Monometálicas**

Enrique Guevara Chapa<sup>1</sup>, S. Mejía Rosales<sup>1</sup>, E. Pérez Tijerina<sup>1</sup>  
y M. José Yacaman<sup>2</sup>.

<sup>1</sup>*Facultad de Ciencias Físico Matemáticas, Universidad Autónoma de Nuevo León  
San Nicolás de los Garza, Nuevo León, 66450, México*

<sup>2</sup>*Department of Chemical Engineering, The University of Texas at Austin,  
Austin Tx. 78712 USA.*

e-mail: eguevara@cfm.uanl.mx

La optimización numérica de nanopartículas ha sido un área de estudio bastante concurrida en los últimos años. La búsqueda de la estructura geométrica con el que se obtenga la menor energía potencial, es un problema de *NP-hard*, por lo que no tiene una solución analítica y su complejidad crece exponencialmente conforme el número de partículas aumenta. Este estudio se ha realizado principalmente en nanopartículas monometálicas de 2 hasta 80 átomos.

El problema se ha atacado por diversos métodos clásicos de optimización global y se han desarrollado métodos nuevos específicamente para estos problemas. A pesar de esto, no existe un método sobre saliente de los demás. Las características que se evalúan en un método son la rapidez y el porcentaje de efectividad para encontrar la mejor estructura posible.

Hemos realizado un estudio comparativo de diversos métodos numéricos de optimización global para tener un parámetro de comparación estándar. También se han combinado diversas estrategias usadas por distintos métodos a fin de mejorar los ya existentes.

Los métodos que se compararon fueron, algoritmos genéticos, montecarlo, tunelamiento aleatorio y búsqueda exhaustiva por barrido.

*Agradecemos al CONACYT el apoyo financiero otorgado para el proyecto NL-2004-C05-60 y a The University of Texas at Austin por el tiempo de computo otorgado.*